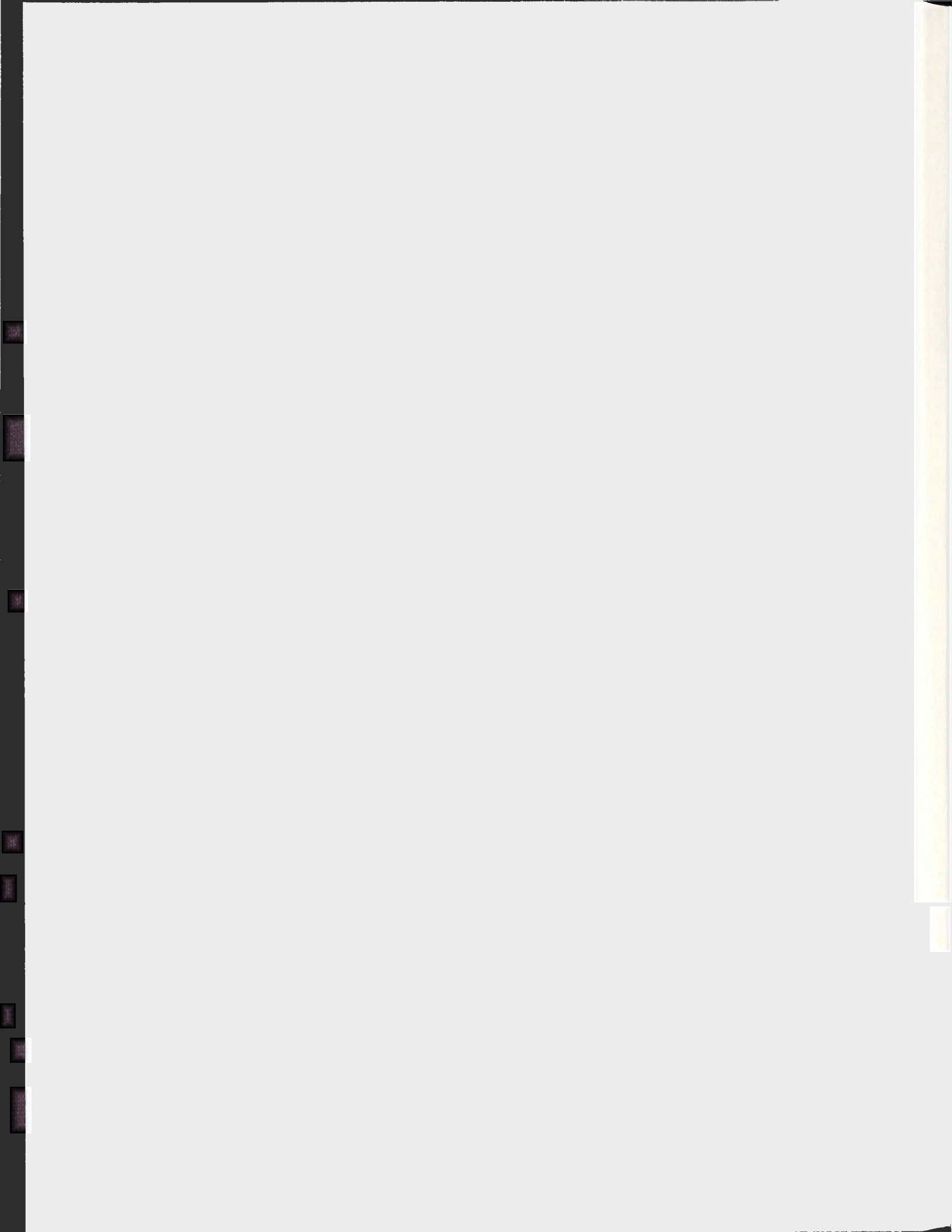


IDENTIFICATION AND CHARACTERIZATION OF A
NOVEL INTERACTION BETWEEN PEROXISOME-
PROLIFERATOR ACTIVATED RECEPTOR GAMMA
(PPAR γ) AND MESODERM INDUCTION-EARLY
RESPONSE 1: IMPLICATIONS FOR ADIPOGENESIS

AMANDA PARSONS



Identification and characterization of a novel interaction between peroxisome-proliferator activated receptor gamma (PPAR γ) and mesoderm induction-early response 1: Implications for adipogenesis

By Amanda Parsons

A thesis submitted to the School
of Graduate Studies in partial
fulfillment of the requirements
for the degree of
Master of Science.

Division of BioMedical Sciences

Faculty of Medicine

Memorial University

October 2008

Abstract

PPAR γ is a nuclear hormone receptor and master regulator of lipid metabolism and adipogenesis. PPAR γ regulates these processes through the recruitment of a diverse set of transcriptional coregulators in a tissue and time specific manner. This study focused on characterizing the interaction between PPAR γ and mesoderm induction early response 1 (MIER1), a transcription factor that has been shown to interact with other nuclear hormone receptors and regulate target gene expression. Glutathione S transferase pull-down assays have revealed that PPAR γ interacts with both MIER1 α and β through the common SANT domain. Coimmunoprecipitations in HEK-293 (human embryonic kidney cells) confirmed that this interaction occurs *in vivo*. A transcriptional reporter assay using luciferase regulated by the PPAR response element (PPRE) demonstrated that MIER1 α and β cause a ligand-independent 2-fold activation of PPAR-driven transcriptional activity and this was similar to the 3-fold activation observed with a known PPAR γ coactivator (PGC1- α). Thus, MIER1 interacts with PPAR in a ligand-independent manner through its SANT domain, and activates PPAR γ -mediated transcriptional activity. PCR analysis showed that MIER1 mRNA expression is upregulated in 3T3-L1 pre-adipocytes during their differentiation into adipocytes. As well, immunocytochemistry revealed that MIER1 α is highly expressed specifically in differentiated 3T3-L1s. Future work will determine the exact role of MIER1 in adipogenesis, using shRNA to knockdown MIER1 α in the well-established 3T3-L1 differentiation system.

Acknowledgements

First and foremost, I would like to extend an earnest thank you to my supervisor, Dr. Gary Paterno, for keeping me motivated and interested in the field of molecular and cellular biology – and for ensuring that I was always aware of my contribution to the ever-expanding knowledge base in the field. I would also like to sincerely thank Corinne Mercer, Gordon Nash and Heather Fifield for their exceptional technical support and guidance. I am also in debt to all of the students at the Terry Fox Cancer Research Labs for their unwavering support and guidance, but more importantly, for their friendship. I also want to thank my supervisory committee for supporting me in my experimental endeavors but also for pulling me back when I got too far ahead of myself. The past two years working at the Terry Fox Labs were truly enjoyable and I will miss everyone.

Funding for this project was provided in part by the National Sciences and Engineering Research Council of Canada, the Canadian Institutes of Health Research and Memorial University of Newfoundland.

Table of Contents

ABSTRACT	II
ACKNOWLEDGEMENTS	III
LIST OF FIGURES	VI
LIST OF TABLES	VII
LIST OF ABBREVIATIONS	VIII
CHAPTER 1 - INTRODUCTION	1
1.1 GENERAL INTRODUCTION	1
1.1.1 THE CENTRAL DOGMA: DNA → RNA → PROTEIN	1
1.1.2 TRANSCRIPTION	1
1.2 MESODERM INDUCTION EARLY RESPONSE 1 (MIER1)	3
1.2.1 MIER1 STRUCTURE/FUNCTION	3
1.3 PEROXISOME PROLIFERATOR-ACTIVATED RECEPTOR (PPAR)	8
1.3.1 PPAR	8
1.3.2 STRUCTURE OF PPARS	9
1.3.3 CLASSICAL MODEL FOR PPAR γ FUNCTION	14
1.3.4 ADIPOGENESIS	18
1.3.5 3T3-L1 MODEL SYSTEM FOR ADIPOGENESIS	19
1.3.6 PPAR γ AND TYPE 2 DIABETES	23
1.4 PURPOSE OF THIS STUDY AND OBJECTIVES	24
CHAPTER 2 – MATERIALS AND METHODS	27
2.1 PLASMIDS	27
2.2 IN VITRO TRANSCRIPTION-TRANSLATION (TNT)	29
2.3 GST PULLDOWN ASSAY	30
2.3.1 GLUTATHIONE SEPHAROSE 4B BEADS	30
2.3.2 GST-FUSION PROTEIN PRODUCTION	31
2.3.3 EXPRESSION OF GST-FUSED PROTEINS	32
2.3.4 GST PULL DOWN ASSAY	33
2.4 CELL CULTURE	34
2.5 TRANSFECTIONS: HEK-293 CELLS	35
2.6 REPORTER ASSAY	38

2.6.1 PPRE-LUCIFERASE ASSAY	38
2.6.2 β -GALACTOSIDASE ASSAY	39
2.7 ADIPOGENESIS ASSAY	39
2.7.1 RNA EXTRACTION	41
2.7.2 PRECIPITATING RNA	42
2.7.3 REVERSE-TRANSCRIPTASE PCR (RT-PCR)	42
2.7.4 WESTERN BLOT FOR ADIPONECTIN OVER COURSE OF ADIPOCYTE DIFFERENTIATION	46
2.7.5 OIL RED O STAINING	47
2.7.6 IMMUNOCYTOCHEMISTRY	48
2.7.7 IMMUNOFLUORESCENCE	50

CHAPTER 3- RESULTS **52**

3.1 IN VITRO INTERACTION BETWEEN MIER1α AND MIER1β WITH PPARγ2	52
3.2 IN VIVO INTERACTION BETWEEN MIER1 AND PPARS	57
3.2.1 MIER1 α AND MIER1 β INTERACT WITH PPAR γ 2 IN HEK-293 CELLS	57
3.2.2 MIER1 α AND MIER1 β INTERACT WITH PPAR β / δ IN HEK-293 CELLS	60
3.3 LIGAND-INDEPENDENT INTERACTION BETWEEN MIER1 AND PPARγ2	63
3.3.1 MIER1 α AND MIER1 β INTERACT WITH PPAR γ 2 IN HEK-293 CELLS, INDEPENDENT OF TROGLITAZONE TREATMENT	63
3.4 EFFECT OF MIER1 ON PPRE-DEPENDENT TRANSCRIPTION	66
3.4.1 MIER1 α AND MIER1 β SERVE AS TRANSCRIPTIONAL ACTIVATORS OF PPRE-DEPENDENT TRANSCRIPTION	66
3.4.2 MIER1 α ACTIVATES PPRE-DEPENDENT TRANSCRIPTION IN A DOSE-DEPENDENT MANNER	70
3.4.3 9-CIS RETINOIC ACID, A LIGAND FOR RETINOID X RECEPTOR, HAS NO EFFECT ON THE ABILITY OF MIER1 α TO ACTIVATE PPRE-DRIVEN TRANSCRIPTION	72
3.5 CHANGES IN MRNA LEVELS OF MIER1 OVER THE COURSE OF ADIPOGENESIS IN 3T3-L1 CELLS	74
3.6 DETERMINATION OF DIFFERENTIATING VERSUS NON-DIFFERENTIATING 3T3-L1 CELLS	76
3.7 IMMUNOCYTOCHEMICAL ANALYSIS OF MIER1α LOCALIZATION IN 3T3-L1 CELLS UNDERGOING ADIPOGENESIS	79

CHAPTER 4 – DISCUSSION **84**

PROPOSED MODEL FOR MIER1 ACTIVATION OF PPARγ2	99
IMPLICATIONS	101
FUTURE STUDIES	103
4.9.1 DETERMINE THE DOMAIN OF PPAR γ 2 THAT INTERACTS WITH MIER1	103
4.9.2 DEMONSTRATE <i>IN VIVO</i> INTERACTION BETWEEN PPAR γ 2 AND MIER1 α	103
4.9.3 DETERMINE THE EFFECT SHRNA-MEDIATED REDUCTION IN MIER1 α LEVELS HAS ON ADIPOGENESIS	104
4.9.4 DETERMINE OTHER BIOLOGICALLY RELEVANT FUNCTIONS OF MIER1 α -MEDIATED ACTIVATION OF PPAR γ 2	105

List of Figures

Figure 1: Domain Structure of MIER1.....	6
Figure 2: Domain Structure of PPAR γ	13
Figure 3: Model for PPAR ligand binding and activation of transcription	17
Figure 4: Epigenetic regulation of the effects of C/EBP and PPAR on adipogenesis.....	22
Figure 5: GST-fused deletion constructs of MIER1 α and β	54
Figure 6: GST pulldown showing interaction between PPAR γ and MIER1 α and β	55
Figure 7: GST pulldown showing interaction between PPAR γ and pieces of MIER1 α	56
Figure 8: PPAR γ 2 interacts with MIER1 α in HEK-293 cells	58
Figure 9: PPAR γ 2 interacts with MIER1 β in HEK-293 cells	59
Figure 10: PPAR β/δ interacts with MIER1 α in HEK-293 cells	61
Figure 11: PPAR β/δ interacts with MIER1 β in HEK-293 cells	62
Figure 12: PPAR γ 2 interacts with MIER1 α and β in HEK-293 cells independent of ligand	64
Figure 13: PPAR β/δ interacts with MIER1 α and β independent of ligand	65
Figure 14: MIER1 α and β activate PPAR γ promoter activity in the presence and absence of PPAR γ agonist (Troglitazone).....	68
Figure 15: MIER1 α and β activate PPAR γ promoter activity in the presence and absence of PPAR γ agonist (fold-change).....	69
Figure 16: A- Dose-dependent increase in PPRE-dependent luciferase activity B & C: Western blot for MIER1 α in HEK-293 cells used for luciferase assay (B: + DMSO, C: +Troglitazone)	71
Figure 17: 9-cis retinoic acid has no effect on MIER1 α ability to increase PPAR-dependent transcription	73
Figure 18: <i>ppary2</i> and <i>mier1</i> mRNA levels increase concomitantly over the course of adipogenesis	75
Figure 19: 3T3-L1 cells stained with Oil Red O at Day 22 of adipogenesis.....	77
Figure 20: Western Blot of Adiponectin over 14 days of adipogenesis.....	78
Figure 21: MIER1 α is expressed in early and late differentiating 3T3-L1 adipocytes	81
Figure 22: MIER1 β is not expressed in early or late differentiating 3T3-L1 adipocytes.....	82
Figure 23: MIER1 α and PPAR γ are colocalized in differentiated 3T3-L1 cells.....	83

List of Tables

Table 1: PPAR γ coregulators and ligands12
Table 2: Mastermix for Reverse Transcription43
Table 3: Primers for PCR44
Table 4: PCR program45

List of Abbreviations

μ g	microgram
μ l	microlitre
aa	amino acid
AD	activation domain
AF1	activation function 1 domain
AF2	activation function 2 domain
AR	androgen receptor
β -gal	β galactosidase
BCS	bovine calf serum
BSA	bovine serum albumin
CBP	CREB-binding protein
DBD	DNA binding domain
DEPC	Diethylpyrocarbonate
DMEM	Dulbecco's modified Eagle's medium
DNA	deoxyribonucleic acid
EDTA	ethyldiamine tetra-acetic acid
ELM2	EGL27 and MTA1 homology 2
ER	estrogen receptor
ERE	estrogen response element
FBS	fetal bovine serum
FGF	fibroblast growth factor
g	gram
GR	glucocorticoid receptor
GST	glutathione S-transferase
GST-MIER1	glutathione S-transferase tagged MIER1
h	hour(s)
HAT	histone acetyltransferase
HDAC	histone deacetylase
<i>mier1</i>	mesoderm induction early response 1 gene (DNA/RNA)
MIER1	mesoderm induction early response 1 protein
HRP	horseradish peroxidase
Hsp40	heat shock protein 40
IP	immunoprecipitation
kDa	kilodalton
LBD	ligand binding domain
LXXLL	L= leucine; X= any amino acid
Luc	luciferase
M	molar
min	minute(s)
ml	millilitre
MLS	membrane localization signal

mM	millimolar
mRNA	messenger ribonucleic acid
NCOR	nuclear receptor corepressor
NLS	nuclear localization signal
nt	nucleotide
°C	degrees Celsius
PBS	phosphate buffered saline
pmoles	picomoles
PCAF	p300/CREB binding protein associated protein
PPAR	peroxisome proliferator activated receptor
PPAR α	peroxisome proliferator activated receptor alpha
PPAR δ/β	peroxisome proliferator activated receptor delta/beta
PPAR γ	peroxisome proliferator activated receptor gamma
PPAR γ 1	peroxisome proliferator activated receptor gamma 1
PPAR γ 2	peroxisome proliferator activated receptor gamma 2
PR	progesterone receptor
RA	retinoic acid
RAR	retinoic acid receptor
RLU	relative luciferase units
RNA	ribonucleic acid
rpm	revolutions per minute
RXR	retinoid X receptor
RXR α	retinoid X receptor alpha
RXR γ	retinoid X receptor gamma
SANT	domain first identified in SWI3, ADA1, NCoR, TFIIB
SDS	sodium dodecyl sulfate
SDS-PAGE	sodium dodecyl sulfate- polyacrylamide gel electrophoresis
SPPARMs	selective PPAR gamma modulators
SH3	src homology domain 3
SMRT	silencing mediator of retinoic acid and thyroid hormone receptor
Sp1	promoter specific transcription factor 1
SRC-1	steroid receptor coactivator 1
SRC-3	steroid receptor coactivator 3
TBP	TATA-binding protein
TFII	transcription factor for RNA polymerase II
TFIII	transcription factor for RNA polymerase III
TFTC	TBP-free TAF containing complex
TGF α	transforming growth factor alpha
TNF	tumor necrosis factor
TR	thyroid hormone receptor
TRABID	TRAF binding domain

CHAPTER 1 - Introduction

1.1 General Introduction

1.1.1 The Central Dogma: DNA → RNA → Protein

The genome of a particular cell dictates the proteins that could potentially be expressed in that given cell at a particular period in the existence of that cell. However, the information in the genome must be translated into the expression of a set of proteins. The mechanism by which the cell translates this information is referred to as the central dogma in cellular biology. Succinctly, deoxyribonucleic acid (DNA) from the nucleus is transcribed into messenger ribonucleic acid (mRNA) that is subsequently translated into protein.

1.1.2 Transcription

Transcription is the synthesis of RNA from the template strand of DNA, and allows for a mobile copy of the information stored in the genome to be translocated to the cytoplasm for translation. The major enzyme responsible for transcription is the RNA polymerase. In eukaryotic cells, there are three different RNA polymerases – RNA polymerase I synthesizes ribosomal RNAs (rRNA), polymerase II synthesizes mRNAs and polymerase III the transfer RNAs (tRNA). The RNA polymerase II can bind to a region of the DNA referred to as the promoter region, with the aid of other proteins referred to as transcription factors. Specifically, the polymerase binds to a region

referred to as the TATA box, with a sequence of 5'-TATAAA-3'. Prior to binding by the polymerase, a TATA-binding protein (TBP) recognizes the TATA box in a complex with transcription factor for polymerase II, fraction D (TFIID). This complex serves as a binding site for other transcription factors including TFIIA and TFIIB, which recruit the polymerase in complex with TFIIF. Once bound to the DNA, the RNA polymerase is changed into its active form by the binding of TFIIIE and TFIIH, and moves along the DNA in a 3' to 5' direction while a protein called DNA helicase unwinds the double-stranded molecule. The RNA polymerase assembles a complementary strand of RNA using nucleotides that form a proper base pair with the nucleotide of the strand of DNA being transcribed. The DNA re-winds itself into a double-stranded molecule and the mRNA is left as a single strand. This mRNA is sometimes shuttled to the cytoplasm where processing can occur. However, most of the eukaryotic mRNA processing occurs in the nucleus. There are three main processing steps; addition of a 5' methylguanosine cap, addition of a 3' polyadenosine (poly[A]) tail, and RNA splicing. The 5' cap prevents degradation of the mRNA by exonucleases and plays a role in initiation of mRNA translation. The 3' poly (A) tail serves as a docking site for proteins involved in processing at the 3' end of the mRNA.

The last processing step of the mRNA includes removal of introns (non-coding regions), and this is referred to as RNA splicing. As with transcription itself, RNA splicing requires precision and a host of enzymes to ensure that not a single nucleotide of the exon sequence is lost, or mistranslation of the mRNA could occur. Splicing usually occurs co-transcriptionally, where the splicing factors could interact with the

transcriptional machinery¹. Once this processing is complete, the mature mRNA is shuttled to the cytoplasm where it can then pass the genetic information on in the form of protein via the process referred to as translation. This study focuses on a novel transcription factor that is intimately tied to the process of transcription – Mesoderm Induction Early Response 1 (MIER1).

1.2 Mesoderm Induction Early Response 1 (MIER1)

1.2.1 MIER1 Structure/Function

Mesoderm Induction Early Response 1 was first isolated in *Xenopus laevis* as a gene that was intimately involved in development. The expression levels of *Xmi-er1* were upregulated after the induction of mesoderm differentiation by fibroblast growth factors (FGF)². A comparison of the amino acid composition of this isoform with the subsequently discovered human ortholog showed 91% similarity on the whole and 100% similarity in the common internal domains. This gene encodes a nuclear protein that has been shown to act as a transcriptional regulator.

Further study into the structure of *mier1* revealed a number of splice variants of the same gene. The chromosomal position is human Chr 1p31.2, and *mier1* spans 63 Kb and consists of 17 exons. Of these exons, there is one skipped exon, a facultative intron and three polyadenylation signals that together can produce 12 different transcripts encoding six proteins³. The six isoforms have a common internal domain but variable N- and C- terminal regions. Specifically, there are three different N-terminal and two C-

terminal variants. The C-terminal variants arise from the use of a facultative intron, and produce the two main isoforms, MIER1 α and MIER1 β . Of these two, only MIER1 β has a nuclear localization signal (NLS) while MIER1 α remains mainly in the cytoplasm⁴. This does not rule out the possibility that MIER1 α could be shuttled into the nucleus via interaction with other nuclear proteins (*e.g.* HDAC1). MIER1 α may also differ in subcellular localization depending upon cell type.

MIER1 α contains in its C-terminus, an LXXLL motif that is not found in MIER1 β . This motif has been shown to function as a nuclear hormone receptor interaction domain in many different coregulators for the nuclear receptors, including RIP-140, SRC-1, TIF-2 and CBP/p300⁵.

Some of the domains in MIER1 are very similar to other transcriptional regulators. There is a well characterized acidic activation domain common to the α - and β - forms of MIER1, as well as an ELM2 domain and a common SANT domain⁶ (Figure 1).

The SANT domain of MIER1 is found in many other transcriptional regulators; the acronym actually originates from the proteins in which it was initially found: SWI3, ADA2, N-CoR and TFIIB. The SANT domain has been implicated in protein-protein interactions, DNA binding and even recruitment of histone acetyltransferases and deacetylases, and thus its function in a specific protein must be determined. The SANT domain is actually a small motif, with approximately 50 amino acids and is often found in nuclear receptor corepressors⁷. It has been hypothesized that the SANT, bromodomains

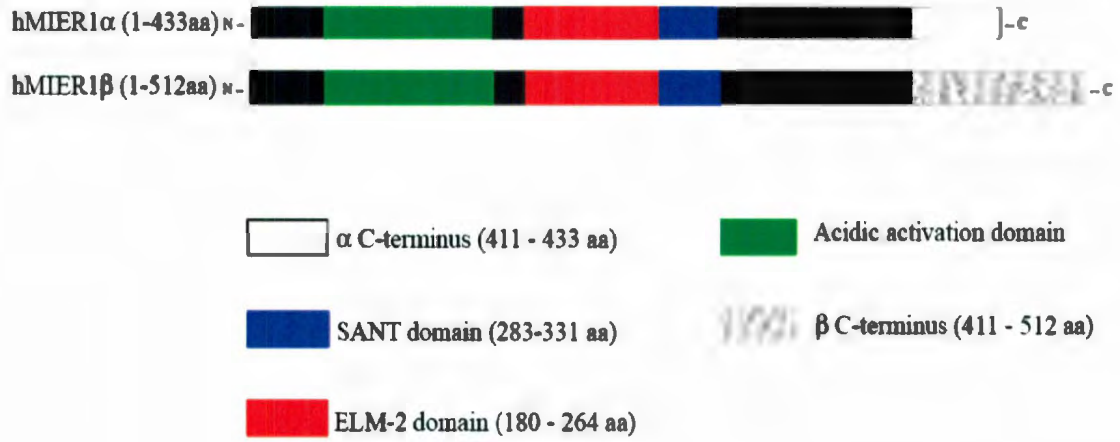


Figure 1: Domain Structure of MIER1

Figure 1 depicts the two most common forms of MIER1, MIER1 α and MIER1 β . These two proteins share a common set of domains listed above, except MIER1 β has an alternate C terminus that arises via the use of a facultative intron.

and chromodomains actually read what has been referred to as the histone code⁷. The histone code hypothesis is based on the fact that specific histone tail modifications, such as acetylation, methylation, phosphorylation and/or ubiquination can make up a code that will determine the transcriptional state of the particular genes⁷. In the case of the SANT domain, it has a binding preference for unmodified histone tails – therefore its interaction with the unacetylated tails could block the binding of histone acetyltransferases (HATs). Also, deacetylation of histone tails could increase binding of SANT-domain containing proteins⁷.

The ELM2 domain has been found in many different proteins, often in conjunction with the SANT domain. It has been found in a number of transcriptional corepressors, including atrophin 2⁸, MTA (metastasis associated family), and CoREST⁹. Several studies have shown that the ELM2 domain is involved in directly binding histone deacetylases 1 and 2 (HDAC1/2)^{10,11}. A recent study on the function of the ELM2 and SANT domains has revealed a distinct mechanism by which the ELM2 domain recruits HDAC1/2 and the SANT domain recruits G9a (histone methyltransferase), resulting in deacetylation followed by stable methylation of histone H3-lysine 9 in atrophin 2¹². Since MIER1 contains both of these domains, and has been shown to have an affinity for both HDAC1/2 and G9a¹³, it may function as a transcriptional repressor in a similar manner.

The presence of the acidic activation domain at the N-terminus¹⁴ gave reason to believe that MIER1 would act as a potent transcriptional activator. However, further study using the G5tkCAT reporter plasmid and GAL4-fused MIER1 α and β showed that

the two isoforms actually function as powerful transcriptional repressors in a number of different cell lines¹⁵. It was subsequently determined that repression occurred through two distinct mechanisms. The first is recruitment of HDAC1 to the ELM2 domain of MIER1¹⁶. The second is via the SANT domain, where MIER1 binds to certain transcription factors (Sp1) and displaces them from their respective binding site¹⁷.

Other putative domains have been identified in MIER1. A study on *Xenopus laevis* xMIER1 indicated there was a proline-rich region that matched the consensus for the Src homology 3 (SH3) binding domain¹⁸. In fact, mutation of proline 365 completely eliminated the effects of xMIER1 on development¹⁸. These SH3 binding domains are usually found in proteins that interact with other proteins via proline-rich peptides, to mediate assembly of larger protein complexes. Some examples of SH3 domain containing proteins include those involved in tyrosine kinase signaling, cytoskeletal organization, and various enzyme complexes¹⁹.

1.3 Peroxisome Proliferator-Activated Receptor (PPAR)

1.3.1 PPAR

The superfamily of nuclear hormone receptors consists of three types: steroid receptors, non-steroid receptors, and orphan nuclear hormone receptors for which there is no known binding partner or ligand. The steroid receptors include the androgen receptor (AR), estrogen receptor (ER), glucocorticoid receptor (GR), progesterone receptor (PR) and mineralocorticoid receptor (MR). The non-steroid receptors include the vitamin D receptor (VDR), retinoic acid receptor (RAR), retinoid X receptor (RXR) and the peroxisome proliferator-activated receptors (PPAR). Some orphan nuclear hormone receptors include PNR (photoreceptor cell-specific nuclear receptor), TLX, TR2 and 4 (thyroid hormone receptors 2 and 4) and NURR1²⁰.

The peroxisome proliferator-activated receptors (PPARs) have an integral role in lipid and glucose metabolism, and have been also implicated in a variety of carcinomas²¹⁻²⁵. Both overexpression of PPAR γ as well as loss-of-function mutations in *ppary* have been implicated in colorectal cancer²¹. PPAR β/δ has been shown to stimulate lung cancer cell growth via the PI3-kinase pathway and inhibition of the phosphatase and tensin homolog (PTEN)²⁶.

There are three isoforms of PPARs including PPAR α , PPAR β/δ and PPAR γ that are expressed in various tissues of the body. PPAR α is found mainly in the liver, muscle, heart and kidneys^{27,28}. Much less is known about PPAR β/δ , which is widely expressed throughout the body including the brain, adipose tissue, liver, muscle, vascular smooth

muscle cells and endothelium²⁹. PPAR γ is expressed mainly in adipose tissue, with some expression also occurring in human skeletal muscle, heart³⁰ and macrophages³¹.

There are three isoforms of PPAR γ , PPAR γ 1, PPAR γ 2 and PPAR γ 3. Both *ppar γ 1* and *ppar γ 3* encode the same protein, while PPAR γ 2 contains an extra 30 amino acids at the NH-2 terminus³². While PPAR γ 1 is ubiquitously expressed, PPAR γ 2 is expressed mainly in adipose tissue³³. Perhaps the most infamous function of PPAR γ 2 is in relation to Type 2 diabetes. Under normal conditions, PPAR γ 2 can be activated by ligands (thiazolidinediones) to promote insulin sensitivity thereby improving the condition of those affected by diabetes³⁴. However, the exact mechanism by which PPAR γ 2 promotes insulin sensitivity has yet to be elucidated.

1.3.2 Structure of PPARs

The overall structure of the PPARs is similar to that of other nuclear hormone receptors. Moving from the N-terminus to the C-terminus, the PPAR gamma gene encodes an A/B domain that stimulates ligand-independent transcriptional activity, which is also called the activation function 1 (AF-1) domain³⁵. This domain also contains conserved MAP-kinase phosphorylation serine sites³². Next is the C domain which contains the DNA binding domain (DBD) consisting of two zinc fingers that facilitate site-specific binding of the receptor to the hormone response element (HRE). In the case of PPAR γ , this response element is called the PPAR γ response element (PPRE). The DBD contains a carboxyl-terminal extension (CTE) of the zinc finger domain that

recognizes the 5'extension of the direct repeat 1 (DR1), which contributes to the specificity and polarity of PPAR DNA binding³². As will be discussed in detail, PPAR response elements (PPRE) consist of a hexameric nucleotide direct repeat of the recognition motif 5'-AGGTCA-3' spaced by one nucleotide, and PPAR binds the 5' direct repeat³⁶. This is in contrast to what is normally seen for heterodimeric partners of the retinoid X receptor (RXR), which tend to bind at the 3' DR.

The D domain is a hinge region that contains the DNA binding domain (DBD), however this domain has also been implicated in ligand binding³⁷. It is highly conserved among the PPARs, and may be involved in nuclear localization³². In 2005, it was discovered that PPAR α is regulated in part by protein kinase C (PKC), through PKC-phosphorylation sites located near the hinge region³⁸. There are a number of other post-translational modifications that affect PPAR. For example, insulin induces both PPAR α and PPAR γ phosphorylation which in turn, leads to an increase in PPAR transcriptional activity³⁹. The mitogen-activated protein kinase pathway can also phosphorylate PPAR γ , via stimulation by α -adrenergic signals³⁹. Certain ligands for the receptor can also lead to ubiquitination and subsequent proteasomal degradation.

Domain E contains the ligand binding domain (LBD) that facilitates dimerization with the retinoid X receptor (RXR) and also binding of a wide range of ligands. The LBD of PPAR γ is hydrophobic, and larger than that of other nuclear receptors, allowing for more promiscuous ligand binding affinity⁴⁰. Also found here is the activation function 2 (AF-2) domain that binds to specific cofactors to facilitate transcriptional regulation. More specifically, it is involved in ligand-dependent transcriptional

activation. Both the D and E/F domains have been shown to interact with Heat Shock protein 90 (HSP90), where it acts as a repressor of both PPAR α and PPAR β/δ activity⁴¹. There are a number of ligands thought to bind this domain of PPAR γ (Table 1). Of the endogenous ligands, there is not a single ligand that has a very high affinity for PPAR γ ; the highest affinity ligand for PPAR γ would be 15-deoxy- Δ -12, 14-prostaglandin J₂⁴². Other less specific ligands include the fatty acids and other eicosanoids.

Table 1: PPAR γ coregulators and ligands

PPARγ Coactivators	PPARγ Corepressors	Endogenous Ligands	Synthetic Ligands
CBP/p300	RIP140	Eicosanoids (e.g. 15-deoxy- Δ -12, 14-prostaglandin J2)	Thiazolidinediones (e.g. rosiglitazone, troglitazone, pioglitazone, ciglitazone)
SRC-1, 2, 3	NCoR		
PGC-1 α , β	SMRT	Fatty acids (e.g. lauric acid, arachidonic acid, linoleic acid, linolenic acid)	Non-steroid anti-inflammatory drugs (NSAIDs) (e.g. aspirin)
PBP			
PRIP			
PRIC285			Statins (e.g. Atorvastatin, Rosuvastatin, simvastatin)
BAF60c			

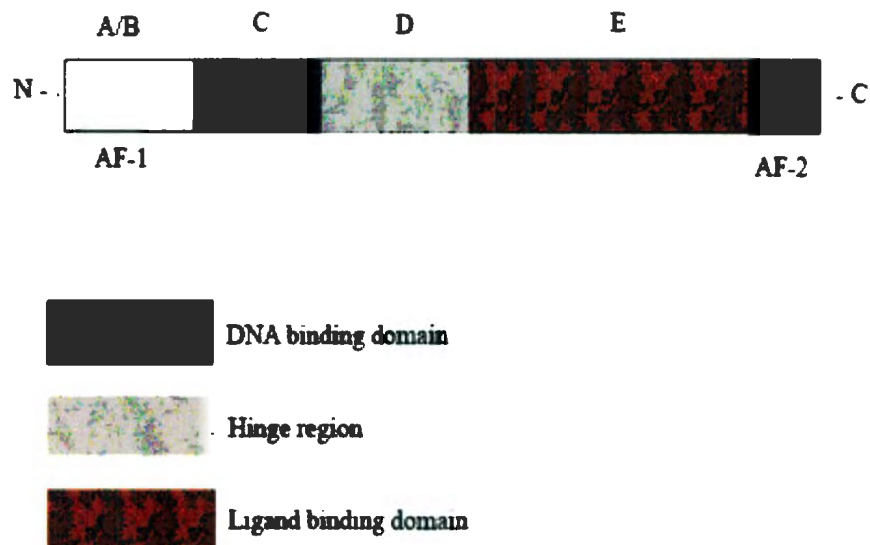


Figure 2: Domain Structure of PPAR γ

The A/B domain at the N-terminus is responsible for ligand-independent transcriptional activity. The C domain contains the DNA binding domain (DBD) that allows PPAR γ to recognize and bind the PPAR response element (PPRE). The D domain is a hinge region that allows for folding of the protein and the E domain contains the ligand binding domain (LBD). The ligand-binding domain along with the AF-2 domain is responsible for ligand-dependent transcriptional activation and also facilitates heterodimerization with the retinoid X receptor (RXR).

1.3.3 Classical Model for PPAR γ Function

Non-steroid nuclear hormone receptors have been implicated in a variety of cellular processes including apoptosis, cellular proliferation, and cell cycle regulation⁴³. PPAR γ specifically has been associated with tissue repair and inflammation. It has also been implicated in a variety of human diseases including Type II diabetes (PPAR γ), leukemia, colon carcinoma, bone cancer and atherosclerosis^{21,44,45}. The general model for PPAR action is conserved among the three isoforms and is triggered by ligand binding to the LBD. After ligand binding, PPAR heterodimerizes with the retinoid X receptor (RXR) and binds to PPREs.

The retinoid X receptor is a ligand-activated nuclear hormone receptor, of which the retinoids or vitamin A derivatives are the major endogenous ligand⁴⁶. Some of the nuclear hormone receptors that RXR binds are PPARs, liver X receptors (LXR), vitamin D receptors (VDR), and the farnesoid X receptor (FXR)⁴⁶. An interesting difference between the heterodimerization of PPAR with RXR as opposed to other nuclear receptors that partner with RXR is that while normally RXR preferentially binds the 5' direct repeat sequence of the particular hormone response element (HRE), in the case of PPAR-RXR, PPAR prefers to bind this 5' sequence. The significance of this difference has not been elucidated.

Binding to PPRE requires that a ligand bind to either PPAR or RXR, although when both receptors are bound by ligand the transcriptional regulation is usually enhanced⁴⁷. These PPAR response elements consist of a hexameric nucleotide direct

repeat of the recognition motif 5'-AGGTCA-3' spaced by one nucleotide⁴⁸. During ligand binding, activation and heterodimerization, the complex recruits coregulators (coactivators or corepressors) to regulate expression of a variety of genes.

Nuclear receptor coregulators are a family of approximately 300 proteins that interact directly or through other proteins with DNA-binding transcription factors to facilitate regulation of gene transcription. These coregulators consist of coactivators (function to activate gene transcription at a particular promoter) and their negative counterpart, the corepressors. These coregulators function in a multicomponent protein complex to assist the cell in regulating the subreactions that together define the process of transcription. As mentioned in the introduction to transcription, this process includes unwinding of DNA from histones, assembly of a large complex including polymerase II, initiation, elongation, RNA splicing and termination.

As if the number of coregulators was not enough to lead to the precise regulation of target gene transcription, coregulators are also controlled by posttranslational modifications of either the coregulator itself, or the associated nuclear receptor. These modifications may include phosphorylation (as in the case of PPAR γ), methylation, acetylation, SUMOylation or ubiquitination⁴⁹. These posttranslational modifications could be a type of code, allowing for the huge diversity of human gene transcripts that cannot be explained by the number of genes alone.

It is human nature to categorize things, and labeling certain proteins as coactivators or corepressors is no exception. However, some of these factors could serve as both coactivators and corepressors, depending upon the circumstances. For example,

SMRT and NCoR are potent transcriptional repressors for a number of nuclear receptors⁵⁰⁻⁵². However, both SMRT and NCoR function as transcriptional activators for TR α (thyroid receptor) through their binding to negative hormone response elements in the promoter region⁵³. Another example, albeit indirect, is SRC-3. SRC-3 has been defined as a growth coactivator in the breast, but can function as a growth repressor in the lymphocytes via cytoplasmic sequestering of I κ K (I κ B kinase) and ultimately inhibiting NF- κ B⁵⁴.

When an agonist binds PPAR (or in some cases, RXR), the complex between PPAR and the corepressor(s) dissociates allowing for the recruitment of coactivators. If bound by an antagonist, the receptor can recruit corepressors. For the PPAR-RXR complex, these two receptors are bound together, even in the absence of agonist⁵⁵. These coregulators can then either recruit histone acetyltransferases (HATs) or deacetylases (HDACs) to modify the chromatin to regulate gene transcription (Figure 3). In some cases, these coregulators actually possess either HAT or HDAC activity⁵⁶.

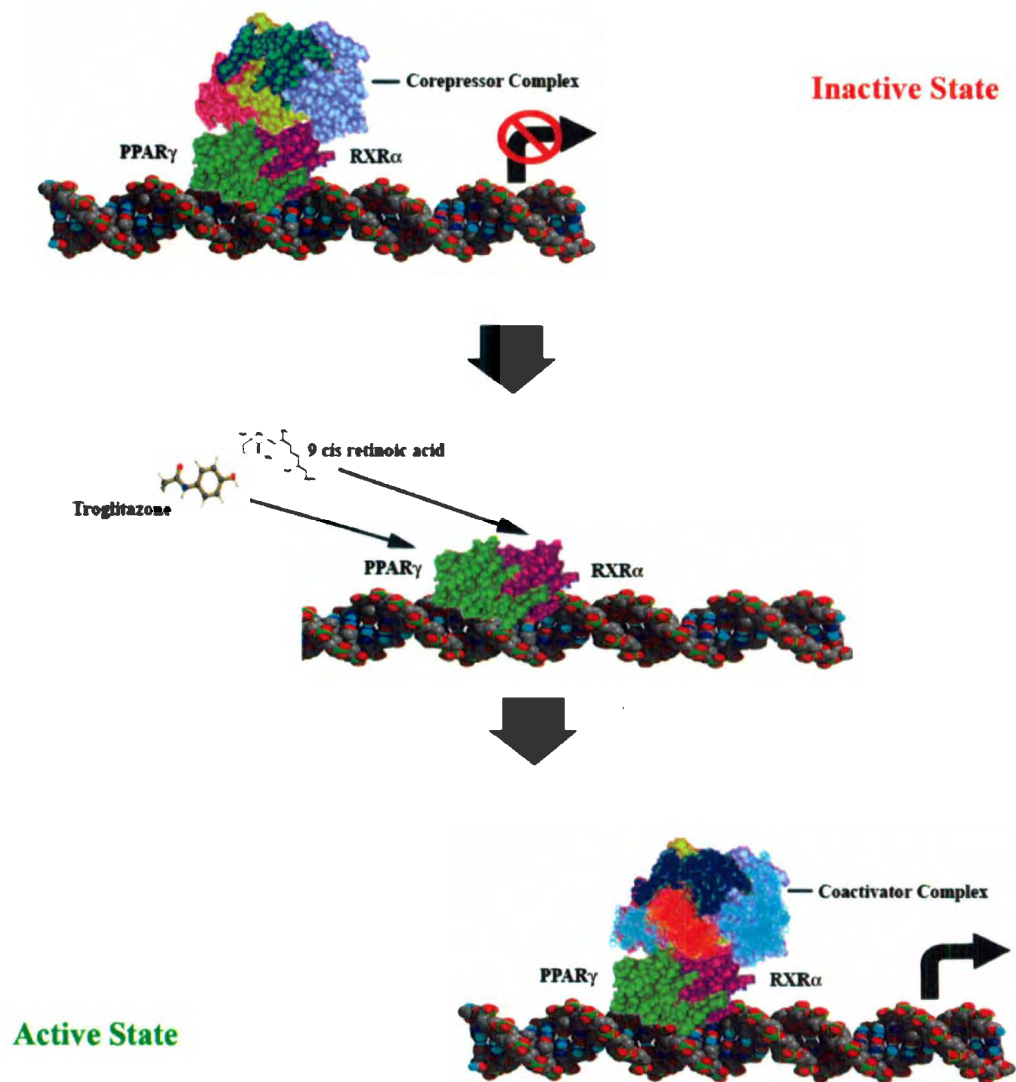


Figure 3: Model for PPAR ligand binding and activation of transcription

PPAR γ forms a complex with retinoid X receptor, and until bound by ligands are inactive and interact with a variety of corepressors containing histone deacetylase (HDAC) activity. When ligands for either PPAR (e.g. troglitazone) or retinoid X receptor (e.g. 9-cis retinoic acid) are present, the heterodimer releases the corepressors complex and recruits coactivators. These coactivators may have histone acetyltransferase (HAT) activity, or recruit HATs to unwind the DNA and allow for efficient transcription of target genes.

1.3.4 Adipogenesis

Until recently, adipose tissue was disregarded as nothing more than a storage depot for excess energy for the body. However in recent years it has achieved a more exciting role, as a *bona-fide* endocrine organ⁵⁷. The adipocytes that make up the adipose tissue are highly specialized cells that respond to environmental stimuli by secreting some of the major bio-regulatory hormones of the body, collectively referred to as adipokines⁵⁸. Over 50 adipokines have been described, as of 2008. Some of the major hormones secreted by this endocrine organ include leptin, adiponectin and resistin. White adipose tissue (WAT), in concert with the pancreas and the liver, plays a central role in the regulation of energy homeostasis. The dysregulation of either of these endocrine organs results in a variety of afflictions including diabetes, hypertension and dyslipidemia⁵⁹.

There are two types of adipose tissue, white adipose tissue (WAT) and brown adipose tissue (BAT) that function to regulate metabolic processes in the body. WAT functions to store energy in the form of triacylglycerol, and can release this stored energy upon stimuli from external sources⁶⁰. BAT, however, dissipates energy in the form of heat to maintain body temperature (thermoregulation)⁶¹. More specifically, the BAT phenotype is characterized by a large number of mitochondria that express uncoupling protein 1 (UCP-1). UCP-1 functions to “uncouple” the electron transport chain from energy production, essentially leading to the production of heat⁶². Human adipose tissue is mainly WAT, with some BAT found mainly in newborns. Recently, it has been

discovered that BAT is found in adult humans, and functions much the same as it does in rodents (who possess large amounts of BAT). The main depots in adult humans are in the supraclavicular and the neck regions, with lesser amounts in the paravertebral, mediastinal, para-aortic, and suprarenal areas⁶³. This BAT could be a target for metabolic disease treatments.

In the case of WAT, adipogenesis occurs when undifferentiated, fibroblast-like pre-adipocytes are differentiated into mature adipocytes⁶⁴. This process occurs via a complex cascade of transcriptional events that leads to the upregulation of PPAR γ along with a few other key adipogenesis factors including CCAAT/enhancer-binding proteins (C/EBPs) and adipocyte determination and differentiation dependent factor 1/sterol response element-binding protein 1c (ADD1/SREBP1c)⁶⁵. This process of adipogenesis is the main biological system used in this particular study; the 3T3-L1 fibroblast model is described here.

1.3.5 3T3-L1 Model System for Adipogenesis

3T3-L1 cells are a continuous strain of the common mouse embryonic fibroblast 3T3 cells, which have been developed through clonal isolation⁶⁶. Since these cells differentiate into mature adipocytes following confluency and treatment with specific drugs (Dexamethasone, 3-isobutyl-1-methylxanthine [IBMX], Insulin), they provide a well-established model for studying adipogenesis⁶⁷.

PPAR γ and the CCAAT/enhancer binding proteins (C/EBPs) are the major regulators of adipogenesis and the formation of white adipose tissue⁶⁸. Stimulation of adipogenesis involves initiation via dexamethasone, IBMX, fetal bovine serum (FBS) and insulin. Specifically, the IBMX stimulates C/EBP β while the dexamethasone stimulates C/EBP δ ⁶⁹. The IBMX is an inhibitor of cAMP and cGMP phosphodiesterases – the turnover of cAMP in the cell is essential for C/EBP β response to particular transcription factors⁷⁰.

These C/EBP proteins begin to accumulate in the cells within 1-4 h of adipogenesis induction, but do not become active until hyperphosphorylated by a cyclin/cdk complex. This cyclin D3 is increased during differentiation of 3T3-L1 adipocytes, which then forms a complex with Cdk2⁷¹. Once activated, C/EBP proteins can bind to the *ppar γ* promoter at consensus C/EBP binding sites and aid in the initiation of transcription⁷².

The primary cocktail of IBMX, Dex, and FBS applied to 3T3-L1 pre-adipocytes causes the upregulation of C/EBP β and C/EBP δ . These proteins then stimulate the expression of PPAR γ while at the same time activating a cascade leading to the synthesis of PPAR γ ligands⁶⁸. Activated PPAR γ subsequently binds to the hormone response element for PPAR, PPRE, of adipogenic target genes that include, for example, adiponectin, leptin, fatty acid binding protein, and lipoprotein lipase^{73,74}.

A number of chromatin-modifying proteins have been shown to be involved in the process of adipogenesis. Since MIER1 interacts with chromatin-modifying proteins,

and adipogenesis regulation involves chromatin modification, a brief review of these epigenetic regulatory mechanisms is required (Figure 4).

C/EBP β is a transcription factor that until phosphorylated is unproductively bound to the *ppar γ 2* and *cebpa* promoters. When the cell enters quiescence at approximately Day 2 of differentiation, the SWI/SNF chromatin remodeling complex is recruited which allows for transcription of PPAR γ . C/EBP β also stimulates C/EBP α transcription which in turn activates its target genes by interacting with a SWI/SNF complex. More important is the epigenetic regulation of PPAR γ activity from this point forward, since it is the only factor described to date that is both necessary and sufficient to promote adipogenesis⁷⁵.

In the undifferentiated cell, PPAR is bound to the promoter of target genes in a repressive complex, which includes retinoblastoma (Rb) and HDAC3. Phosphorylation of Rb allows for the dissociation of this complex, while ligands for PPAR (*ie.* troglitazone) stimulate PPAR to recruit coactivators like CBP/p300. At the level of the cell cycle, PPAR is also regulated by Cyclin D3-CDK6. This kinase phosphorylates PPAR at the A/B domain, causing increased transcription of the adipogenic target genes⁷⁶.

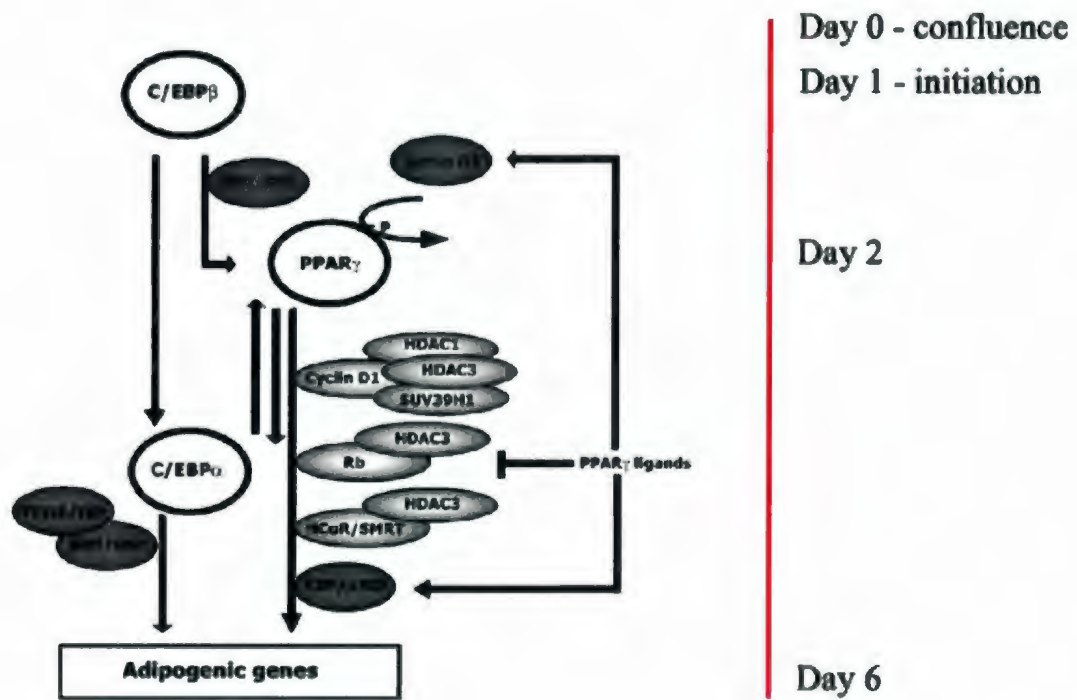


Figure 4: Epigenetic regulation of the effects of C/EBP and PPAR on adipogenesis

After initiation of adipogenic program, C/EBP β becomes phosphorylated and upregulates C/EBP α on Day 2 of adipogenesis. C/EBPs upregulate PPAR γ expression which is regulated in part by the cyclin/cdk complex and phosphorylation of Rb. The PPAR γ ligands allow for the release of corepressor complexes (Rb/HDAC3, CyclinD1/HDAC1/HDAC3/SUV39H1, and NCoR/SMRT) and stimulate PPAR to recruit coactivators (CBP/p300). PPAR γ binds to the PPARE of target adipogenic genes (adiponectin, leptin, fatty acid binding protein, lipoprotein lipase, etc), which continue to accumulate in the cytoplasm of differentiating 3T3-L1 cells after Day 6. Retrieved from (Musri *et al.*, 2007)⁴⁴ with modifications.

1.3.6 PPAR γ and Type 2 Diabetes

Type 2 Diabetes is a metabolic disorder that results in hyperglycemia (abnormally high blood sugar levels). This is most often the direct result of low levels of circulating insulin or an increased resistance to the effects of insulin in various tissues with no compensatory production. There are three subtypes of *diabetes*; type 1, type 2, and gestational diabetes (during pregnancy). All three forms are associated with a reduction in β -cell function in the Islets of Langerhans in the pancreas. Type 1 is the result of an autoimmune attack on the β -cells, while Type 2 relies on higher than normal insulin resistance in potential insulin-responsive tissues. More specifically, this is resistance to insulin-stimulated glucose uptake⁷⁸. In the case of Type 2 diabetes, development of this affliction involves some loss of β -cell function, in addition to the insulin resistance mentioned above. The role of adipose tissue in Type 2 diabetes has also been widely studied⁷⁹. Gestational diabetes occurs when pregnancy hormones affect the individual's insulin sensitivity – usually there is a genetic predisposition⁸⁰.

In 1995, PPAR γ was identified as the receptor responsible for the insulin-sensitizing effects of the thiazolidinedione (TZD) class of drugs⁸¹. However, the exact mechanism by which the TZDs increase insulin sensitivity is unknown. A few hypotheses have been proposed. The first hypothesis is referred to as the “lipid steal” hypothesis⁸², and suggests that TZDs are likely to act on adipose tissue by enhancing its capacity to act as a depot for dietary fatty acids. This keeps the lipids in adipocytes and away from other insulin-sensitive tissues such as skeletal muscle⁸³.

Another way TZDs could enhance insulin sensitivity is through modifying the profile of hormones secreted from adipose tissue. More specifically, TZDs increase adiponectin (one of the adipokines secreted by adipose tissue) gene expression and plasma protein levels⁸⁴. Adiponectin plasma levels also correlate directly with insulin sensitivity, and thus this mechanism could be how TZDs exert their effect. If PPAR γ 2 is regulated in some way by MIER1, it is possible that MIER1 may serve as a potential target for Type 2 diabetes treatment.

1.4 Purpose of this Study and Objectives

Since MIER1 α has been shown to interact with nuclear hormone receptors ER α / β ⁸⁵, RXR α ⁸⁶ and RAR α / β / γ ⁸⁶, it is possible that it also interacts with the PPAR isoforms since they share a very similar domain structure. There has also been evidence that MIER1 α plays a role in the regulation of ER α activated transcription (unpublished data). **Given the above information, the purpose of this study was to determine if MIER1 α interacts with PPAR γ both *in vitro* and *in vivo* and whether or not this interaction affects the regulation of transcription of PPAR γ target genes. Since PPAR γ is the master regulator for adipocyte differentiation, the role of MIER1 in this process was investigated.**

Objective 1: *Determination of a possible interaction between MIER1 and the PPAR isoforms*

GST pulldown assays were completed with GST-MIER1 α or GST-MIER1 β and *in vitro* translated ^{35}S -labeled PPAR γ to determine the possibility of an interaction between PPAR γ and MIER1.

Objective 2: *Identification of the region of MIER1 responsible for interaction with the PPAR isoforms (PPAR γ and PPAR β/δ)*

To further characterize the interaction between PPAR γ and MIER1, GST-MIER1 deletion constructs were used to determine the region of MIER1 responsible for the interaction.

Objective 3: *Characterization of the *in vivo* interaction between MIER1 and the PPAR isoforms*

A human embryonic kidney cell line (HEK-293) was transfected with MIER1 α or MIER1 β and PPAR, and coimmunoprecipitations were conducted in order to determine whether MIER1 interacts with PPAR γ and PPAR β/δ *in vivo*.

Objective 4: *Characterization of the role of MIER1 in PPRE-dependent transcription*

MIER1 has been shown to act as a potent transcriptional regulator via the use of both the ELM2 and SANT domains for recruitment of transcription factors and histone modifiers. For example, MIER1 has been shown to regulate ERE-driven transcription⁸⁷ and has the ability to recruit HDAC1 through the ELM2 domain. As well, since MIER1 contains a SANT domain common to many coregulators, it may regulate PPAR-dependent transcription.

Objective 5: *Determination of the role of MIER1 in Adipogenesis*

Since PPAR is a master regulator of adipogenesis, and if MIER1 regulates PPAR, it may play a vital role in the differentiation process. We examined the mRNA levels of MIER1 by RT-PCR and protein expression using immunocytochemistry (ICC) over the time course of adipocyte differentiation. Immunocytochemical analysis of differentiated 3T3-L1 cells was performed to determine if MIER1 was being expressed specifically in the cells forming lipid droplets. Furthermore, confocal microscopy was used to determine if colocalization of MIER1 α and PPAR γ occurred in adipocytes.

CHAPTER 2 - Materials and Methods

2.1 Plasmids

A. pcDNAflag *ppary2*, pSVsport *ppary2*, pBABEpuro *pparβ/δ*

These plasmids were purchased from Addgene. Both pSVsport *ppary2* (Spiegelman, B.) and pBABE puro *pparβ/δ* (Spiegelman, B.) were used to transfect HEK-293 cells for immunoprecipitation.

B. CS3+MT, CS3+MT-*mier1 α/β*

CS3+MT is a myc-tagged vector and was a gift from Drs. David Turner and Ralph Rupp (University of Michigan). *Hmier1α* and β were cloned into this vector by Corinne Mercer.

C. GST-*mier1 α/β*

Deletion constructs of MIER1 α and β were cloned by Zhihu Ding into the pGEX vectors (containing a GST-tag for GST-pulldown assays) (Amersham).

D. pGL3-Basic

This plasmid (Promega) lacks the eukaryotic promoter and enhancer sequences required for transcriptional activation and it is used as a control for background luciferase activity.

E. pPPRE-X3-TK-luc

This plasmid was purchased from Addgene (Spiegelman, B.). This plasmid contains three PPAR response elements (PPREs) upstream of the luciferase reporter gene.

F. pSV- β Gal

This plasmid was purchased from Promega (Hall, 1983). It encodes the bacterial β -galactosidase enzyme under control of the constitutive Rous Sarcoma virus promoter and it is used as a way to normalize for transfection efficiency. The β -galactosidase (β -gal) assay measures the ability of β -galactosidase to convert o-nitrophenyl- β -D-galactopyranoside to O-nitrophenol (which can be measured at 415nm with a spectrophotometer).

2.2 In vitro Transcription-Translation (TnT)

In order to produce proteins for use in GST pull down assays, coupled transcription-translation reactions were performed using a TnT kit (Promega) as per protocol obtained from the manufacturer. Briefly, plasmid DNA is incubated with rabbit reticulolysate and the required amino acids. In order to make radiolabeled protein, amino acids deficient in methionine are added instead of all the amino acids. To this particular reaction, [³⁵S]-methionine is added for incorporation into the protein. To make both radiolabeled and non-radiolabeled protein at the same time, a mastermix was first prepared in 1.7ml centrifuge tubes and separated prior to the addition of [³⁵S]-methionine. The following reaction components were added in order, with a quick vortex between each reagent: 75 µl rabbit reticulolysate, 6 µl TnT reaction buffer, 3 µl amino acids minus methionine, 57 µl DEPC water, 3 µl of ribonuclease inhibitor (RNA Guard; Amersham Biosciences) and 6 µl T7 polymerase. From this mastermix, 44 µl was put in a 1.7 ml tube for the non-radiolabeled TnT production. The following was then added to the non-radiolabeled tube: 1.5 µl amino acids minus methionine, 2.5 µl amino acids minus leucine and 1 µl of plasmid DNA. 10 µl of [³⁵S] methionine was added to the remaining mastermix. From the mastermix, 49 µl were put in another 1.7 ml tube for the radiolabeled protein production, and 1 µl of plasmid DNA was added. In place of plasmid DNA, 1 µl of DEPC water was added to the negative control TnT. All three reactions were incubated at 30°C for 90 min.

In order to determine the efficiency of the reaction, TCA (trichloroacetic acid) precipitation assays were conducted. In this case, 2 μ l of the TnT product was incubated with 98 μ l of a 1N NaOH/2% H_2O_2 solution at 37 °C for 10 min. Subsequently, 900 μ l of 25% TCA/2% casamino acids (Merck) was added to each reaction and they were incubated on ice for 30 min. These are amino acids hydrolyzed from casein. The resultant precipitate was collected via filtration onto filter paper and dissolved in Biodegradable counting scintillant (Amersham) and counted in a liquid scintillation counter (Beckman LS 3801).

2.3 GST Pulldown Assay

2.3.1 Glutathione Sepharose 4B Beads

Glutathione Sepharose 4B beads (GE-Biosciences) were prepared according to manufacturers instructions. After gentle mixing of original 75% slurry of beads, 1.33 ml was dispensed into a 15 ml falcon tube. This solution was centrifuged at 500 x g for 5 min. The supernatant was aspirated off and the beads were washed with 10 ml of cold PBS. Again, the solution was centrifuged at 500 x g for 5 min and the supernatant removed by aspiration. The beads were then resuspended in 1 ml of 1 x PBS containing 0.2% azide to produce a 50% slurry of beads that were stored at 4 °C.

2.3.2 GST-fusion protein production

Glycerol stocks of transformed BL21 cells were streaked onto an ampicillin plate and left to grow at 37 °C overnight. The next morning, this plate was removed from heat and placed at 4 °C until the afternoon. At this time, a single colony was used to inoculate a 5 ml culture of luria broth (LB) medium [10 g peptone, 5 g yeast, 10 g NaCl, 1 L dH₂O, autoclaved] plus ampicillin (50µg/ml). This was left at 37 °C overnight, shaking. The next morning, 250ml of LB + ampicillin was inoculated with 1 ml of the overnight culture. This was grown up for approximately 4 h, at which point the optical density (OD) at 595 nm was verified to be between 0.6 and 0.8 using a spectrophotometer. Next, 25 µl of 1M IPTG (isopropyl-β-D-thiogalactopyranoside) was added to induce the production of protein and this culture was left shaking at 37 °C for another 3 h. The culture was then transferred aseptically into a 250 ml Nalgene bottle and centrifuged at 4000 rpm at 4 °C for 10 min. Supernatant was removed and pellet was resuspended in 5 ml ice-cold 1 x PBS. The suspension was transferred to a 50 ml falcon tube, and 50 µl of the protease inhibitor 0.2 M PMSF (phenylmethylsulphonyl fluoride) was added. The sample was then placed on ice and sonicated for 2 min with 30 sec bursts, after which the sample was transferred to a 30 ml Corex tube. To the sonicated sample, 500 µl of 10% TritonX-100 in 1 x PBS was added and the sample was centrifuged at 10,000 rpm at 4 °C for 15 min. The supernatant was transferred into 1.7 ml tubes in 1 ml aliquots and stored at -70 °C. The concentration of these fusion proteins was determined by SDS-PAGE (sodium dodecyl sulfate – polyacrylamide gel electrophoresis).

2.3.3 Isolation and detection of GST-fused proteins

50 μ l of a 50% slurry of Glutathione Sepharose 4B beads was dispensed into clean 1.7 ml tubes. The beads were washed twice with 1 ml of 1 x PBS. Briefly, 1 ml of 1 x PBS was added to beads, vortexed lightly and centrifuged for 1.5 min at 5,000 x g to pull the beads to the bottom of the tube. The supernatant was aspirated off by vacuum. After washing, 250 μ l of soluble GST-fused protein was added to each tube with beads. To bring the total volume to 1 ml, 700 μ l of 1 x PBS + PI (protease inhibitors) was added to the sample and rotated at 4 °C for 1 hour. After incubation, the beads were washed x 5 with 1 x PBS + 0.2% NP-40 (Igepal; Sigma). To the washed beads, 30 μ l of 2 x SSB (Sodium dodecyl sulfate [SDS] Sample Buffer) was added and the samples were vortexed lightly then boiled for 3 min to denature the proteins. The samples were allowed to cool on ice for 2 min before centrifugation at 5000 x g for 3 min to bring the beads to the bottom of the tube. These supernatants were then run on an 8% SDS-PAGE gel and stained with Coomassie Blue Stain (Coomassie Blue; Biorad) for 1 hour. The gel was then destained overnight in 1 L of destain (740ml dH₂O, 200 ml methanol, 60 ml glacial acetic acid) and dried under vacuum for 90 min.

2.3.4 GST pull down assay

GST pulldown assays were used in order to determine if the proteins in question, that is, PPAR γ and MIER1, interact *in vitro*. PPAR γ and ER α were labeled with [35 S]-methionine incorporation via the transcription/translation reactions described previously. Prior to the start of the GST pull down, GST pull down buffer was prepared as follows. A 300 ml solution was made (0.4 mM Tris, pH 7.5, 150 mM NaCl, 1 mM EDTA and 10% glycerol). This stock was frozen at -20°C until use. On the day of use, an aliquot was made up to 0.5% Bovine serum albumin (BSA) from powder and 0.2% NP40. Another aliquot was made up to 0.2% NP40 and 1 x PI (protease inhibitors).

For each reaction in the GST pull down, 50 μ l of a 50% slurry of Glutathione-sepharose beads were washed twice with 500 μ l of GST pull down buffer + BSA + NP40. Briefly, buffer was added and tubes were vortexed lightly then centrifuged at 5000 x g for 1.5 min to pull the beads to the bottom and allow aspiration of the buffer by vacuum. Subsequently, beads were resuspended in 500 μ l of GST pull down buffer + BSA + NP40 + PI. The beads were then rotated for 1 h at 4°C with the GST-fused MIER1 proteins as indicated in the corresponding figures.

After incubation, beads were washed seven times with 1 ml of GST pull down buffer (-) BSA (+) NP40. Beads were then resuspended in 1 ml GST pull down buffer (+) BSA (+) NP40 (+) PI along with [35 S]-methionine labeled PPAR γ or ER α TnTs (100,000 cpm) and rotated another 2 h at 4°C. Beads were subsequently washed x 4 with 1 ml of GST pull down buffer (-) BSA (+) NP40, x 4 with 1 ml of GST pull down buffer

(-) BSA (-) NP40 and an additional x 2 with 1 ml of 150 mM NaCl. The last wash was aspirated off completely and the beads were resuspended in 30 μ l of 2 x SSB (SDS sample buffer [0.125 M Tris HCl, 2% SDS, 5% β -mercaptoethanol, 20% glycerol]) + bromophenol blue (dye). The samples were boiled for 3 min, centrifuged to collect the beads at the bottom of the tube, and the supernatant was loaded on an 8% SDS-polyacrylamide gel. Samples were subsequently analyzed using autoradiography. PPAR γ and ER α input lanes (total PPAR or ER transfected into cells) were loaded with 1/20th of the volume used in each reaction.

2.4 Cell culture

Cell culture was performed in order to determine if PPARs and MIER1 interact *in vivo*. Here, human embryonic kidney cells (HEK-293) were cultured in Dulbecco's Modified Eagle Medium (Gibco) supplemented with 10% serum [25% fetal bovine serum (FBS) and 75% calf serum (CS)], 1% Na-pyruvate and 0.5% penicillin/streptomycin. Also, a substrain of mouse embryonic fibroblasts (3T3-L1) that undergo a pre-adipocyte to adipocytes conversion after stimulation were obtained from the American Type Culture Collection (ATCC) and grown up at 37 °C in 5% CO₂ in DMEM containing 10% calf serum. These 3T3-L1 cells were subcultured every 3 days by first aspirating media from the 100 mm culture vessel. Next, cells were washed with 10 ml of 1 x PBS and this was aspirated and replaced with 1.5 ml of a 1% trypsin/EDTA/PBS solution. The culture vessel was swirled lightly to promote detachment of cells, and these were resuspended in

8.5 ml of media. 1 ml of this resuspension was added to a new 100 mm culture vessel already containing 9 ml of media for an ~ 1:10 subcultivation ratio. Both HEK-293 cells and 3T3-L1 cells were grown at 37°C and 5% CO₂.

To initiate differentiation of 3T3-L1 cells, DMEM containing 10% fetal bovine serum (FBS), 0.5% penicillin/streptomycin (Pen/Strep), and 1% Na-pyruvate was supplemented with 0.5 mM isobutyl-methylxanthine (IBMX) and 1 μM Dexamethasone (Dex) purchased as a component of the Adipogenesis Assay Kit (Chemicon, ECM950).

2.5 Transfections: HEK-293 cells

Cells were seeded into 6-well plates at a density of 5×10^5 cells/well 24 h prior to transfection. All transfections were performed in triplicate in 6-well plates with 6 μl Lipofectamine and 6 μl of PLUS reagent per well, according to manufacturer's instructions (Life Technologies Inc.) along with indicated amounts of DNA. Complexes were left on cells for 4 h, and then the medium containing Lipofectamine and PLUS was aspirated from the cells and replaced with 2 ml of supplemented DMEM. Cells were allowed to grow for an additional 24 h, at which point a potent and specific ligand for PPAR γ , 20 μM Troglitazone (Sigma), was added to the cells in DMEM. This troglitazone was purchased from Sigma in powder form, and was dissolved in DMSO to a final stock concentration of 11.3 mM and stored at -20°C. Alternatively, vehicle alone (dimethylsulfoxide, DMSO) was dissolved in DMEM and added to the cells. The final

concentration of DMSO administered to cells did not exceed 0.1% DMSO in DMEM. 24 h later the cells were harvested according to protocols designed for each type of subsequent experiment (ie: luciferase assay, western blot, immunoprecipitation).

For *in vivo* **immunoprecipitation (IP)** assays, HEK-293 cells were transfected (per well) with 0.5 μ g each of pSVsport PPAR γ 2, and pCS3+MT-*MIER1* α or pCS3+MT (empty vector). 48 h post transfection, cells were lysed as follows. Each well was washed x 2 with 1ml of 1 x PBS. For each condition, two of the three wells were extracted with 1ml of 1 x Triton solution diluted from a 10 x stock (0.1 M Tris pH 7.5, 0.1 M EDTA, 0.2% sodium-azide, 10% Triton X-100 in dH₂O). Immediately prior to immunoprecipitation, 100 μ l of 100 x PI was added to the 1 x Triton lysis solution. The third well was extracted in 500 μ l of 2 x SSB. Once solutions were added to the cells, they were scraped gently with cell lifters (Fisher Scientific) and incubated on ice for 20 min. Subsequently, lysate was pulled through a 1ml syringe x 20 in order to shear the DNA. The lysate was transferred to labeled, chilled 1.7 ml tubes. The cellular debris was removed by centrifugation at 12,000 x g for 10 min at 4 °C. The supernatant was transferred to another chilled 1.7 ml tube. For immunoprecipitation, 1.5 μ g (7.5 μ l) of PPAR γ antibody (Santa Cruz, H-100) was added to 1 ml of cell lysate and rotated at 4 °C overnight.

After the overnight incubation, 50 μ l of a 50% slurry of Protein G beads (Amersham) was added to the samples and they were left to rotate at 4 °C for 1 h. After rotation, beads were washed three times with the 1 x Triton solution (with 1 x PI), and twice with 150 mM NaCl. After each wash, beads were centrifuged at 500 x g for 1 min

to pellet the beads. The beads were then resuspended in 30 μ l of 2 x SSB plus bromophenol blue dye and boiled for 3 min. The beads were then centrifuged again (as described above) and the resulting supernatant was loaded on an 8% SDS-PAGE gel. Gels were run for approximately 1.5 h at 30 mA in order to separate out the component proteins and molecular weight markers. Once the gels were run, they were washed for a total of 15 min in a total of 1 L of 1 x Transfer buffer [200ml 5 X stock (60.54g Tris, 288.4 g glycine, and 3L dH₂O), 200 ml of 100% methanol, and 600 ml dH₂O] with frequent washes to remove as much SDS as possible. The separated proteins were then transferred for 2 h at 60 V onto a Hybond-ECL nitrocellulose membrane (Amersham) as described previously⁸⁸. Subsequently, the membrane was blocked in 5% skim milk powder/1 x TBS-T [20 mM Tris pH 7.6, 150 mM NaCl, 0.1% Tween-20, and dH₂O] at room temperature for 1 h. Western blot analysis was performed with a 1:1000 dilution of mouse monoclonal anti-myc (Day 7, obtained from 9E10 cells) antibody⁸⁹ in 5% skim milk, shaking overnight at 4°C. Subsequent to overnight agitation, membranes were washed for 1 h with a total of 1 L of 1 x TBS-T, then agitated with a 1:3000 dilution of sheep anti-mouse conjugated to horseradish peroxidase (HRP) secondary antibody (Amersham) in 5% skim milk powder/1 x TBS-T for 1 h. Lastly, the membranes were washed for another 1 h at room temperature with frequent washes for a total of 1 L 1 x TBS-T, then analyzed with ECL Western Blotting System and visualized on Hyperfilm ECL (Amersham).

2.6 Reporter Assay

2.6.1 PPRE-Luciferase Assay

HEK-293 cells were seeded at a density of 5×10^5 cells/well in 6-well dishes 24 h prior to transfection. Transfections were performed as described in Section 2.5 with 0.5 μ g of PPRE-X3-TKLuc (PPAR γ response element with luciferase), 0.5 μ g of PPAR γ 2 and combinations of *myc-mier1 α* , *myc-mier1 β* and/or *pgcl- α* (known PPAR γ coactivator). 24 h post-transfection, cells were treated with 20 μ M troglitazone (PPAR γ ligand) or vehicle alone (DMSO) for another 24 h. Subsequently, cells were lysed in 1 x cell lysis buffer (provided in Luciferase Assay Kit, Promega). Cell lysate was then transferred into 1.7 ml tubes and spun at 12,000 rpm for 10 sec at room temperature. The supernatant was then transferred to a clean 1.7 ml tube and stored at -70 °C until use. On the day of luciferase readings, cell lysate was kept on ice and the luciferase assay substrate, luciferin (Promega), was brought to room temperature in a covered water bath for a minimum of 30 min. Luciferase activity was then read in a Monolight 2010 Luminometer (Analytical Luminescence Laboratory) by mixing 10 μ l of cell lysate with 50 μ l of luciferase assay substrate. All readings were normalized to transfection efficiency using the β -galactosidase assay described here. For example, the relative luciferase units were divided by the β -galactosidase reading for each sample.

2.6.2 β -Galactosidase Assay

HEK-293 cells were transfected as previously described with the plasmids given above, along with 0.2 μg of pCMV- βgal . 10 μl of the extracted protein in cell lysis buffer was then added to 1.7 ml tubes, and incubated with 200 μl β -gal buffer [100% Z-buffer (16.1g/L $\text{Na}_2\text{HPO}_4 \cdot 7\text{H}_2\text{O}$, 5.5 g/L $\text{NaH}_2\text{PO}_4 \cdot \text{H}_2\text{O}$, 0.75 g/L KCl, 0.246 g/L $\text{MgSO}_4 \cdot 7\text{H}_2\text{O}$), 4g/L ONPG (o-nitrophenyl- β -D-galactopyranoside), and 0.27% β -mercaptoethanol) at 37 $^\circ\text{C}$ for 3 min (until a yellow color developed). The reaction was halted by adding 200 μl of 1 M Tris, pH 11.0 and the absorbance was read in a plate reader at 415 nm.

2.7 Adipogenesis Assay

A substrain of mouse embryonic fibroblast 3T3 cells referred to as 3T3-L1s (ATCC) were initiated to differentiate into fully formed adipocytes in this assay. First of all, the 3T3-L1s were seeded at a density of 6×10^4 cells/well in a 24-well plate, with each condition done in triplicate. There were a total of nine sets of three, seeded into three separate 24-well plates in order to facilitate extraction with minimal exposure to possible contaminants. These cells were cultured in regular 3T3-L1 propagation media (DMEM containing 10% calf serum, 1% sodium pyruvate [NaPyr] and 0.5% penicillin/streptomycin). The next day was set as Day 0, and on this day the first set of

triplicates was trypsinized and pelleted for storage at -80°C until all of the cells had been collected.

To trypsinize these cells, the media was aspirated from each well and the cells were washed with 1 ml of 1 x PBS. Subsequently, 400 μl of a solution of 1 x PBS + EDTA + 1 % trypsin was added to each well, and the plate was rocked gently to facilitate the detachment of cells from the bottom of the well. To this solution of trypsin and detached cells, 600 μl of 3T3-L1 propagation media was added and the solution was pipetted up and down over the bottom of the well. The cells were then transferred to a 1.7 ml tube, and centrifuged at room temperature in a table-top microcentrifuge at 5,000 rpm for 5 min. The trypsin solution was then aspirated off and the pellet was washed in 1 x PBS, centrifuged again at 5,000 rpm for 5 min, and stored at -80°C until further use.

On Day One, all of the remaining 3T3-L1s that were seeded into 24-well plates were initiated to undergo differentiation using the 3T3-L1 maintenance media (described in Section 2.4) that was also supplemented with a final concentration in media of 1 μM dexamethasone and 0.5 mM isobutyl-methylxanthine. These cells were left overnight and on Day Two, the second set of triplicate wells of 3T3-L1s were trypsinized, centrifuged and stored for further use. On Day Three, all of the cells were treated with 3T3-L1 maintenance media supplemented with a final concentration of 10 $\mu\text{g/ml}$ insulin. Two days later, media was replaced with 3T3-L1 maintenance media and this was repeated every two days until all the cells had been collected. Cells were trypsinized and pelleted for storage every other day.

2.7.1 RNA Extraction

The RNA (ribonucleic acid) was extracted from the collected 3T3-L1 cells using procedures described in the Qiagen RNeasy Mini Kit (Qiagen, Mississauga, Canada). Pelleted 3T3-L1 cells were obtained from cryogenic storage, and 350 μ l of Buffer RLT (Qiagen) was added to each sample. The lysate was then pulled through a 1 ml insulin syringe x 10 in order to shear the cells. Next, 350 μ l of 70% ethanol was added to the homogenized lysate, and this was mixed via pipetting. The sample was then transferred to an RNeasy spin column (Qiagen) attached to a 2 ml collection tube, and centrifuged at 8000 x g for 15 sec. After discarding the flow-through, 700 μ l of Buffer RW1 (Qiagen) was added and again the tubes were centrifuged as noted above. Then 500 μ l of Buffer RPE was used to wash the spin column membrane, and this too was centrifuged through and discarded. To dry the membrane, the spin column was transferred to a new 2 ml collection tube and centrifuged at full speed for 1 min. Elution of RNA from the column into a new 1.5 ml collection tube was done by adding 30 μ l of RNase-free water to the column and spinning it at 8000 x g for one minute. RNA yield was then determined using a spectrophotometer and measuring the absorbance at both 260 nm and 280 nm. The absorbance at 260 nm is used to give the RNA concentration by using that value in the following calculation:

$$\text{Concentration of RNA } [\mu\text{g}] = 40(\text{extinction coefficient}) \times A_{260} \times \text{dilution factor}$$

The purity of each sample was then determined by calculating the ratio of A_{260}/A_{280} . A number close to 2 gives an indication of relative purity⁹⁰. The concentration of RNA for each sample was required in order to make cDNA from the same amount of total RNA.

2.7.2 Precipitating RNA

One tenth of the volume of 3 M sodium acetate, pH 5.2 was added, along with 2.5 x the volume of 100 % ethanol. This solution was placed at -80°C for 2.5 h, then taken out and centrifuged at 4°C for 20 min to pellet the RNA. The pellet was then washed with 70 % ethanol, vortexed, and centrifuged again at 4°C for 20 min. The ethanol was then carefully decanted and the pellet was left to air dry on a paper towel, before being resuspended in an appropriate volume of DEPC water for further use.

2.7.3 Reverse-transcriptase PCR (RT-PCR)

For each sample and negative control, 1 μg of total RNA was diluted in 10 μl using DEPC water. These samples were then incubated at 65°C in a PCR thermocycler for 10 min, and then transferred directly to ice. To the sample tubes, 12 μl of the mastermix solution listed below was added. To each of the negative control tubes, 12 μl of the mastermix solution was added, along with 10 μl of dH_2O .

Table 2: Mastermix for Reverse Transcription

Reagent	Amount/tube (μ l)	Number of Tubes (1.1X)
5 X First Strand Buffer	4	79.2
100 ng/ μ l Random Primers	2	39.6
100 mM DTT (dithiothreitol)	2	39.6
10mM total dNTPs (nucleotide triphosphates)	2	39.6
MMLV-RT (Moloney Murine Leukemia Virus- Reverse Transcriptase)	1	19.8
RNA Guard	1	19.8
H ₂ O	Only in negative control.	

The sample tubes containing the mastermix were then incubated at 37 °C for 75 min and then the enzymes were heat inactivated at 95 °C for 15 min. The resulting cDNA was then used in PCR reactions with primers for the specific genes of interest. In this case, primers were designed against *ppar γ 2*, human β -actin (*hbc*), and *mier1*.

Table 3: Primers for PCR

Gene of Interest	Nucleotide Sequence	Size of Amplicon
<i>mier1</i> forward	CAA GGG CTG AAG GCC TAT GG	150 bp
<i>mier1</i> reverse	CCA AAT CGT GTT TGC TGA GC	
<i>pparγ2</i> forward	CAA GAA TAC CAA AGT GCG ATC AA	68 bp
<i>pparγ2</i> reverse	GAG CTG GGT CTT TTC AGA ATA ATA AG	
<i>h-bac</i> forward	ATC TGG CAC CAC ACC TTC TAC AAT GAG CTG CG	150 bp
<i>h-bac</i> reverse	ATC GCT GGG GTG TTG AAG GTC TC	

Both *ppar γ 2* and *mier1* primers were used in the following PCR cycles using 2 μ l of cDNA from each sample. Each sample reaction included 0.1 μ l Taq DNA polymerase, 2 μ l of 10 mM dNTPs (nucleotide triphosphates), 1 μ l of MgCl₂ (magnesium chloride), 2.5 μ l of 10 X PCR reaction buffer and 1 μ l of each primer diluted to 200 ng/ μ l. H₂O was added to a final volume of 25 μ l.

Table 4: PCR program

Temperature (°C)	Time (seconds)	No. of Cycles
94	240	1
60	30	
72	60	26
94	30	
60	30	
72	300	1
30	1	

The samples were run on a 100 ml, 1.6% agarose gel and visualized with ethidium bromide (EtBr). For *β-actin*, mRNA levels are high so only 20 cycles (as described in Table 4) were run. This was done to ensure that the PCR reaction was in the linear range.

2.7.4 Western Blot for Adiponectin over course of adipocyte differentiation

3T3-L1 cells were seeded at a density of 6×10^5 cells/well in 60 mm culture dishes and initiated to undergo differentiation as described in Section 2.7. Cells were collected from the 60 mm dishes every second day as follows. 60 mm culture dish was washed x 1 with 3 ml of 1 x PBS. This was aspirated from cells and replaced with 300 μ l of 2 x SSB. Cells were scraped with a cell scraper and incubated on ice for 20 min. The lysate was then transferred to a 1.7 ml tube and the lysate was pulled through a 1 ml syringe x 10. The resulting cell lysate was spun down at 12,000 rpm for 10 min, and supernatant was transferred to a chilled 1.7 ml tube. For samples from Day 2 to Day 14, 10 μ l of dH₂O + bromophenol blue was added to 30 μ l of lysate (to dilute out the 2 x SSB) and all 40 μ l were loaded on an 8% polyacrylamide gel. For β -actin, 15 μ l of each sample was diluted in 10 μ l of dH₂O + bromophenol blue and all 25 μ l were loaded on the gel. The gel was run as described in Section 2.5 under Immunoprecipitation, and transferred for 2 h at 60 V. The membrane was probed using a 1:2000 dilution of anti-adiponectin polyclonal antibody (Abcam, ab3455) for 3 h at room temperature. A 1:2000 dilution of DAR-HRP secondary antibody (Amersham) was used and the results were visualized by ECL detection. For the β -actin blot, a 1:4000 dilution of anti- β -actin monoclonal antibody was added to the membrane for 1 h at room temperature. SAM-HRP was added at a dilution of 1:4000 for 1 h at room temperature.

2.7.5 Oil Red O staining

Lipid droplets form in 3T3-L1 cells as they differentiate into mature adipocytes. In order to determine that the organelle-like structures inside the cells were lipid droplets, cells were stained with Oil Red O. This is a lipophilic dye that stains lipid droplets bright red. Cells were seeded at a density of 4×10^5 per well in 6-well culture dishes and initiated to undergo adipogenesis as described in Section 2.7, except cells were not trypsinized every second day but maintained in maintenance media. On Day 22 of adipogenesis, cells were stained with Oil Red O as per the protocol outlined in the Adipogenesis Assay Kit (Chemicon, ECM950). Briefly, cells were washed x 2 with 1 ml of 1 x PBS. This was aspirated and replaced with 1 ml of Oil Red O solution (0.36% Oil Red O solution in 60% isopropanol) and this was incubated for 15 min at room temperature. Stain solution was then aspirated and wells were washed x 3 using 2 ml of wash solution (Chemicon, 90360) each time. The wash solution was aspirated from the wells and pictures were taken at 8x magnification under the Olympus dissecting microscope. For quantification of lipid content, a dye extraction solution (Chemicon, 90359) could be added to the wells (1 ml in a 6-well culture dish). After agitation for approximately 15-30 min, extracted dye could be removed from the well and placed in a 96-well culture dish for quantification in a plate reader. Optimal absorbance for Oil Red O is 520 nm (Chemicon, Adipogenesis Assay Kit), but it can also be quantified with lower efficiency at 490 nm. A blank well lacking cells was subjected to the same protocol in order to account for nonspecific binding of the Oil Red O to the culture dish.

2.7.6 Immunocytochemistry

In order to determine whether MIER1 was specifically upregulated in differentiating cells, 3T3-L1 cells were first seeded in 8-well chamber slides (BD Biosciences, Falcon) at a density of 1×10^5 cells/well. The next day, cells were confluent and ready to be differentiated according to the methodology described in the Adipogenesis Assay section. On Day 4 or Day 14 of differentiation, culture slides were removed from the incubator and washed in 250 ml of 1 x PBS and subsequently fixed by adding 200 μ l of 4% paraformaldehyde to each well and incubating in a moist container for 30 min. After incubation, cells were washed x 2 in a beaker containing 250 ml of 1 x PBS and then placed in a 250 ml beaker of 0.1% Triton in 1 x PBS for 5 min. The 0.1% Triton/PBS was aspirated from wells, and replaced with 200 μ l of 5% donkey serum Blocking Buffer (Normal Donkey Serum diluted in 1 x PBS). Cells were incubated in this blocking buffer for 1 h, after which point they were washed as described above in a 250 ml beaker of 1 x PBS. After aspirating the excess PBS from each well, primary antibody was added to each well. In this case, anti-MIER1 α antibody⁹¹ or anti-MIER1 β antibody was added at a final dilution of 1:500 in 3% BSA/PBS (Bovine Serum Albumin, RIA Grade) in a final volume of 200 μ l per well. Primary antibody was left on overnight at 4°C, after which point the antibody was aspirated from each well and slides were immersed x 1 in 500 ml of 0.1% Triton/PBS for 5 min. Slides were then washed x 1 with 200 μ l of 1 x PBS per well. After aspirating the excess PBS, 200 μ l of 0.6% hydrogen peroxide (H₂O₂) was added to each well. This was done to inactivate any endogenous

peroxidase from the cells. This was incubated at 4 °C for 30 min. Following this incubation, Donkey-anti-rabbit horseradish-peroxidase (DAR-HRP) antibody was diluted 1:200 in a 3%BSA/PBS solution and 200 µl added to each well. This secondary antibody was incubated for 1 h at 4 °C. After incubation, cells were again washed x 1 with 500 ml of 0.1% Triton/PBS, and then with 200 µl of 1 x PBS for 5 min. Again, excess PBS was aspirated from cells and 3,3'-diaminobenzidine (DAB)(Sigma) was diluted in deionized water (1 pellet Urea H₂O₂, 1 pellet DAB per ml of dH₂O) and added to each well. This catalyzes a reaction between the peroxidase attached to the secondary antibody, producing a brownish chromagen product that can be visualized under a microscope. This reaction was left to proceed for 10 min, after which time the excess DAB was aspirated from cells and the slides were subsequently washed in 1 x PBS and incubated there for 3 min. The excess PBS was aspirated and the gasket was carefully detached from the slide. To each well of the slide, a few drops of 10% glycerol diluted in 1 x PBS was added and a coverslip was placed over the slide. This coverslip was sealed with clear nail polish and left to dry for approximately 20 min. Staining was visualized using an Olympus BH-2 compound microscope and pictures were taken using the CoolSnap camera and software system, at 50x magnification in both brightfield and phase contrast.

2.7.7 Immunofluorescence

To look at possible colocalization of both MIER1 α and PPAR γ in differentiating 3T3-L1 cells, immunocytochemistry was performed using fluorescent-linked secondary antibodies. 3T3-L1 cells were seeded and differentiated as per methodology in the Adipogenesis Assay. On Day 11 of adipogenesis, culture slides were removed from the incubator and washed in 250 ml of 1 x PBS (see ICC) and subsequently fixed by adding increasing amounts of 4% paraformaldehyde to each well. The cells were incubated in paraformaldehyde for 15 min, then washed twice in a 250 ml beaker of 1 x PBS. Slides were then incubated in a 0.1% Triton/PBS solution for 10 min. After this incubation, 200 μ l of 5% donkey blocking buffer (5% donkey serum diluted in 1 x PBS) was added to each well, and this was incubated for 30 min. After the incubation, cells were again washed in 1 x PBS. The excess PBS was aspirated from culture slides and replaced with primary antibodies. In this case, a 1:500 final dilution of anti-MIER1 α antibody (Leo purified polyclonal antibody, Bleed 1) and a 1:100 dilution of PPAR γ monoclonal antibody (E-8, Santa Cruz) were mixed together in 3% BSA/PBS to a final volume of 2 ml. To each well of the culture slide, 200 μ l of this antibody solution was added and left for overnight incubation at 4°C in a container with paper towels soaked in 1 x PBS.

The next day, the primary antibody solution was aspirated from all wells and the culture slide was washed in 0.1% triton/PBS in a 250 ml beaker. The excess solution was aspirated from each well and replaced with 5% donkey blocking buffer for another 15 min incubation. Cells were briefly washed in 1 x PBS and then secondary antibody was prepared and added. For this particular experiment, a 1:200 dilution of both FITC-DAR

(fluorescein isothiocyanate- donkey-anti-rabbit) and CY3-DAM (cyanine3-donkey-anti-mouse) were diluted in 3% BSA/PBS and 200 μ l of this solution was added to each well. Cells were incubated with conjugated antibodies for one hour and covered in tin foil since the fluorescent antibodies are light sensitive. After the 1 h incubation, the antibodies were aspirated from the cells and the culture slides were washed x 1 in 0.1% Triton/PBS in a 250 ml beaker. This was done twice, incubating the slides for 10 min in 0.1% Triton/PBS each time. After the second wash, a 1:5000 dilution of DAPI (4', 6-diamidino-2-phenylindole) which stains DNA was added to each well of the culture slide, and incubated for 10 min. After incubation, this was aspirated from the wells and the slide was washed two times in 1 x PBS. Once these washes were complete, the excess 1 x PBS was aspirated from cells and the gasket was carefully removed. To each well of the slide, a few drops of 10% glycerol diluted in 1 x PBS was added and a coverslip was placed over the slide. This coverslip was sealed with clear nail polish and left to dry for approximately 20 min. Fluorescent staining was visualized by confocal microscopy using an Olympus Fluoview Confocal microscope, and images were analyzed and saved using the associated Fluoview program.

CHAPTER 3- Results

3.1 In Vitro interaction between MIER1 α and MIER1 β with PPAR γ 2

In order to determine whether MIER1 α and/or MIER1 β interact *in vitro* with PPAR γ 2, a set of GST-pulldowns were completed using *in vitro* translated [³⁵S]-labeled PPAR γ 2 and GST-fused MIER1 α and MIER1 β . For this experiment, GST-fused deletion constructs (Figure 5) of MIER1 α were used along with [³⁵S]-labeled PPAR γ 2. As a positive control for these assays, *in vitro* translated [³⁵S]-labeled ER α was used since it has been shown to interact strongly with MIER1⁹².

For each of these GST pulldowns, a constant amount of *in vitro* translated ³⁵S-labeled PPAR γ 2 was used (100,000 cpm). For the MIER1 GST-fusion constructs, equimolar amounts of protein were used in each case. To account for differences in the molecular weights of each of the fusion proteins (mass effect), the amount of protein was adjusted according to the largest molecular weight fusion construct (which was MIER1 β). These relative amounts for each protein are shown on the Coomassie Blue stained polyacrylamide gels immediately under the autoradiography image (Figure 6B and 7B).

These initial GST pulldowns showed that PPAR γ 2 interacts with both the α and β forms of MIER1 (Figure 6A, lanes 4, 5), however it interacts more strongly with MIER1 α (Figure 6A, lane 4). Another set of GST pulldowns were completed to

determine which domains of MIER1 were responsible for the interaction between the two proteins (Figure 6 and 7).

PPAR γ interacts most strongly with $\Delta 19$ of MIER1, which is only the SANT domain (Figure 7, lane 6), and does not interact with $\Delta 11$ which lacks the SANT domain completely (Figure 7, lane 2). These data show that PPAR γ interacts with the SANT domain of MIER1 α . The SANT domain is located in the C-terminus of MIER1, but PPAR γ also interacted weakly with $\Delta 4$ (Figure 6, lane 2) which is the N-terminus of MIER1. This is not background, since the GST protein alone did not bind to PPAR γ . There was an interaction between PPAR $\gamma 2$ and the region of the N-terminus (MIER1 $\Delta 4$, aa 1-283) that did not possess the SANT domain. There may be two binding sites between PPAR γ and MIER1.

The PPAR γ TnT (shown in the input lane of Figure 6A) runs slightly lower than the bands observed from the interaction between MIER1 α and PPAR γ . The ER α input lane also runs slightly lower than the interaction band in the positive control lane. It is unclear why this occurred.

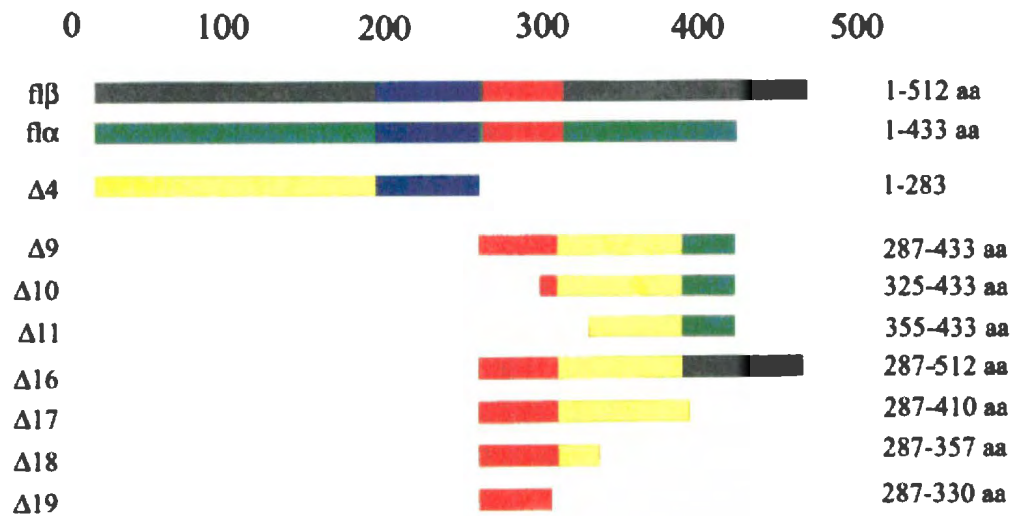


Figure 5: GST-fused deletion constructs of MIER1 α and β

This diagram shows the GST-fused MIER1 α and MIER1 β deletion constructs that were used in the GST pulldowns given in Figure 2 and Figure 3. Blue bar represents the ELM2 domain, red – SANT domain, dark green – C-terminus of MIER1 β , light green – C-terminus of MIER1 α .

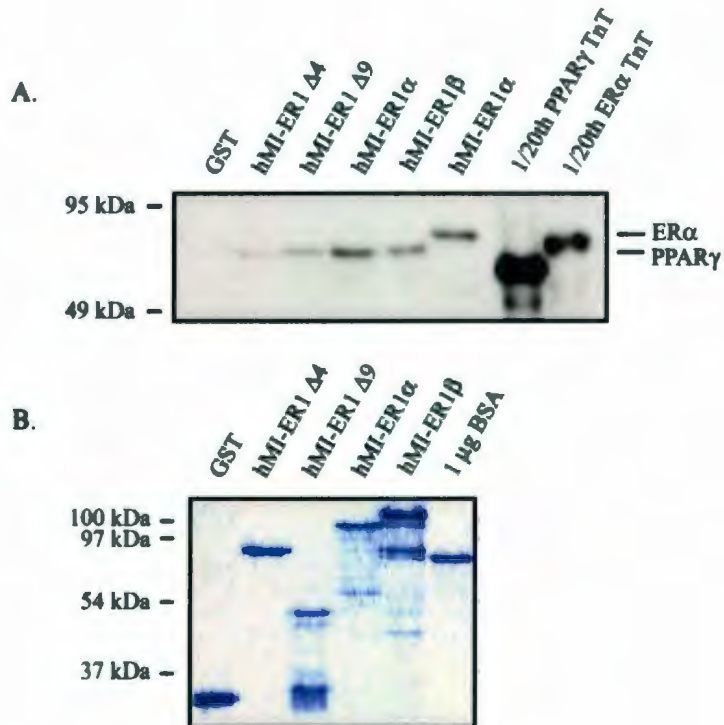


Figure 6: GST pull-down showing interaction between PPAR γ and MIER1 α and β

GST fusion proteins were prepared according to protocol given in Materials and Methods section. Equimolar amounts of the fusion proteins (not exceeding 1 μ g) were incubated with [35 S]-labeled PPAR γ protein (100,000 cpm) and purified by binding to glutathione sepharose beads (Amersham). The protein complex was then separated from the beads and run on an SDS-PAGE gel. The gel was dried and exposed to film overnight. Figure 6A shows the GST pull-down exposed to film, and Figure 6B indicates the Coomassie Blue-stained gel that shows the relative amount of protein loaded for each lane. The lane labeled GST does not contain a MIER1 deletion construct, but contains the GST tag alone. BSA is bovine serum albumin and is used as a control for protein amounts loaded.

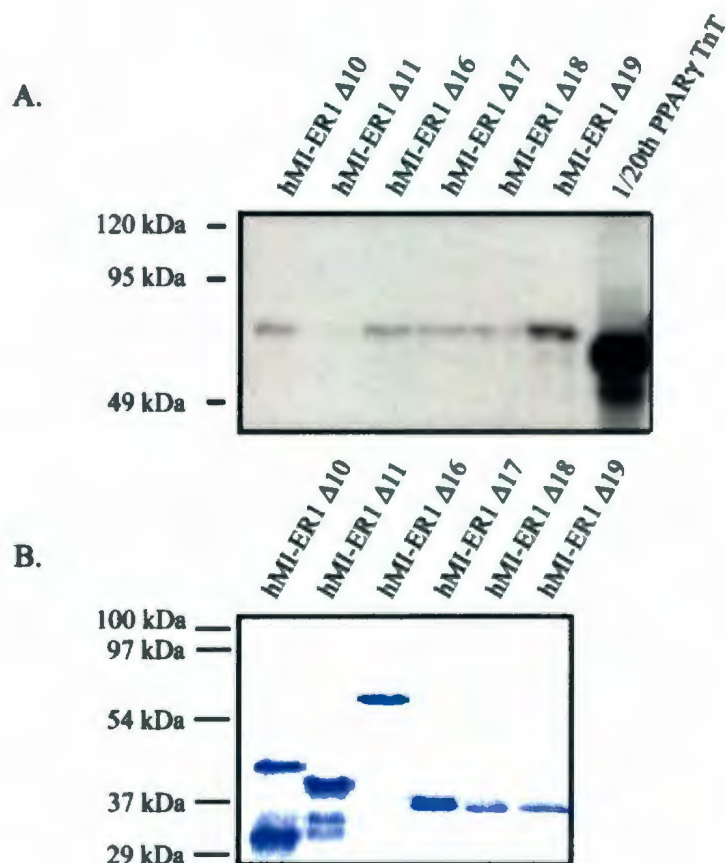


Figure 7: GST pull-down showing interaction between PPAR γ and pieces of MIER1 α

GST fusion proteins were prepared according to protocol given in Materials and Methods section. Equimolar amounts of the fusion proteins (not exceeding 1 μ g) were incubated with [35 S]-labeled PPAR γ protein (100,000 cpm) and purified by binding to glutathione sepharose beads (Amersham). The protein complex was then separated from the beads and run on an SDS-PAGE gel. The gel was dried and exposed to film overnight. Figure 7A shows the GST pull-down exposed to film, and Figure 7B indicates the Coomassie Blue-stained gel that shows the relative amount of protein loaded for each lane. Figure 7A shows the GST pull-down exposed to film, and Figure 7B indicates the Coomassie Blue-stained gel that shows the amount of protein loaded for each lane.

3.2 In Vivo Interaction between MIER1 and PPARs

3.2.1 MIER1 α and MIER1 β interact with PPAR γ 2 in HEK-293 cells

To determine whether the interaction observed *in vitro* (GST pulldown assays) was also occurring *in vivo*, HEK-293 cells were transiently transfected with pCS3+MT vector (Myc-tagged empty vector), pCS3+MT-*mier1 α* or pCS3+MT-*mier1 β* and pSV-*ppary2*. Cell extracts were immunoprecipitated with anti-PPAR polyclonal antibody and probed with anti-Myc⁹³ antibody to detect MIER1. In each experiment, expression of MIER1 was verified in whole cell lysates which were run alongside the immunoprecipitates. Cell extracts were also subjected to immunoprecipitation with anti-PPAR γ polyclonal antibody (Santa Cruz, H-100) followed by Western blot analysis with 9E10 antibody. Both MIER1 α and MIER1 β immunoprecipitated with transfected PPAR γ in HEK-293 cells (Figure 8 and 9, respectively). These studies indicate a strong *in vivo* interaction between MIER1 α or β and PPAR γ .

The molecular weight of the bands for myc-MIER1 α and myc-MIER1 β was approximately 100 and 110 kDa, respectively. While the true molecular weight of MIER1 α is 60kDa, the untagged protein actually runs higher on a gel due to an acidic domain near the N-terminus^{94,95}. This, taken together with the myc-tag which adds approximately 14 kDa to the molecular weight of the protein of interest, can account for the difference in molecular weight observed in the western blot. These proteins run at the same molecular weight shown in previous publications⁹⁶.

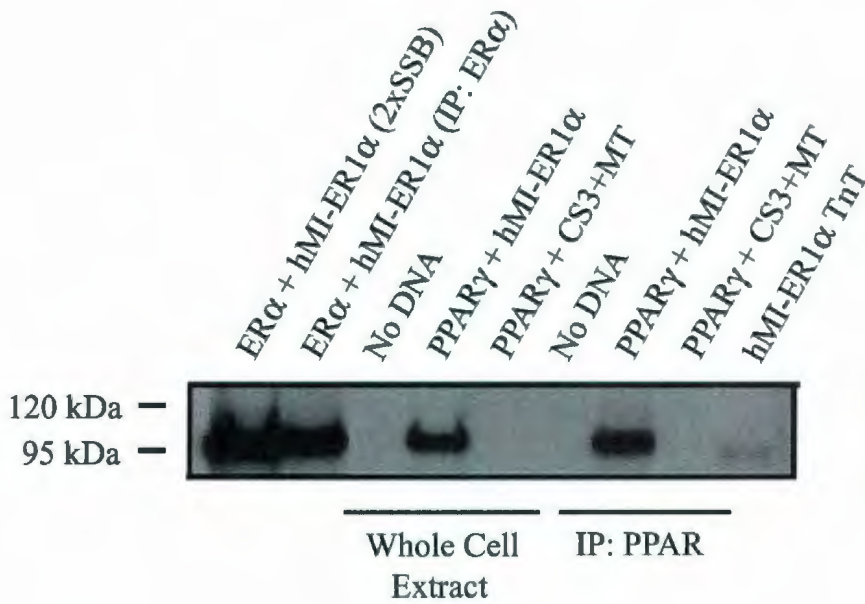


Figure 8: PPAR γ 2 interacts with MIER1 α in HEK-293 cells

HEK-293 cells were seeded at a density of 5×10^5 cells/well of a 6-well plate and grown in DMEM for approximately 18 h. Cells were then transfected with 0.5 μ g of pCS3+MT vector, pCS3+MT-*mier1 α* and pSV-sport-*ppary2* or ER α . Cell lysates were prepared (and immunoprecipitated) as described in detail in the Materials and Methods section, and loaded directly onto the gel (lanes 1-8) for western blot. *In vitro* translated MIER1 was loaded as a positive control. The position of marker proteins is indicated to the left.

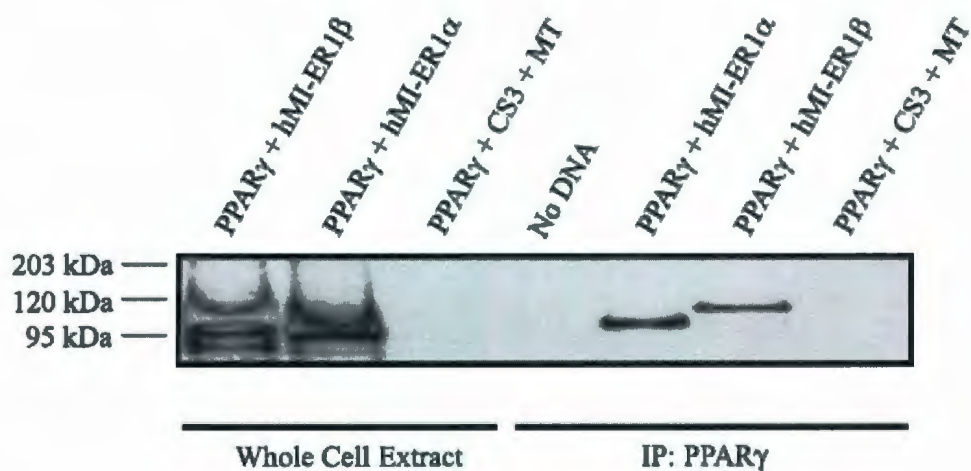


Figure 9: PPAR γ 2 interacts with MIER1 β in HEK-293 cells

HEK-293 cells were seeded at a density of 5×10^5 cells/well of a 6-well plate and grown in DMEM for approximately 18 h. Cells were then transfected with 0.5 μ g of pCS3+MT vector, pCS3+MT-*mier1 α* , or pCS3+MT-*mier1 β* and pSV-sport-*ppar γ 2*. Cell lysates were prepared (and immunoprecipitated) as described in detail in the Materials and Methods section, and loaded directly onto the gel (lanes 1-7) for western blot. The position of marker proteins is indicated to the left.

3.2.2 MIER1 α and MIER1 β interact with PPAR β/δ in HEK-293 cells

Both MIER1 α and MIER1 β immunoprecipitated with transfected PPAR β/δ in HEK-293 cells (Figure 10, 11 respectively). These studies indicate a strong *in vivo* interaction between MIER1 α or β and PPAR β/δ . To determine this, HEK-293 cells were transiently transfected with pCS3+MT vector, pCS3+MT-*mier1 α* or pCS3+MT-*mier1 β* and pBABEpuro *ppar β/δ* . Expression of Myc-tagged MIER1 α and β was verified for each experiment by Western blot analysis of whole cell lysate (extracted in 2 X SSB) using 9E10 antibody and run alongside the immunoprecipitation results. Cell extracts were also subjected to immunoprecipitation with anti-PPAR β/δ polyclonal antibody (H-74, Santa Cruz) followed by Western blot analysis with anti-Myc 9E10.

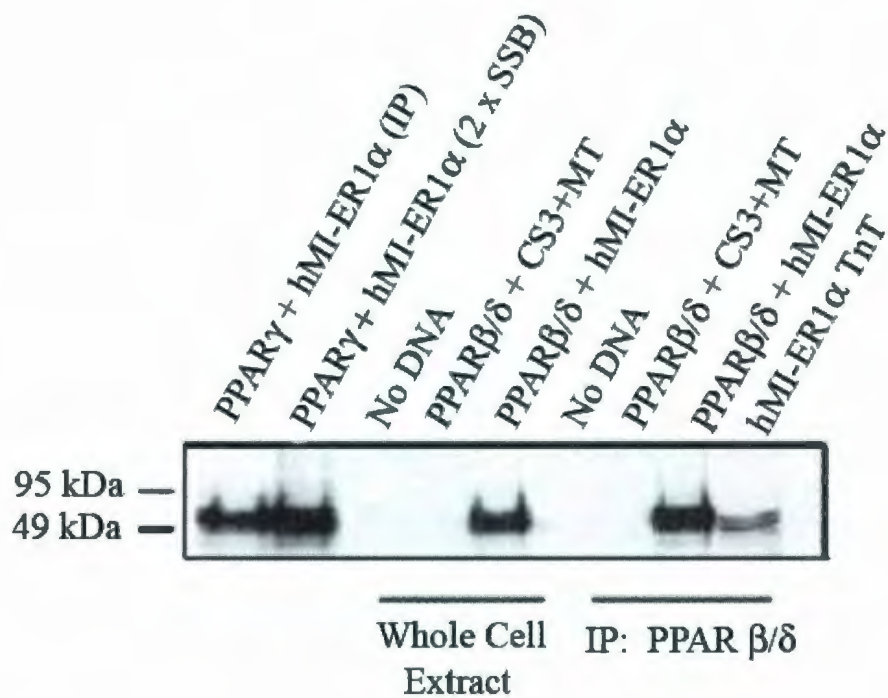


Figure 10: PPARβ/δ interacts with MIER1α in HEK-293 cells

HEK-293 cells were seeded at a density of 5×10^5 cells/well of a 6-well plate and grown in DMEM for approximately 18 h. Cells were then transfected with 0.5 μ g of pCS3+MT vector, pCS3+MT-*mier1α* or pCS3+MT-*mier1β* and pBabe-puro-*pparβ/δ*. Cell lysates were prepared as described in detail in the Materials and Methods section, and loaded directly onto the gel (Lanes 1-8) for western blot. *In vitro* translated MIER1 was loaded as a positive control. The position of marker proteins is indicated to the left.

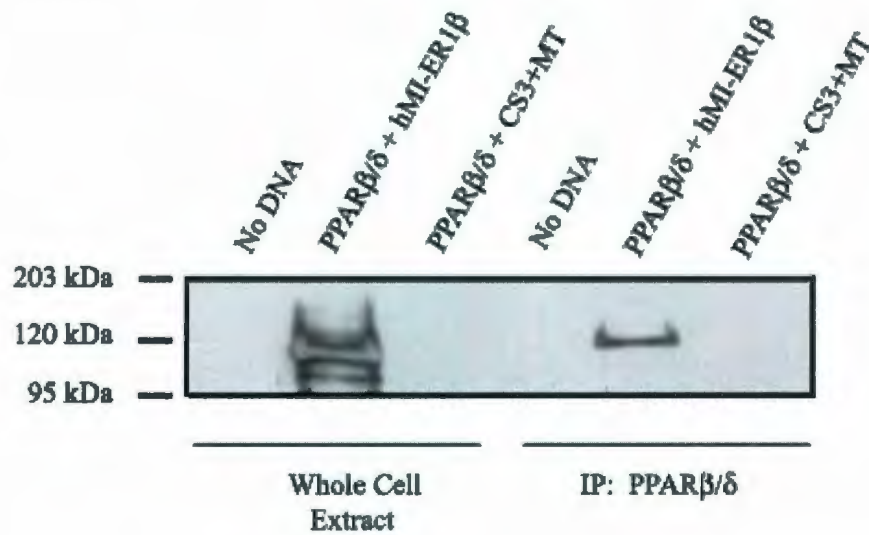


Figure 11: PPARβ/δ interacts with MIER1β in HEK-293 cells

HEK-293 cells were seeded at a density of 5×10^5 cells/well of a 6-well plate and grown in DMEM for approximately 18 h. Cells were then transfected with 0.5 μ g of pCS3+MT vector, pCS3+MT-*mier1 α* or pCS3+MT-*mier1 β* and pBABEpuro *ppar β/δ* . Cell lysates were prepared as described in detail in the Materials and Methods section, and loaded directly onto the gel (Lanes 1-6) for western blot.

3.3 Ligand-Independent Interaction between MIER1 and PPAR γ 2

3.3.1 MIER1 α and MIER1 β interact with PPAR γ 2 in HEK-293 cells, independent of troglitazone treatment

To determine whether the interaction between PPAR γ 2 and MIER1 α and MIER1 β is dependent on the presence of ligand, HEK-293 cells were transiently transfected with pCS3+MT vector (Myc-tagged empty vector), pCS3+MT-*mier1 α* or pCS3+MT-*hmier1 β* and pSV-sport-*ppar γ 2* or pBABEpuro *ppar β/δ* . 24 h after transfection, cells were treated with 20 μ M Troglitazone or vehicle alone (DMSO). Cell extracts were subjected to immunoprecipitation with anti-PPAR γ 2 antibody (Santa Cruz, H-100) or anti-PPAR β/δ (Santa Cruz, H-74) followed by Western blot analysis with 9E10 antibody. Both MIER1 α and MIER1 β immunoprecipitated with transfected PPAR γ 2 in HEK-293 cells in the presence or absence of Troglitazone (Figure 12). This indicates that the interaction is ligand-independent, in the case of troglitazone. Similarly, PPAR β/δ also interacts with MIER1 α and β , independent of troglitazone action (Figure 13). Further experiments are required to determine if the troglitazone-independent action of MIER1 applies in the presence of other PPAR γ ligands.

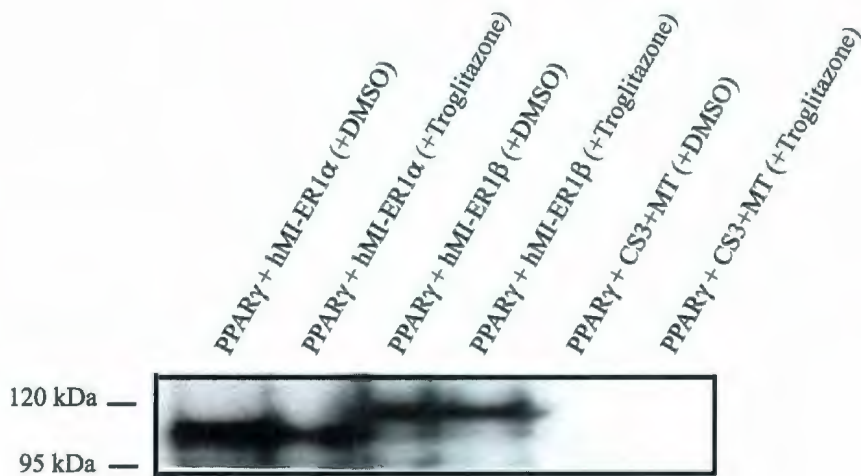


Figure 12: PPAR γ 2 interacts with MIER1 α and β in HEK-293 cells independent of ligand

HEK-293 cells were seeded at a density of 5×10^5 cells/well of a 6-well plate and grown in DMEM for approximately 18 h. Cells were then transfected with 0.5 μ g of pCS3+MT vector, pCS3+MT-*mier1 α* or pCS3+MT-*mier1 β* and pSV-sport-*ppary2*. 24 h later, cells were treated for 24 h with 20 μ M of Troglitazone or dimethyl sulfoxide (DMSO). Cell lysates were prepared as described in detail in the Materials and Methods section, and loaded directly onto the gel (Lanes 1-6) for western blot.

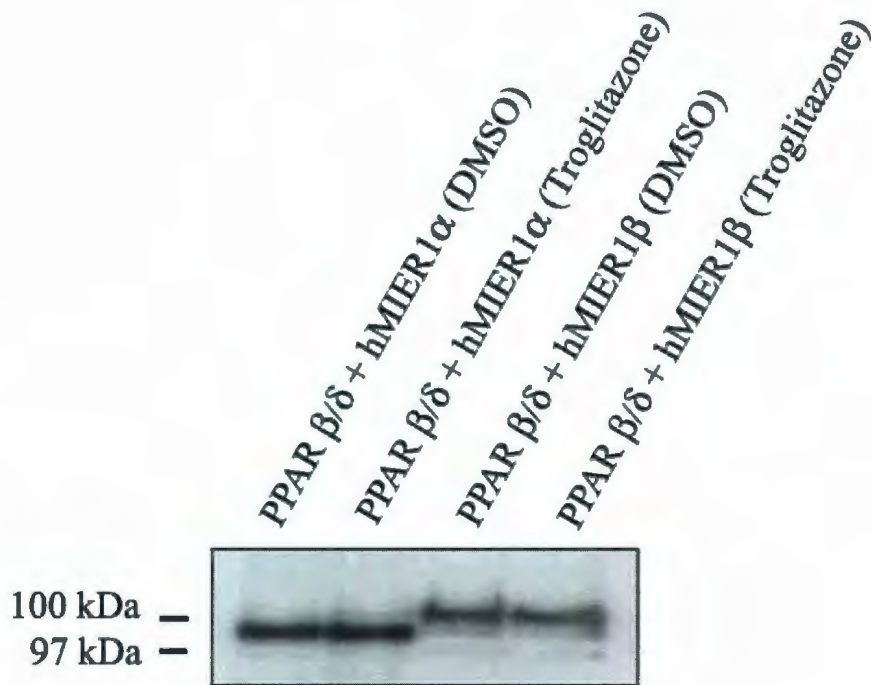


Figure 13: PPAR β/δ interacts with MIER1 α and β independent of ligand

HEK-293 cells were seeded at a density of 5×10^5 cells/well of a 6-well plate and grown in DMEM for approximately 18 h. Cells were then transfected with 0.5 μg of pCS3+MT vector, pCS3+MT-*mier1 α* or pCS3+MT-*mier1 β* and pBabe-puro-PPAR β/δ . 24 h later, cells were treated for 24 h with 20 μM of Troglitazone or dimethyl sulfoxide (DMSO). Cell lysates were prepared as described in detail in the Materials and Methods section, and loaded directly onto the gel (Lanes 1-4). Figure 11 shows a western blot with no immunoprecipitation of PPAR β/δ with CS3+MT indicating that the interaction is MIER1-specific, and is not dependent on the myc-tag.

3.4 Effect of MIER1 on PPRE-dependent Transcription

3.4.1 MIER1 α and MIER1 β serve as transcriptional activators of PPRE-dependent transcription

Since both MIER1 α and MIER1 β were found to interact with PPAR γ 2 *in vitro* and *in vivo*, we wished to determine what effect (if any) this interaction had on the ability of PPAR to activate transcription at the PPRE. HEK-293 cells were transfected using the reporter construct pPPRE-X3-TK-luc (Tk: thymidine kinase; Luc: luciferase) along with either pCS3+MT, pCS3+MT-*mier1 α* , pCS3+MT-*mier1 β* , or pSVsport-*pgc-1 α* . PGC-1 α , a known PPAR γ 2 coactivator, was transfected into HEK-293 cells to serve as a positive control. All HEK-293 cells were transfected with pSVsport *ppar γ 2*. These HEK-293 cells were incubated for 24 h, and then treated with 20 μ M Troglitazone or dimethylsulfoxide (DMSO, vehicle). After an additional 24 h, these cells were lysed and harvested for luciferase assays as described in detail in the Materials and Methods section. The effects of MIER1 α and MIER1 β can be determined by comparing the relative luciferase units (RLUs) for these samples to those for the Myc-tagged CS3+MT empty vector. β -galactosidase assays were performed to normalize to transfection efficiency, as described in Materials and Methods. In three separate experiments done in triplicate, expression of MIER1 α or MIER1 β resulted in stimulation of PPAR-dependent activity by approximately 2-fold (Figure 14 and 15). This stimulation occurred in the presence and in the absence of 20 μ M Troglitazone (PPAR ligand). More specifically,

troglitazone stimulates in all cases and this is augmented by PGC-1 α , MIER1 α or MIER1 β . In addition, both MIER1 α and MIER1 β stimulated a similar 2-fold increase in the absence of ligand; this was comparable to stimulation by PGC-1 α (Figure 15).

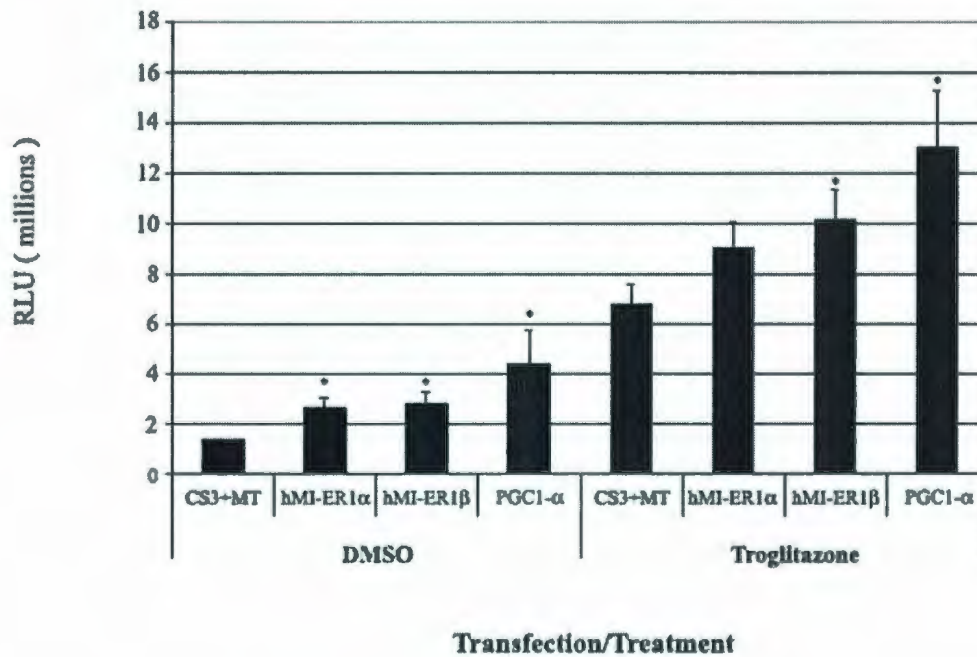


Figure 14: MIER1 α and β activate PPAR γ promoter activity in the presence and absence of PPAR γ agonist (Troglitazone)

HEK-293 cells were transfected with 0.5 μ g of pPPRE-X3-TK-luc reporter plasmid, 0.5 μ g of CS3+MT vector, pCS3+MT-*mier1 α* , pCS3+MT-*mier1 β* , or pSVsport *pgc-1 α* and pSVsport *ppary2*. PGC-1 α is a known PPAR γ 2 coactivator, and it was transfected into HEK-293 cells to serve as a positive control. Cells were treated with either 20 μ M Troglitazone or DMSO (vehicle). Cells were harvested approximately 48 h after transfection and the amount of relative luciferase units (RLU) was determined as described in Materials and Methods. Values were normalized by measuring transfection efficiency (β -galactosidase assay). Each of these bars represents an experiment repeated three times in triplicate, and error bars are given. Student t-tests were conducted to determine significance ($p < 0.05$, compared to CS3+MT for each treatment).

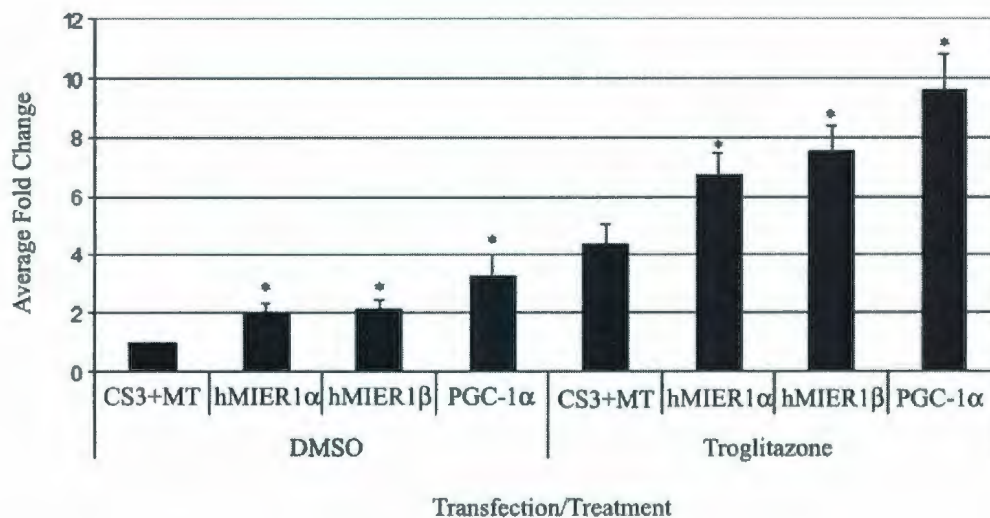


Figure 15: MIER1 α and β activate PPAR γ promoter activity in the presence and absence of PPAR γ agonist (fold-change)

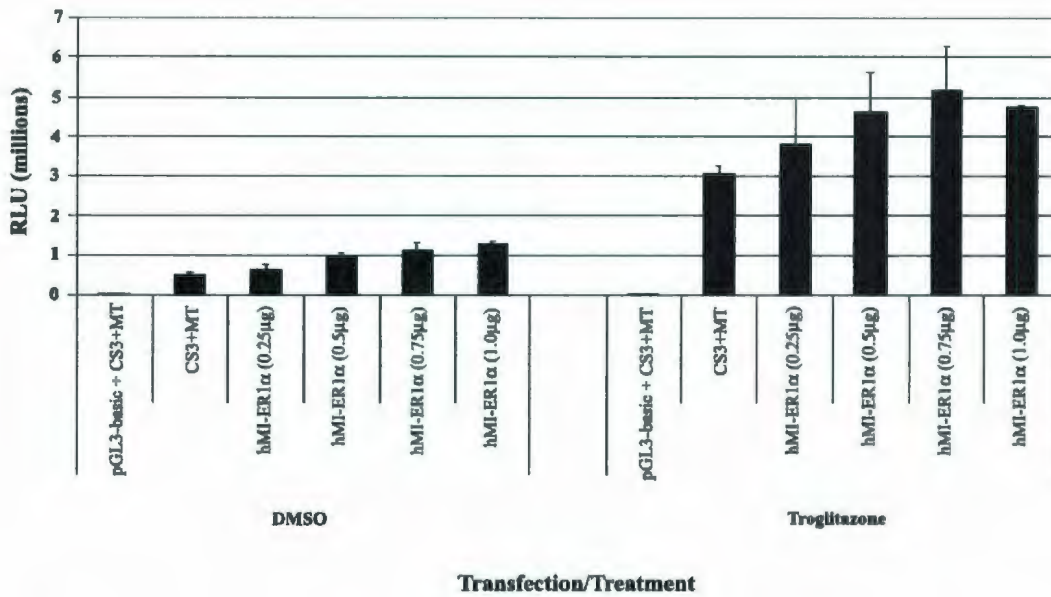
The results of the luciferase assay displayed in Figure 14 have been normalized to show average fold change as opposed to relative luciferase units (RLU). Specifically, CS3+MT (empty vector) was set as 1, and the fold change for each condition was compared to the empty vector. Each of these bars represents an experiment repeated three times in triplicate, and error bars are given. Student t-tests were conducted to determine significance ($p < 0.05$, compared to CS3+MT for each treatment).

3.4.2 MIER1 α Activates PPRE-dependent Transcription in a Dose-dependent Manner

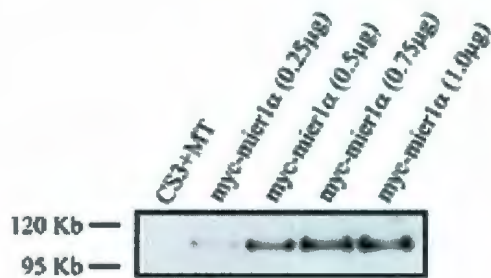
Since MIER1 α led to activation of PPRE-dependent transcription, it was important to ensure that this activation was a specific result of the overexpression of MIER1. Specific effects would increase with increasing concentration of MIER1 α , therefore, varying amounts of MIER1 α were transfected into HEK-293 cells and the luciferase activity was measured. Amounts of 0.25, 0.5, 0.75 and 1 μ g of MIER1 α were transfected into HEK-293 cells along with the pPPRE-X3-TK-luc reporter plasmid and pSVsport *ppar* γ 2.

Figure 16A demonstrates a dose-dependent increase in PPRE-dependent transcription, both in the presence and absence of troglitazone. Figure 16 B and C indicate the relative amounts of *myc-mier1* α transfected into the cells for each condition.

A.



B.



C.

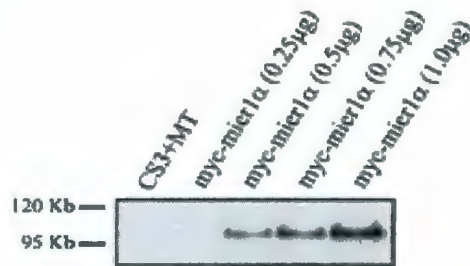


Figure 16: A- Dose-dependent increase in PPRE-dependent luciferase activity B & C: Western blot for MIER1α in HEK-293 cells used for luciferase assay (B: + DMSO, C: +Troglitazone)

HEK-293 cells were transfected with 0.5 μg of pPPRE-X3-TK-luc reporter plasmid, 0.5 μg of CS3+MT vector, pSVsport *pparγ2* and increasing amounts of pCS3+MT-*mier1α* as indicated in the above figure. Cells were treated for 24 h with either 20 μM Troglitazone or DMSO (vehicle). Cells were harvested approximately 48 h after transfection and the amount of relative luciferase units (RLU) was determined as described in Materials and Methods. Values were normalized by measuring transfection efficiency (β-galactosidase assay). Each of these bars represents an experiment repeated three times in triplicate, and error bars are included.

3.4.3 9-cis Retinoic Acid, a ligand for retinoid X receptor, has no effect on the ability of MIER1 α to activate PPRE-driven transcription

In order to determine whether a ligand for the retinoid x receptor (RXR) could affect the ability of MIER1 α to bind to PPAR γ 2 and activate transcription at the PPRE, HEK-293 cells were transfected as described in Figure 15, and treated with 1.0×10^{-8} M 9-cis retinoic acid (or ethanol). These results rely on the presence of endogenous RXR in HEK-293 cells⁹⁷, since RXR was not transfected into the cells. The results show that MIER1 α activated PPRE-driven transcription to the same level (no significant difference) in the presence and in the absence of 9-cis retinoic acid.

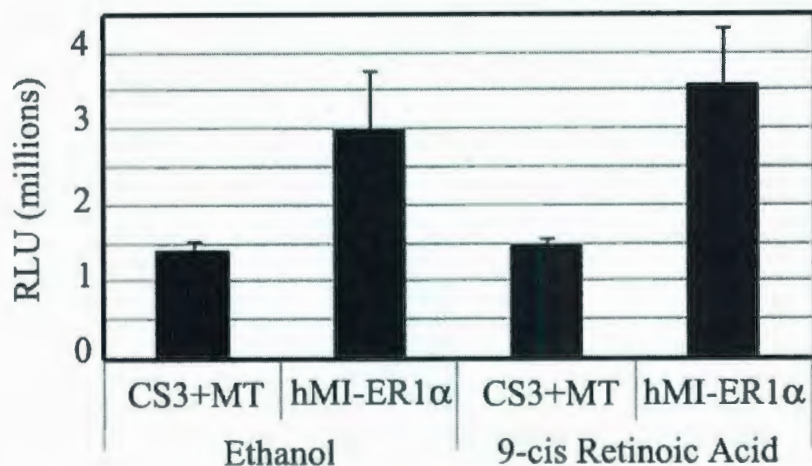


Figure 17: 9-cis retinoic acid has no effect on MIER1α ability to increase PPAR-dependent transcription

HEK-293 cells were transfected with 0.5 μg of pPPRE-X3-TK-luc reporter plasmid or pGL3-basic, pSVsport *ppary2* and 0.5 μg of CS3+MT vector or pCS3+MT-*mier1α*. Cells were treated with either 1.0×10^{-8} M 9-cis retinoic acid or ethanol (vehicle). Cells were harvested approximately 48 h after transfection and the amount of relative luciferase units (RLU) was determined as described in Materials and Methods. Values were normalized by measuring transfection efficiency. Each of these bars represents an experiment repeated three times in triplicate, and error bars are included.

3.5 Changes in mRNA levels of MIER1 over the course of adipogenesis in 3T3-L1 cells

In order to determine the biological significance of an interaction between PPAR γ 2 and MIER1 α , 3T3-L1 cells were seeded in 24-well plates and initiated to undergo adipogenesis. Cells were harvested every second day until all of the cells had been harvested (16 days total). RNA was extracted from the cells and cDNA was made to perform semiquantitative RT-PCR for levels of *mier1* mRNA and *ppar γ 2* mRNA over the course of adipogenesis. *ppar γ 2* increases over the course of adipogenesis⁹⁸, while *mier1* mRNA levels increase concomitantly. *Hmier1* mRNA levels are low at Day 0 and increase up to Day 6 and then level off. *ppar γ 2* mRNA levels continue to increase from Day 0 up to Day 10-12 and start to level off. *β -actin* was used as a load control and the levels after 20 cycles were equal, indicating saturation of the amplification. The primer pair used for *mier1* amplifies both the α - and β - isoforms.

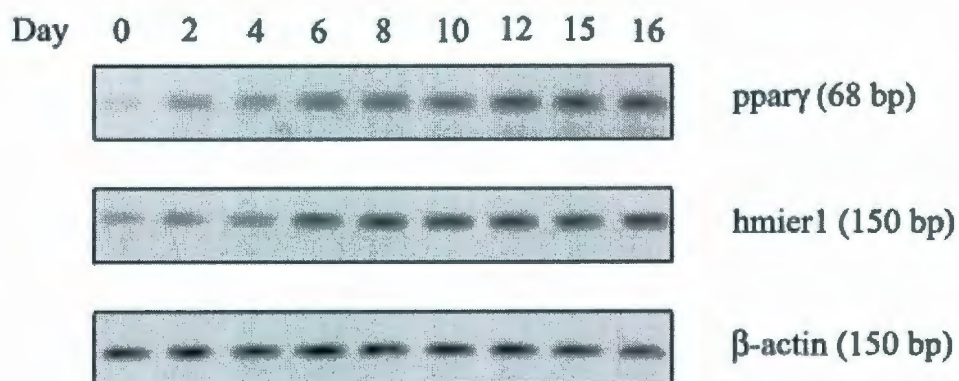


Figure 18: *pparγ2* and *mier1* mRNA levels increase concomitantly over the course of adipogenesis

3T3-L1 cells were initiated in 24-well plates to undergo adipogenesis, and cells were harvested every second day as described in Materials and Methods. *β-actin* was used as a control (20 cycles). Both *pparγ* and *mier1* were amplified with 26 cycles. Equal amounts of cDNA were used for each PCR reaction.

3.6 Determination of differentiating versus non-differentiating 3T3-L1 cells

Differentiation into mature adipocytes is determined by the presence of lipid droplets in the cell. The lipid droplets appeared as clear, birefringent, subcellular organelles. Lipid droplets were visible under phase contrast microscopy and were confirmed to be lipid droplets by Oil Red-O staining (Figure 19). In the case of immunocytochemistry, the lipid droplets appeared under the microscope as circular areas with no staining inside (Figure 21). Intracellular lipid droplets were first observed at approximately Day 4 of adipogenesis and continued until the end of the experiment (Day 14). Since not all of the cells had differentiated, incubating them in maintenance media for an extended period of time would result in the accumulation of even more differentiated adipocytes. Cells were initiated upon confluence, and the number of cells in a particular well remained constant over the course of adipogenesis. Only the number of cells differentiating into adipocytes (forming lipid droplets) increased.

Adiponectin is expressed as the cells differentiate into mature adipocytes⁹⁹, and is a frequently-used adipogenic marker. Adiponectin is upregulated as 3T3-L1s differentiate into mature adipocytes; therefore a western blot was performed for adiponectin using the cell lysate obtained over 14 days of adipogenesis (see Section 2.7). Figure 20 indicates that adiponectin is upregulated at approximately Day 8 of adipogenesis and continues to accumulate until Day 14.

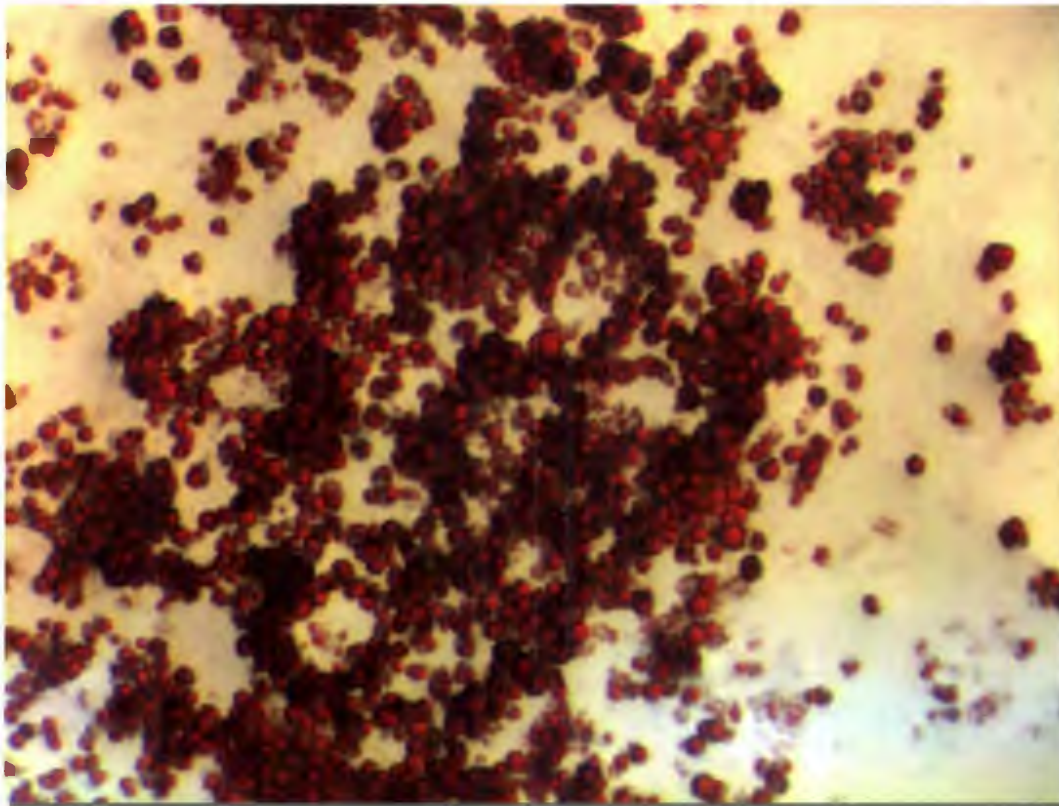


Figure 19: 3T3-L1 cells stained with Oil Red O at Day 22 of adipogenesis

3T3-L1 cells were seeded into 6-well culture dishes and initiated to undergo adipogenesis as described in Materials and Methods. On Day 22 of adipogenesis, cells were stained according to the protocol for Oil Red O stain obtained with the Adipogenesis Assay Kit (Chemicon, ECM950) (Section 2.7.5). Pictures were taken under a dissecting scope at 8x magnification.

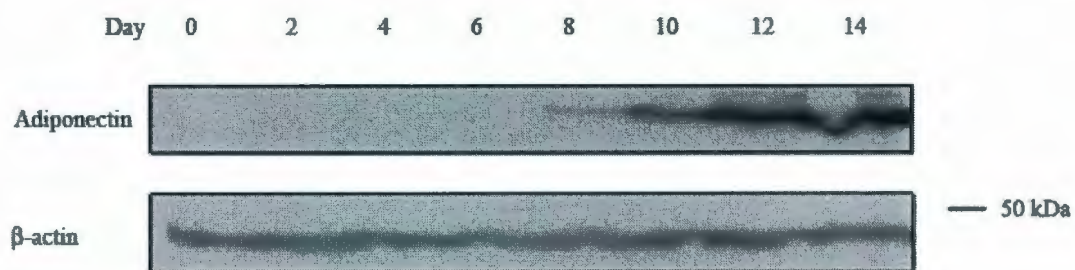


Figure 20: Western Blot of Adiponectin over 14 days of adipogenesis

3T3-L1s were seeded into 60 mm dishes and initiated to undergo adipogenesis as described in Materials and Methods (Section 2.7.4). Cell lysates were collected every second day as described in Section 2.7.4, and a western blot was performed on the lysate using a 1:2000 dilution of anti-adiponectin antibody (Abcam, ab3455).

3.7 Immunocytochemical analysis of MIER1 α localization in 3T3-L1 cells undergoing adipogenesis

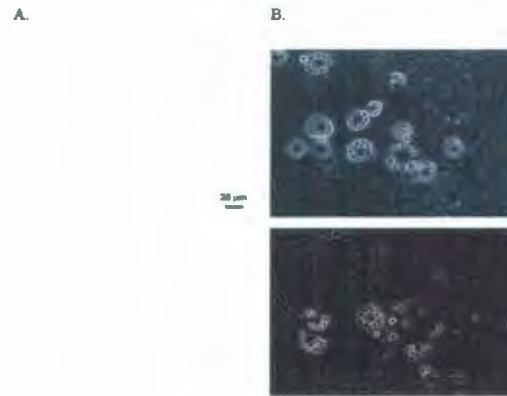
In order to determine whether MIER1 α is expressed specifically in 3T3-L1 cells that are differentiating into mature adipocytes, 3T3-L1s were induced to differentiate as described in detail in the Materials and Methods. On Day 4 and Day 14 of the adipogenic program, chamber slides were stained with either purified anti-MIER1 α - or β -specific antibody or purified preimmune antibody. Cells that contained lipid droplets (as determined by phase contrast microscopy and Oil Red-O staining (Figure 19)) were the only cells that stained for MIER1 α (Figure 21). There was no staining for MIER1 β in either differentiated or undifferentiated 3T3-L1 cells (Figure 22), indicating that MIER1 α is the important isoform in adipogenesis.

Cytoplasmic staining of MIER1 α was observed in 3T3-L1s undergoing adipogenesis. Specifically, phase contrast was used to visualize the cells that were undifferentiated and that had not been positively stained. Cells that had not yet differentiated did not stain for MIER1 α (phase contrast microscopy, Figure 21), and those differentiated adipocytes were on top of the fibroblast (pre-adipocyte) layer due to the accumulation of triglycerides. These adipocytes became more rounded as they accumulated lipid droplets and were much larger than the underlying, undifferentiated fibroblasts. As well, the accumulating lipid droplets started out as tiny drops inside a cell, then as more developed, fused to form one large lipid droplet that filled nearly the entire cytoplasm of the adipocyte (late differentiation). It was also noticed that the differentiation of adipocytes in one area of the chamber slide would lead to more

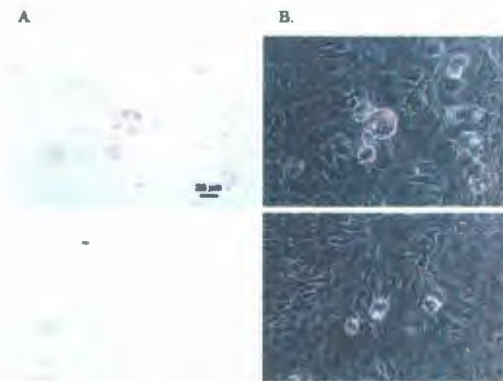
adipocytes differentiating in that same area. It appears that the differentiating cells secrete factors that help stimulate neighboring fibroblast cells (pre-adipocytes). If cells were left to differentiate for too long (23 days – data not shown), the adipocytes would start to lift off the plate in the middle of a section of very late differentiated adipocytes.

Immunofluorescence was performed at Day 11 of adipogenesis. Anti-MIER1 α purified polyclonal antibody (Leo, Bleed 1) and anti-PPAR γ monoclonal antibody (Santa Cruz, E-8) were used for detection of each protein. The majority of MIER1 α staining was cytoplasmic, and found only in the differentiated 3T3-L1 cells. For PPAR γ , the staining was both nuclear and cytoplasmic (Figure 23). Colocalization of both proteins was observed in the nucleus of a small minority of differentiated 3T3-L1 cells (Figure 23). The bottom three panels of Figure 23 show subcellular localization of PPAR γ , MIER1 α , and their colocalization in the nucleus of a differentiating 3T3-L1 cell. This phenomenon was only observed in a small percentage of differentiated adipocytes – these adipocytes appeared to be at a later stage in differentiation (larger cells, fused lipid droplets). The majority of the differentiated cells expressed MIER1 α in the cytoplasm, and PPAR γ was expressed in both the nucleus and the cytoplasm (Figure 23, top panel).

Preimmune Day 4



Immune Day 4



Immune Day 14

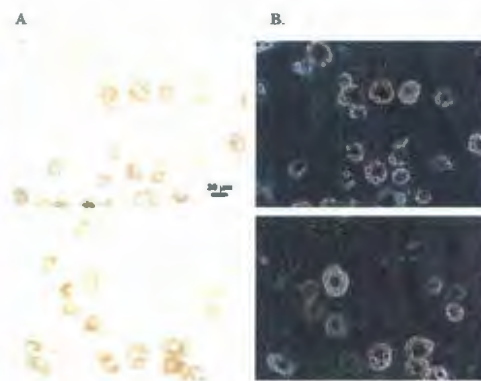
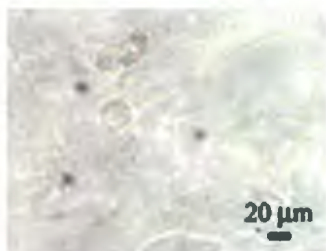


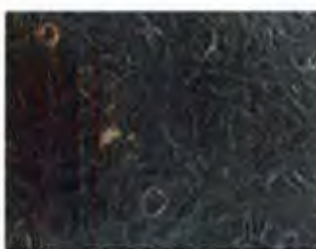
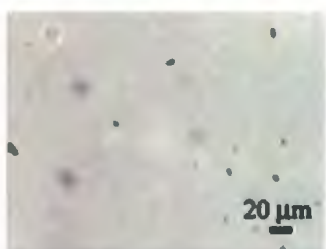
Figure 21: MIER1 α is expressed in early and late differentiating 3T3-L1 adipocytes

3T3-L1 cells were seeded in 8-well chamber slides and initiated to undergo adipogenesis as described in Materials and Methods. On Day 4 and Day 14 of adipogenesis, cells were stained using an anti-MIER1 α polyclonal antibody (labeled Day 4, Day 14) or a pre-immune polyclonal antibody and visualized by DAB (dark brown-red stain) staining of horseradish peroxidase-linked secondary antibody (Donkey anti-rabbit-HRP). Pictures were taken at 50x magnification under both brightfield (Column A) and phase-contrast (Column B). Figures include pictures of 2 wells for preimmune, Day 4, and Day 14.

Preimmune Day 4



Immune Day 4



Immune Day 14

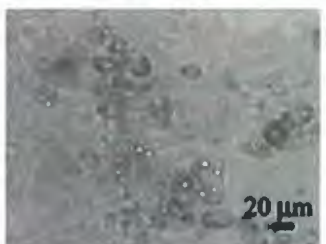


Figure 22: MIER1 β is not expressed in early or late differentiating 3T3-L1 adipocytes

3T3-L1 cells were seeded in 8-well chamber slides and initiated to undergo adipogenesis as described in Materials and Methods. On Day 4 and Day 14 of adipogenesis, cells were stained using an anti-MIER1 β polyclonal antibody or a pre-immune polyclonal antibody and visualized by DAB (dark brown-red stain) staining of horseradish peroxidase-linked secondary antibody (Donkey anti-rabbit-HRP). Pictures were taken at 50x magnification under both brightfield (left column) and phase-contrast (right column).

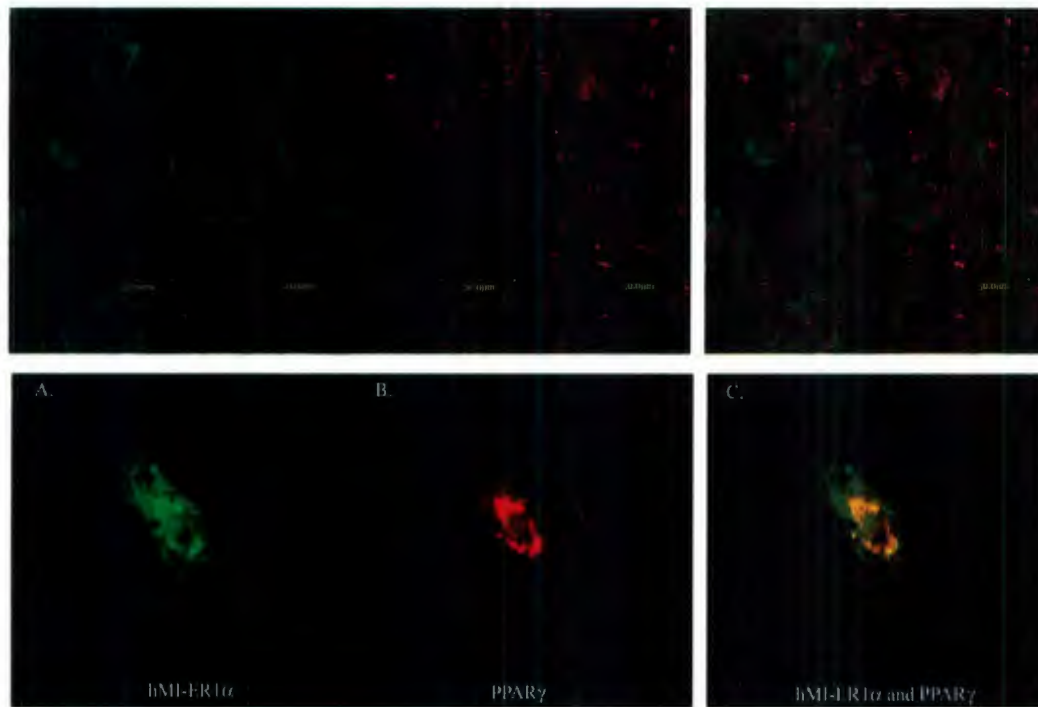


Figure 23: MIER1 α and PPAR γ are colocalized in differentiated 3T3-L1 cells

3T3-L1 cells were seeded in 8-well chamber slides and initiated to undergo adipogenesis as described in Materials and Methods. On Day 11 of adipogenesis, cells were stained using an anti-MIER1 α polyclonal antibody and an anti-PPAR γ monoclonal antibody (Santa Cruz, E-8) and visualized using FITC-DAR and CY3-DAM secondary antibodies, respectively, and confocal microscopy. Green fluorescent staining indicates MIER1 α (A) and red fluorescent staining indicates PPAR γ (B). Panel C on the right shows colocalization (yellow) of both proteins.

CHAPTER 4 – Discussion

The purpose of this study was to determine the implications of an interaction between PPAR γ 2 and the transcriptional coregulator, MIER1. Since PPAR γ 2 is one of the master regulators for adipogenesis (differentiation of precursor cells into mature, lipid-filled adipocytes), MIER1 may also play a role in this important physiological process.

Peroxisome proliferator-activated receptors (PPARs) have been shown to play an integral role in the control of energy homeostasis in the body, especially through their ability to sense environmental cues (e.g. free fatty acids) and translate that into a cellular response and augmentation of gene expression. PPAR family members interact with a number of cofactors in order to either increase or decrease transcriptional activity at target genes through various mechanisms, one of these being its binding to the PPRE. In this study, a transcriptional coregulator that has previously been shown to act as a transcriptional repressor (MIER1) has been determined to function as a transcriptional activator for PPAR γ 2. Moreover, the ability of MIER1 to bind to and activate PPAR γ 2-dependent transcription is characteristically similar to that of a known PPAR γ 2 coactivator, PGC-1 α (PPAR γ coactivator 1 alpha). Not only do mRNA levels of *mier1* increase over the same time period as *ppar γ 2* during adipogenesis, but the expression of MIER1 protein in differentiating adipocytes follows the same trend as shown by immunocytochemistry at two distinct time periods over the course of adipogenesis (early and late).

PGC-1 α is a coactivator that functions as a platform for the recruitment of regulatory protein complexes that can affect gene transcription in a multitude of ways¹⁰⁰. Just as PGC-1 α can recruit proteins with histone acetyltransferase (HAT) activity (ex: CREB-binding protein/p300, steroid receptor coactivator-1 [SRC-1]), MIER1 has been shown to interact with CBP/p300 (one of these histone-modifying proteins)¹⁰¹. In fact, both MIER1¹⁰¹ and PGC-1 α ¹⁰² interact with CBP/p300 via their amino-terminal region. Given the similarity between these proteins and others which will be discussed in detail as they arise, it is logical to predict that MIER1 may serve as a novel coactivator for PPAR γ 2.

While it has been shown that MIER1 interacts with other nuclear hormone receptors, there was no indication that MIER1 interacted with PPAR γ up to this point. Initial pulldowns gave evidence that PPAR γ 2 interacted with both MIER1 α and MIER1 β , although the interaction was stronger between PPAR γ 2 and MIER1 α than with MIER1 β . More specifically, more MIER1 α bound to PPAR γ 2 than MIER1 β . This was not dependent upon protein mass, and is similar to what has been shown with MIER1 β and ER α as well¹⁰³.

The difference between the α and β forms of MIER1 lies within the C-terminal domain. This is the location of the LXXLL motif in MIER1 α that is not present in MIER1 β . Since PPAR γ 2 interacted with both the isoforms, the LXXLL motif was determined to be an unlikely interaction site for the two proteins. As has been previously shown with a wide variety of LXXLL-containing proteins, this motif is not always

required for an interaction with nuclear hormone receptors^{104,105}. In the case of the protein inhibitor of activated STAT family (PIASy), the LXXLL domain is not required for the interaction between the corepressors and STAT1, but is essential for the transrepression of STAT1 activity¹⁰⁵. Recently, the LXXLL-motif was ruled out as a potential interaction site between MIER1 and ER α ¹⁰⁶. Since PPAR γ and PPAR β/δ interact with both isoforms of MIER1 (Figures 8, 9, 10 and 11), this rules out the LXXLL-motif as the interaction site between these two proteins. However, LXXLL may be contributing to the stronger binding between MIER1 α and PPAR γ compared to MIER1 β . The fact that MIER1 β interacts less strongly with PPAR γ than MIER1 α (which contains the LXXLL motif) is evidence that cooperative binding with the LXXLL domain may allow for a stronger interaction between MIER1 α and PPAR γ .

While the LXXLL motif is one explanation for the stronger binding between MIER1 α and PPAR γ , the presence of a longer C-terminus on MIER1 β may also be important. The tail of MIER1 β may be folding in such a way that it blocks the binding to a specific site in the C-terminus. In this case, the data indicates that MIER1 α and β are interacting with PPAR γ through their common SANT domain. Therefore this specific site that β could be partially blocking is the SANT domain of MIER1.

The SANT domain is found in many nuclear hormone corepressors, including NCoR and CoREST and SMRT¹⁰⁷. In these proteins, and other chromatin-remodelling proteins, the SANT has been shown to function in binding and regulating histone deacetylases (HDAC)⁷. However, the SANT domain also has a function in binding histone acetylases (HAT), G9a (histone methyltransferase) and even histones directly^{7,108}.

In this case, MIER1 is serving as a coactivator for PPAR γ 2. One of the ways MIER1 could stimulate PPRE-dependent transcription is via recruitment of proteins with HAT activity. Since MIER1 has already been shown to interact with CBP/p300 (unpublished data) which contains HAT activity, it may be stimulating activity by recruiting CBP/p300 to the PPRE. As mentioned in recent publications, the SANT domain has been implicated in using the histone code in order to regulate transcription⁷.

While the interaction with PPAR γ 2 was stronger with the C-terminus (GST-fusion construct Δ 9) of MIER1 than the N-terminus (GST-fusion construct Δ 4), there was still an interaction between PPAR γ 2 and the N-terminus. The region of the N-terminus used for the pulldown (MIER1 Δ 4, aa 1-283) did not possess the SANT domain at all. This indicates that there may be multiple binding sites for PPAR γ 2 and MIER1. For example, MIER1 may fold into a specific conformation that allows it to bind PPAR γ 2 via the SANT domain and another area of the N-terminus. This type of interaction has been shown recently with CCPG (Constitutive Coactivator of PPAR γ) and PPAR γ , where both the C- and N-terminus interact with PPAR γ ¹⁰⁹. As well, CBP/p300 has been shown to bind PPAR γ 2 via both the AF-1 and the AF-2 domains – allowing for both ligand-dependent and ligand-independent activation of transcription¹¹⁰.

Future studies should use deletion constructs of PPAR γ 2 in a GST pulldown experiment in order to determine what domain(s) of PPAR γ 2 interact with MIER1. This will better define the interaction between the two proteins and also explain how MIER1 may be stimulating transcription at the PPRE. The GST pulldown is an *in vitro* assay that

uses deletion constructs of a protein of interest, so the tertiary structure of that region may be affected. As well, there may be accessory proteins involved in the binding of PPAR γ to MIER1 α , which are not present in the *in vitro* assay. For these reasons, an *in vivo* assay is required to better characterize the interaction. These possibilities may explain why the interaction between PPAR γ and either MIER1 α or β was of similar intensity *in vivo*, contrary to what was observed in the GST pulldowns. This indicates that there may be some protein present in HEK-293 cells that may be facilitating the interaction between MIER1 α and β , and PPAR γ 2. In fact, preliminary studies have shown that MIER1 α interacts with RXR *in vitro*⁸⁶. PPAR γ and RXR are obligate heterodimer partners, and interact with each other even in the absence of ligand¹¹¹. RXR may therefore be facilitating the interaction between PPAR γ and MIER1. Future studies using cell lines lacking RXR (or siRNA-mediated knockdown of RXR) should be completed in order to determine the effect of RXR on the ability of MIER1 to bind PPAR γ *in vivo*.

The interaction of PPAR β/δ with MIER1 was expected, since all of the PPAR isoforms have the same basic nuclear receptor structure¹¹². As well, the entire PPAR family of nuclear receptors have been implicated in similar metabolic processes¹¹². However, PPAR β/δ is the only PPAR in the family that is not a target of current drugs for metabolic disorders¹¹³. PPAR β/δ has been implicated in reducing weight gain, increasing skeletal muscle metabolic rate and endurance, and improving insulin sensitivity and cardiovascular function¹¹³. Most importantly, since many drugs targeting PPAR γ lead to atherogenic inflammation¹¹⁴, a protein that could target both PPAR γ and PPAR β/δ would

be ideal. In fact, newer drugs for Type 2 diabetes are targeting both proteins in an effort to thwart the side effects of PPAR γ agonists alone¹¹⁵. MIER1 may therefore be a potential dual agonist for metabolic disorders. The effects of MIER1 on PPAR β/δ are outside the scope of this project, but future studies should aim to better characterize this interaction.

To determine whether the interaction between MIER1 α and β and PPAR γ 2 was ligand dependent, HEK-293 cells were treated with the thiazolidinedione, Troglitazone. Troglitazone is an agonist for PPAR γ which binds to the AF2 ligand-binding domain and is used in the treatment of Type 2 Diabetes. It can target PPAR γ 2 in the pancreas, skeletal muscle, and adipose tissue. Troglitazones mechanism of action, as a thiazolidinedione, involves the recruitment of GLUT4 receptors to the surface of cells in adipose tissue¹¹⁶ which allows for more efficient uptake of glucose and effectively lowering blood-glucose levels. At the molecular level, as a ligand for PPAR γ 2, it binds to PPAR at the ligand-binding domain and facilitates a conformational change that allows for the release of corepressor complexes and the recruitment of coactivator complexes.

The interaction between MIER1 and PPAR was ligand independent, when cells were treated with troglitazone for a period of 24 h. A similar ligand-independent interaction is observed with a known PPAR γ 2 coactivator (PPAR gamma coactivator-1 alpha, PGC-1 α)¹¹⁷. The LXXLL motif is common for ligand-dependent interactions¹¹⁷, and since the LXXLL motif was not responsible for the interaction between MIER1 and PPAR γ 2, the data fits this theory. More recently, CCPG (Constitutive Coactivator of PPAR γ) has been shown to also interact with PPAR γ 2 independent of the LXXLL

domain¹¹⁸. A 24 h treatment time is quite long when looking at transient interactions, therefore further studies should look at the treatment with ligand over a shorter time period (e.g. 1.5 h) to determine immediate effects of ligand on the interaction between PPAR and MIER1.

Since the interaction between the two isoforms of MIER1 and PPAR γ 2 have been confirmed in HEK-293 cells, the next step was to determine what effect this interaction had on the genomic function of PPAR γ 2. Our data demonstrates that MIER1 can function as a potent PPAR coactivator, with a similar stimulation of transcription as that seen with PGC-1 α . Similar to PGC-1 α , this stimulation occurred in both the presence and absence of troglitazone. This is in contrast to the ligand-dependent stimulation observed with most nuclear receptor-coactivator complexes^{119,120}. Without MIER1 α transfected into HEK-293 cells, treatment with troglitazone led to a significant increase in PPRE-dependent transcription, as expected. However, in the presence of MIER1 α and troglitazone, the fold activation above that seen with empty vector (CS3+MT) alone was the same as that seen with MIER1 α alone. In other words, MIER1 α augments activation at the PPRE independent of ligand – it functions as a novel coactivator. This ligand-independent activation of transcriptional activity should be further investigated between MIER1 and PPAR γ .

Since our data does not rule out the possibility that there are other PPAR γ 2 ligands present in HEK-293 cells that are bound to PPAR γ 2 and allowing for the recruitment of MIER1 to the coactivator complex. PGC-1 α was used as a positive

control, and as expected for a PPAR γ 2 coactivator, it augmented the activation of transcription at the PPRE in the presence and absence of troglitazone. In the absence of MIER1 there was a 7-fold increase in transcriptional activity at the PPRE when the cells were treated with troglitazone. This is expected since troglitazone is a ligand for PPAR and allows for recruitment of coactivators (in this case, endogenous coactivators) and transcription of the luciferase gene.

The data shows that MIER1 α and β interact with PPAR γ 2 independent of ligand as seen with PGC-1 α ¹²¹, and these proteins also increase transcriptional activity similar to PGC-1 α . The PGC-1 α protein has features (motifs) in common with MIER1 in that it contains a number of nuclear receptor boxes, such as the LXXLL motif¹²². PGC-1 α also contains a potent activation domain near the N-terminus, that can interact with other transcriptional coactivators¹¹⁷, as does MIER1¹²³. Future work should aim to look at whether the increase in transcriptional activity with MIER1 α or β is synergistic with PGC-1 α . If there is indeed a synergistic effect, it may suggest that MIER1 α or β are a part of a much larger transcriptional activation complex that also includes PGC-1 α . Previous work has shown that the mediator complex, a multiprotein complex of coactivators, is required to bridge the transcription factors to the transcriptional machinery and plays a pivotal role in adipocyte differentiation by coactivating PPAR γ ¹²⁴. MIER1, as a coactivator for PPAR γ 2, is likely involved in this complex. This can be determined by interaction studies with other components of this complex, including MED1, TRAP220 and DRIP205¹²⁴.

Since PPAR γ forms an obligate heterodimer with RXR, it was necessary to determine whether a ligand for RXR α had any effect on the ability of MIER1 to stimulate PPRE-dependent transcription. There was no significant difference between activation by MIER1 α in the presence or absence of 9-cis retinoic acid (Figure 17). This suggests that MIER1 may be stimulating transcription solely via its binding to PPAR γ and not indirectly via binding to RXR. Conversely, there was no increase in activation of PPRE-driven transcription after the addition of 9-cis retinoic acid in the control cells (lacking MIER1) either. This means that 1) the 9-cis retinoic acid is not working, 2) there are other endogenous ligands for RXR present in HEK-293 cells, or 3) RXR is the limiting protein in the system since it is not transfected into the cells. Other studies have shown that in cells transfected with the PPRE and treated with 9-cis retinoic acid alone, there was no significant increase in PPRE-driven transcription¹²⁵. In all of the PPRE-luciferase assays completed in this study, the use of HEK-293 cells provided endogenous retinoid x receptor (RXR) which is an obligate partner for PPAR γ to regulate transcription. At the same time, since RXR was not transfected into HEK-293 cells, the amount of endogenous RXR is the rate limiting component of this system which could be attenuating the amount of transcriptional activation seen with MIER1 α or β . If the cell had access to unlimited amounts of RXR (via overexpression), MIER1 α or β may cause an even greater increase in transcriptional activity at the PPRE. While these results suggest that MIER1 is acting independent of ligand for either PPAR γ or RXR, the rate-limiting factor in these cells is the presence of endogenous RXR. Since RXR was not transfected into these cells, but PPAR γ was transfected in (in excess), further studies are

required to determine if the activation by MIER1 α is actually higher than that shown in Figures 14, 15, 16, and 17.

It is well known that one of the most important physiological roles of PPAR γ 2 is in the process of adipogenesis⁶⁸. The dysregulation of this process can result in the development of cardiovascular disease, obesity and most notably, diabetes¹²⁶. Since both isoforms of MIER1 (α and β) caused significant activation of PPRE-driven transcription via interaction with PPAR γ 2, it was important to elucidate the biological relevance of this interaction. The 3T3-L1 model for adipogenesis has been well-established, and both MIER1 overexpression and knockdown studies (described in detail in Future Studies section) could be performed in this system.

PPAR γ 2 increases over the course of adipogenesis via a complex set of regulatory mechanisms¹²⁷. More specifically, after the induction of differentiation (Day 1) with a cocktail of IBMX, Dex and fetal bovine serum (FBS), ppar γ 2 mRNA levels increase up to approximately Day 8, and then level off¹²⁷. As a positive control, this exact trend was exhibited after PCR analysis of ppar γ 2 mRNA levels over 16 days of differentiation (Figure 16). Other coactivators have exhibited a similar trend over the course of the differentiation process in 3T3-L1 cells. For example, ADD1/SREBP-1 mRNA levels are upregulated very early on in the adipogenic program¹²⁸. ADD1 is a helix-loop-helix transcription factor that is expressed in differentiating adipocytes and regulated during differentiation of cultured adipocyte lines¹²⁹. A novel coactivator for PPAR γ , CCPG, has recently been shown to increase from Day 0 of adipogenesis and peak at Day 4¹³⁰.

This coincides with the pattern of expression observed for MIER1 (Figure 18). The importance of MIER1 in the regulation of adipogenesis has yet to be elucidated.

The importance of coactivators in the adipogenesis program cannot be stressed enough, and determining all of the components involved in the regulation of this differentiation process is paramount to understanding how adipose tissue acts as an endocrine organ. The expression of specific coactivators at specific times during this program can determine the ultimate fate of the specific cell. For example, PGC-1 α , which bears many similarities (physically and functionally) to MIER1, can induce the conversion of white adipose tissue (WAT) into brown adipose tissue via the upregulation of uncoupling protein 1 (UCP-1)¹³¹. UCP-1 is involved in the dissipation of energy as heat, and brown adipose tissue is abundant in rodents and human newborns, but very little in human adults. It is likely that the conversion of WAT to BAT (or at least, a BAT phenotype) could have therapeutic advantages in human adults¹³². Specifically, the induction of UCP-1 could increase fatty acid oxidation and lead to a decrease in fat mass¹³³. This is evidence that the expression of specific coactivators can contribute to the phenotype of adipose tissue and have implications in disease. If MIER1 acts like PGC-1 α , it may be functioning as a switch to transform pre-adipocytes into brown adipose versus white adipose tissue.

Since the mRNA levels of MIER1 increase from Day 0 of adipogenesis up to Day 6 and then levels off, the next step was to look *in vivo* at the cells by immunocytochemistry. Cells were stained on Day 0, Day 4 and Day 14 of adipogenesis using an anti-MIER1 α or β antibody and visualized by DAB staining. On Day 0 of

adipogenesis, there were no differentiated adipocytes and staining for MIER1 α and β was not observed. On Day 4 of adipogenesis, some staining of MIER1 α was observed, but there was no MIER1 β detected. On Day 14 of adipogenesis, MIER1 α staining was much stronger than on Day 4, but no staining was observed for MIER1 β . Therefore, MIER1 α is most likely the isoform involved in adipogenesis. Further work in characterizing the role of MIER1 in adipogenesis should focus on the α -isoform.

Only the 3T3-L1 cells that were differentiating/differentiated had MIER1 protein present – underlying undifferentiated cells did not contain MIER1. This was determined via phase-contrast microscopy, which allowed the observer to note underlying 3T3-L1 fibroblasts that had not changed morphology or begun to acquire lipid droplets in the cytoplasm, and were not positive for MIER1 α . The phase-contrast pictures are given along with the brightfield pictures, showing birefringent lipid droplets in the cytoplasm of differentiated adipocytes (Figure 21, 22). These lipid droplets could also be discerned by staining with Oil Red O (Figure 19). Another way of determining that the cells were differentiating (aside from visual cues) was the production of a known adipogenic protein, adiponectin. This protein is produced by differentiated 3T3-L1 cells, and was detected via western blot (Figure 20). It was not detected by western blot until Day 6, which is expected since the differentiated adipocytes did not appear until Day 4 and would require some time to produce detectable levels of adiponectin. At the same time, since only a subset of the cells were differentiating, the protein may have been present but undetectable.

Since the MIER1 protein levels start to increase and are still increasing up to Day 6 after initiation, and MIER1 α serves as a coactivator for PPAR γ 2, it is likely that MIER1 is involved in the second stage (differentiation) rather than the first stage (determination) of adipogenesis. The adipogenesis process is initiated by the IBMX-stimulated upregulation of C/EBP β and the DEX-stimulated upregulation of C/EBP δ . These proteins in turn facilitate the transcription of both C/EBP α and PPAR γ 2 (which is considered the second or differentiation stage of adipogenesis). C/EBP α is expressed at approximately Day 2 of adipogenesis, and is then phosphorylated (activated) by Cyclin D3-Cdk2 complex and can bind to and activate transcription of *ppar* γ 2¹³⁴. Therefore, MIER1 α levels are at their peak when PPAR γ 2 levels are high and activating transcription of target genes that contain a PPRE. This is further evidence that MIER1 α is a potent transcriptional activator for PPAR γ 2 and is found in the “right place at the right time” to serve this purpose.

The localization of MIER1 α in these 3T3-L1 adipocytes appears to be both cytoplasmic and nuclear, with the majority of staining around the lipid droplets. Since the cytoplasm in late differentiated adipocytes is merely a thin layer surrounding the lipid droplets, MIER1 α is concentrated in this area. This is consistent with earlier work that has shown MIER1 α is localized in the cytoplasm of NIH-3T3 cells¹³⁵, which are the cells from which the 3T3-L1 cells were derived. However, localization of MIER1 is cell type dependent⁸⁹. There may be a regulating complex that shuttles MIER1 to and from the cytoplasm. Others have shown that PPAR γ 2 staining in adipocytes during the later stages

of adipogenesis is concentrated around the forming lipid droplets, indicating a colocalization between these two interacting proteins in adipocytes⁹⁵. This is different from the expression pattern in other cell types, where PPAR γ is mostly nuclear^{136,137}. Consistent with the literature, Figure 23 indicates that the majority of PPAR γ staining is localized to the nucleus, with some PPAR γ present in the cytoplasm. Again, since the cytoplasm is greatly reduced due to the formation of lipid droplets, it is somewhat difficult to discern the exact pattern of staining. As well, the data shows that the temporal expression of MIER1 α protein occurs concomitantly with PPAR γ expression. This is interesting, since the localization of MIER1 α in neoplastic breast tissue is cytoplasmic, but nuclear in normal breast tissue⁸⁹. The reason for this has not yet been elucidated, but it has been shown that xMIER1 is retained in the cytoplasm by some sort of cytoplasmic anchoring protein, via the acidic activation domain¹³⁸.

Taken a step further, mammary adipose tissue has been shown to secrete factors (adipokines) that, compared to other stromal cell-secreted factors, is able to promote increased cell motility, migration and the capacity for angiogenesis¹³⁹. Therefore, not only is MIER1 α implicated in breast cancer via its interaction with the estrogen receptor (ER), but it may also play a role through its interaction with PPAR γ in mammary adipose tissue.

The immunofluorescence assay to look at colocalization clearly showed that both MIER1 α and PPAR γ were colocalized in the nucleus of a subset of differentiated 3T3-L1 cells. This was restricted to large, terminally differentiated adipocytes. This is important if MIER1 α is acting as a coactivator for PPAR γ -mediated transcription, since it must be

present in the nucleus to directly regulate gene transcription. Further studies are required to determine the proportion of these differentiated 3T3-L1 cells that have subcellular localization of both PPAR γ 2 and MIER1 α , to further define the relationship between these two proteins.

Since the majority of MIER1 α staining is cytoplasmic, and PPAR γ in 3T3-L1s is also cytoplasmic, a mechanism of non-genomic action of MIER1 α may be possible. PPAR γ has a number of non-genomic effects via signal transduction pathways. Most recently described is the effect of MAPK kinases on PPAR γ subcellular localization¹³⁶. MEKs can translocate to the nucleus (where PPAR γ normally resides), but are rapidly exported out of the nucleus by their nuclear export signal (NES). As they are exported from the nucleus they take their interacting partner, PPAR γ , into the cytoplasm as well¹³⁶. MIER1 α may be performing a similar role late in the adipogenic program when PPAR γ is no longer required.

There was less PPAR γ and MIER1 α present in terminally differentiated (late) adipocytes at Day 16, as revealed by immunofluorescence analysis (data not shown). This follows what is observed in the literature, since PPAR γ 2 has transcribed the required genes for the differentiation portion of the adipogenic program and is no longer useful to the mature adipocyte. At the same time, MIER1 α , functioning as a coactivator for PPAR γ 2, would be redundant after adipogenesis has occurred. Further studies should follow the subcellular localization of MIER1 α and PPAR γ over each day of adipogenesis

to determine the exact mechanism by which these proteins influence the subcellular location of each other.

Proposed model for MIER1 activation of PPAR γ 2

The localization of MIER1 α in 3T3-L1 cells appears to be mainly cytoplasmic, while PPAR γ 2 is both nuclear and cytoplasmic. Since PPAR γ 2 exerts some of its effects in the nucleus and MIER1 α has been shown to act as a coactivator for PPAR γ 2, the localization of MIER1 could fit with this coactivator theory. However, the transcription assays in this study were undertaken in HEK-293 cells, while the localization of MIER1 α was determined in 3T3-L1 cells. While this is one possible mechanism for PPAR γ stimulation by MIER1 α , the subcellular localization of MIER1 α in HEK-293 cells should be determined to support this model. The exact mechanism by which MIER1 α exerts its effect on PPAR γ 2 has yet to be elucidated, but based on the similarity of MIER1 α to one of the well-characterized coactivators for PPAR γ 2 (PGC-1 α) this mechanism is one possibility.

The mechanism of action for PGC-1 α involves binding of PPAR γ 2, followed by a conformational change that allows docking of other coactivators that contain histone acetyltransferase activity (e.g. CBP/p300, SRC-1). This has been referred to as the “spring-trap” model¹⁴⁰, since PPAR γ 2 opens up like a trap-door to provide more binding sites for other transcriptional cofactors. Since MIER1 α has been shown to interact with CBP/p300 and has a similar fold-activation of PPRE-driven transcription, it may be acting as a coactivator for PPAR γ 2 in a similar mechanism as PGC-1 α .

Based on the large amount of cytoplasmic staining for MIER1 α observed in differentiated 3T3-L1 cells, a mechanism of non-genomic action of this protein should also be discussed. MIER1 α has been determined to contain the well characterized EF-hand, which is a calcium (Ca²⁺) binding site. EF-hand proteins have been implicated in the non-genomic pathways associated with nuclear receptors. For example, the Modulator of Nongenomic Activity of ER (MNAR) is a scaffolding protein containing an EF-hand that can affect ER interaction with Src tyrosine kinases and can lead to stimulation of the MAPK pathway¹⁴¹. In the case of PPAR γ , it has been demonstrated in vascular smooth muscle cells that PPAR agonists rapidly induce ERK activation and *c-fos* mRNA expression, suggesting a non-genomic function of these ligands¹⁴². However, it has not been determined whether this non-genomic signaling is PPAR γ dependent or independent. Immunofluorescence has demonstrated that PPAR γ is present in both the cytoplasm and in the nucleus (Figure 21), consistent with the findings in the literature which show PPAR γ 2 surrounding the lipid droplets in later stages of adipogenesis¹⁴³. HMI-ER1 α , with the EF-hand domain, may regulate its non-genomic effects through calcium signaling pathways in the cell. It has also recently been discovered that MIER1 α also contains a calmodulin binding site (O'Day, D., personal communication, 2008), that together with the EF-hand could allow MIER1 α to serve as a signaling intermediate in calcium-dependent pathways.

Another possibility is that MIER1 may be regulating the subcellular localization of PPAR γ 2, similar to PPAR γ 2 shuttling via interaction with MAPK kinases¹³⁶. Since

PPAR γ 2 surrounds the lipid droplets at later stages of adipogenesis¹⁴³, and MIER1 α staining is mainly cytoplasmic (specifically surrounding lipid droplets), it may be acting as an anchor to keep PPAR γ 2 in the cytoplasm. In the very late stages of adipogenesis, when the cells are full of lipid and there is virtually no visible cytoplasm left, MIER1 α may move into the nucleus (as shown in Figure 23, bottom panel) and regulate PPAR γ 2-dependent transcription.

Implications

The implications of an interaction between PPAR γ and MIER1 α are significant and seem to be intimately tied to hormone signaling between adipose tissue, the pancreas, and the rest of the body. Ligands that activate PPAR γ in both adipose tissue and the pancreas have been made famous via their ability to reduce insulin resistance and hyperglycemia in type 2 diabetes¹⁴⁴. Recent work on the location of MIER1 in mouse tissues has shown that MIER1 α is highly expressed in the Islets of Langerhans in the pancreas. Combined with this study which has shown MIER1 α is expressed in 3T3-L1 adipocytes, MIER1 is in the right places to serve as a target for type 2 diabetes therapy. While its role in the pancreas has not yet been elucidated, the possibility that MIER1 α activates PPAR γ transcriptional activity in 3T3-L1 adipocytes suggests it may do the same in the β -cells of the pancreas. It has been shown that troglitazone (an agonist for PPAR γ 2) actually functions in part by maintaining or preserving β -cell mass¹⁴⁵.

It would be interesting to see if MIER1 α is downregulated in the β -cells of the pancreas or adipose tissue in type 2 diabetes. This would provide a mechanism whereby loss of MIER1 α would result in decreased activity of PPAR γ (a hallmark of type 2 diabetes) and progression of the disease. The MIER1 α knockdown experiments suggested in future studies should demonstrate the requirement for MIER1 α in the adipogenic program. It is hypothesized that a knockdown of this coactivator for PPAR γ 2 would prevent the differentiation process. Taken a step further, a reduction in the level of MIER1 α in both the pancreas and the adipose tissue would dysregulate PPAR γ 2 activity and eventually lead to type 2 diabetes.

As mentioned briefly in the model for MIER1 α activation of PPAR γ 2, MIER1 α has an EF-hand involved in calcium binding. If we look at the role of the β -cells in insulin secretion, a role for MIER1 α is not difficult to discern. It has been shown that β -cells sense glucose through its metabolism. This results in an increase in the ATP/ADP ratio, which closes the K_{ATP} channels and leads to plasma membrane depolarization, the influx of Ca^{2+} , and, finally, insulin secretion¹⁴⁶. This influx of calcium may trigger MIER1 α to bind to PPAR γ 2 and initiate transcription of key target genes involved in the release of insulin from the β -cells (e.g. uncoupling protein-2, UCP-2). Therefore, MIER1 α may serve as a novel therapeutic target for type 2 diabetes through its regulation of PPAR γ 2 transcriptional activity in these particular endocrine organs (adipose tissue and pancreas).

Future Studies

While much progress has been made in terms of the biological function of MIER1 in regulating PPAR γ 2 activity and the process of adipogenesis, more work is required to determine the exact mechanism by which MIER1 α activates PPAR γ 2. Once this mechanism has been extensively characterized, the potential for MIER1 to serve as a novel therapeutic target for Type 2 Diabetes or obesity can be determined. Given below are some of the experiments that should be completed or are in progress in order to probe deeper into possible mechanisms of MIER1 activity.

4.9.1 Determine the domain of PPAR γ 2 that interacts with MIER1

To determine the exact mechanism by which MIER1 interacts with and activates PPAR γ 2, it is necessary to determine which domain of PPAR γ 2 is involved in the interaction between these two proteins. The best way to determine this interaction site would be through immunoprecipitation using deletion constructs of PPAR γ 2. These deletion constructs have been used in another study to assess the interaction domain between PPAR γ 2 and CCPG¹⁴⁷.

4.9.2 Demonstrate *in vivo* interaction between PPAR γ 2 and MIER1 α

The *in vivo* interaction between PPAR γ 2 and MIER1 α has been demonstrated in this study via the transfection of HEK-293 cells with both PPAR γ 2 plasmid and myc-

tagged MIER1 α plasmid, followed by subsequent immunoprecipitation and immunoblot. However, this involves overexpression of both proteins in the cell. A better way to confirm this interaction would be to do an immunoprecipitation and immunoblot relying on endogenous levels of both proteins in the cell, since this is more physiologically relevant. For this experiment, a cell line that expresses both PPAR γ 2 and MIER1 α would have to be used. Since both of these proteins are present at high levels during adipogenesis in 3T3-L1 cells, this would be an excellent cell line to use.

4.9.3 Determine the effect shRNA-mediated reduction in MIER1 α levels has on adipogenesis

MIER1 α has been shown here to act as a transcriptional activator for PPAR γ 2, with strikingly similar characteristics to another known coactivator, PGC-1 α . Also determined here is the fact that MIER1 protein and mRNA levels increase over the course of adipogenesis in a pattern comparable to that seen for PPAR γ 2 protein and mRNA levels. Therefore the exact role of MIER1 α in this differentiation process must be determined. Future work is in progress in using short hairpin RNA (shRNA) developed against specific regions of MIER1 α . These shRNA will be transfected into 3T3-L1 preadipocytes in order to knockdown expression levels of MIER1 α and determine the effect on adipogenesis. In another study that looked at a novel coactivator for PPAR γ 2, the knockdown of that protein (CCPG) resulted in significantly less adipocyte differentiation as measured by Oil Red-O staining of lipid droplets and western blot of

adipocyte-specific markers adiponectin and perilipin¹⁴⁸. It is hypothesized that a knockdown of MIER1 α , which functions as a transcriptional activator for PPAR γ 2, will either prohibit or severely impair the differentiation of 3T3-L1 fibroblasts into mature adipocytes.

4.9.4 Determine other biologically relevant functions of MIER1 α -mediated activation of PPAR γ 2

While the majority of research on PPAR γ 2 has focused on adipogenesis and implications of PPAR γ 2 for type 2 diabetes, there are a number of other biological functions for this nuclear receptor. Specifically, PPAR γ 2 plays an important role in the pancreatic islet cells and it has been recently discovered that MIER1 α is expressed in the islets of Langerhans in the mouse pancreas¹⁴⁹. The first thing to determine here is whether PPAR γ 2 and MIER1 α are colocalized in the same types of cells in the islets (either the α , β or δ cells) using immunohistochemistry and co-staining with either glucagon, insulin or somatostatin for the specific cells of the islets. From there, further work could focus on the exact role of MIER1 α on PPAR γ 2 function in the pancreas.

An exciting field of research has been focusing on mouse models, and it would be advantageous to this study if a conditional knockout mouse was generated – specifically, knockdown of MIER1 α in the pancreas or in the adipose tissue. The phenotype of this knockout mouse would provide more insight into the function of MIER1 in the aforementioned metabolic regulation processes. Similarly, the effect of overexpressing MIER1 in a mouse model that has Type 2 diabetes could also be determined. There is

virtually no limit to the amount of data that could be harvested from mouse models like this. If results of these expression experiments in mice mirror the data obtained thus far with PPAR γ and MIER1 α , this brings MIER1 α to the forefront of potential drug targets for a wide array of metabolic disorders.

Reference List

1. Wang,Z. & Burge,C.B. Splicing regulation: From a parts list of regulatory elements to an integrated splicing code. *RNA* 14, 802-813. 2008.
2. Paterno,G.D. *et al.* Genomic organization of the human mi-er1 gene and characterization of alternatively spliced isoforms: regulated use of a facultative intron determines subcellular localization. *Gene* 295, 79-88 (2002).
3. Paterno,G.D. *et al.* Genomic organization of the human mi-er1 gene and characterization of alternatively spliced isoforms: regulated use of a facultative intron determines subcellular localization. *Gene* 295, 79-88 (2002).
4. Paterno,G.D. *et al.* Genomic organization of the human mi-er1 gene and characterization of alternatively spliced isoforms: regulated use of a facultative intron determines subcellular localization. *Gene* 295, 79-88 (2002).
5. Heery,D.M., Kalkhoven,E., Hoare,S. & Parker,M.G. A signature motif in transcriptional co-activators mediates binding to nuclear receptors. *Nature* 387(12), 733-737. 1997.
6. Ding,Z., Gillespie,L.L. & Paterno,G.D. Human MI-ER1 alpha and beta function as transcriptional repressors by recruitment of histone deacetylase 1 to their conserved ELM2 domain. *Mol. Cell Biol.* 23, 250-258 (2003).
7. de la Cruz,X., Lois,S., Sanchez-Molina,S. & Martinez-Balbas,M.A. Do protein motifs read the histone code? *BioEssays* 27(2), 164-175. 2005.
8. Wang,L., Charroux,B., Kerridge,S. & Tsai,C. Atrophin recruits HDAC1/2 and G9a to modify histone H3K9 and to determine cell fates. *European Molecular Biology Organization* 9(6), 555-562. 28-3-2008.
9. Lee,M.G. *et al.* Functional Interplay between Histone Demethylase and Deacetylase Enzymes. *Mol.Cell Biol.* 26(17), 6395-6402. 2006.
10. Wang,L., Charroux,B., Kerridge,S. & Tsai,C. Atrophin recruits HDAC1/2 and G9a to modify histone H3K9 and to determine cell fates. *European Molecular Biology Organization* 9(6), 555-562. 28-3-2008.
11. Ding,Z., Gillespie,L.L. & Paterno,G.D. Human MI-ER1 alpha and beta function as transcriptional repressors by recruitment of histone deacetylase 1 to their conserved ELM2 domain. *Mol. Cell Biol.* 23, 250-258 (2003).

12. Wang,L., Charroux,B., Kerridge,S. & Tsai,C. Atrophin recruits HDAC1/2 and G9a to modify histone H3K9 and to determine cell fates. *European Molecular Biology Organization* 9(6), 555-562. 28-3-2008.
13. Wang,L., Charroux,B., Kerridge,S. & Tsai,C. Atrophin recruits HDAC1/2 and G9a to modify histone H3K9 and to determine cell fates. *European Molecular Biology Organization* 9(6), 555-562. 28-3-2008.
14. Paterno,G.D., Li,Y., Luchman,H.A., Ryan,P.J. & Gillespie,L.L. cDNA cloning of a novel, developmentally regulated immediate early gene activated by fibroblast growth factor and encoding a nuclear protein. *J.Biol.Chem.* 272, 25591-25595. 1997. Memorial University of Newfoundland.
15. Ding,Z., Gillespie,L.L. & Paterno,G.D. Human MI-ER1 alpha and beta function as transcriptional repressors by recruitment of histone deacetylase 1 to their conserved ELM2 domain. *Mol. Cell Biol.* 23, 250-258 (2003).
16. Ding,Z., Gillespie,L.L. & Paterno,G.D. Human MI-ER1 alpha and beta function as transcriptional repressors by recruitment of histone deacetylase 1 to their conserved ELM2 domain. *Mol. Cell Biol.* 23, 250-258 (2003).
17. Ding,Z., Gillespie,L.L., Mercer,F.C. & Paterno,G.D. The SANT domain of human MI-ER1 interacts with Sp1 to interfere with GC box recognition and repress transcription from its own promoter. *J Biol. Chem.* 279, 28009-28016 (2004).
18. Teplitsky,Y., Paterno,G.D. & Gillespie,L.L. Proline 365 is a critical residue for the activity of xMIER1 in *Xenopus* embryonic development. *Biochem.Biophys.Res.Comm.* 308, 679-683. 2003.
19. Buday,L. Membrane-targeting of signalling molecules by SH2/SH3 domain-containing adaptor proteins. *Biochimica et Biophysica Acta* 1422(2), 187-204. 1999.
20. Shi,Y. Orphan nuclear receptors in drug discovery. *Drug Discovery Today* 12(11-12), 440-445. 2007.
21. Wang,D. & Dubois,R.N. Peroxisome proliferator-activated receptors and progression of colorectal cancer. *PPAR. Res* 2008, 931074 (2008).
22. Schug,T.T. *et al.* Overcoming retinoic acid-resistance of mammary carcinomas by diverting retinoic acid from PPARbeta/delta to RAR. *Proc. Natl. Acad. Sci. U. S. A* 105, 7546-7551 (2008).

23. Prasad,K.N., Saxena,A., Ghoshal,U.C., Bhagat,M.R. & Krishnani,N. Analysis of Pro12Ala PPAR gamma polymorphism and Helicobacter pylori infection in gastric adenocarcinoma and peptic ulcer disease. *Ann. Oncol.* (2008).
24. Matsuyama,M. & Yoshimura,R. Peroxisome Proliferator-Activated Receptor-gamma Is a Potent Target for Prevention and Treatment in Human Prostate and Testicular Cancer. *PPAR. Res* 2008, 249849 (2008).
25. Roman,J. Peroxisome proliferator-activated receptor gamma and lung cancer biology: implications for therapy. *J Investig. Med.* 56, 528-533 (2008).
26. Han,S., Ritzenthaler,J.D., Zheng,Y. & Roman,J. PPAR beta/delta agonist stimulates human lung carcinoma cell growth through inhibition of PTEN expression: the involvement of PI3K and NF-kappaB signals. *Am.J.Physiol Lung Cell Mol Physiology* 294(6), L1238-L1249. 2008.
27. Rosenson,R.S. Effects of peroxisome proliferator-activated receptors on lipoprotein metabolism and glucose control in type 2 diabetes mellitus. *Am. J. Cardiol.* 99, 96B-104B (2007).
28. Rosenson,R.S. Effects of peroxisome proliferator-activated receptors on lipoprotein metabolism and glucose control in type 2 diabetes mellitus. *Am. J. Cardiol.* 99, 96B-104B (2007).
29. Rosenson,R.S. Effects of peroxisome proliferator-activated receptors on lipoprotein metabolism and glucose control in type 2 diabetes mellitus. *Am. J. Cardiol.* 99, 96B-104B (2007).
30. Mukherjee,R., Jow,L., Croston,G.E. & Paterniti Jr,J.R. Identification, characterization and tissue distribution of human ppar isoforms ppar gamma 2 versus ppar gamma 1 and activation with retinoid x receptor agonists and antagonists. *J.Biol.Chem.* 272(12), 8071-8076. 1997.
31. Escher,P. *et al.* Rat PPARs: Quantitative analysis in adult rat tissues and regulation in fasting and refeeding. *Endocrinology* 142(10), 4195-4202. 2001.
32. Fournier,T., Tsatsaris,V., Handschuh,K. & Evain-Brion,D. PPARs and the Placenta. *Placenta* 28(2-3), 65-76. 2006.
33. Stumvoll,M. & Haring,H. The peroxisome proliferator-activated receptor-gamma2 Pro12Ala polymorphism. *Diabetes* 51, 2341-2347 (2002).

34. Kintscher,U. & Law,R.E. PPARgamma-mediated insulin sensitization: the importance of fat versus muscle. *Am. J. Physiol Endocrinol. Metab* 288, E287-E291 (2005).
35. Andersen,O., Eijsink,V.G. & Thomassen,M. Multiple variants of the peroxisome proliferator-activated receptor (PPAR) gamma are expressed in the liver of atlantic salmon (*Salmo salar*). *Gene* 255, 411-418 (2000).
36. Chen,J.G. *et al.* Identification of a peroxisome proliferator responsive element (PPRE)-like cis-element in mouse plasminogen activator inhibitor-1 gene promoter. *Biochem. Biophys. Res. Commun.* 347, 821-826 (2006).
37. Tomaru,T. *et al.* Isolation and characterization of a transcriptional cofactor and its novel isoform that bind the deoxyribonucleic acid-binding domain of peroxisome proliferator-activated receptor-gamma. *Endocrinology* 147, 377-388 (2006).
38. Gray,J.P., Burns,K.A., Leas,T.L., Perdew,G.H. & Vanden Heuvel,J.P. Regulation of Peroxisome Proliferator-activated receptor alpha by protein kinase C. *Biochemistry* 44(30), 10313-10321. 2005.
39. Torra,I. *et al.* Peroxisome proliferator activated receptors: from transcriptional control to clinical practice. *Lipidology* 12(3), 245-254. 2001.
40. Stanley,T.B. *et al.* Subtype specific effects of peroxisome proliferator-activated receptor ligands on corepressor affinity. *Biochemistry* 42, 9278-9287 (2003).
41. Sumanasekera,W.K. *et al.* Heat shock protein 90 (Hsp90) acts as a repressor of ppar alpha and ppar beta activity. *Biochemistry* 42(36), 10726-10735. 2003.
42. Kim,J.B., Wright,H.M., Wright,M. & Spiegelman,B.M. ADD1/SREBP1 activates PPARgamma through the production of endogenous ligand. *Proc.Natl.Acad.Sci.U.S.A* 95(8), 4333-4337. 1998.
43. Lee,S. & Privalsky,M.L. Heterodimers of Retinoic Acid Receptors and Thyroid Hormone Receptors Display Unique Combinatorial Regulatory Properties. *Molecular Endocrinology* 19, 863-878 (2005).
44. Semple,R.K., Chatterjee,V.K.K. & O'rahilly,S. PPARg and human metabolic disease. *J.Clin.Invest* 116(3), 581-589. 2006.

45. Saiki, M. *et al.* Pioglitazone inhibits the growth of human leukemia cell lines and primary leukemia cells while sparing normal hematopoietic stem cells. *Int. J. Oncol.* 29, 437-443 (2006).
46. Ziouzenkova, O. & Plutzky, J. retinoid metabolism and nuclear receptor responses: new insights into coordinated regulation of the PPAR-RXR complex. *FEBS Letters* 582, 32-38. 2008.
47. Kersten, S., Desvergne B & Wahli, W. Roles of PPARs in health and disease. 421-424. 25-5-2007.
48. Chen, J.G. *et al.* Identification of a peroxisome proliferator responsive element (PPRE)-like cis-element in mouse plasminogen activator inhibitor-1 gene promoter. *Biochem. Biophys. Res. Commun.* 347, 821-826 (2006).
49. Lonard, D.M. & O'Malley, B. Nuclear Receptor Coregulators: judges, juries, and executioners of cellular regulation. *Mol. Cell* 27, 691-700. 9-7-2007.
50. Chen, J.G. *et al.* Identification of a peroxisome proliferator responsive element (PPRE)-like cis-element in mouse plasminogen activator inhibitor-1 gene promoter. *Biochem. Biophys. Res. Commun.* 347, 821-826 (2006).
51. Horlein, A.J. *et al.* Ligand-independent repression by the thyroid hormone receptor mediated by a nuclear receptor co-repressor. *Nature* 377, 397-404. 1995.
52. Sande, S. & Privalsky, M.L. Identification of TRACs, a family of co-factors that associate with and modulate the activity of nuclear hormone receptors. *Mol. Endocrinol.* 10, 813-825. 1996.
53. Lonard, D.M. & O'Malley, B. Nuclear Receptor Coregulators: judges, juries, and executioners of cellular regulation. *Mol. Cell* 27, 691-700. 9-7-2007.
54. Coste, A. *et al.* Absence of the steroid receptor coactivator-3 induces B-cell lymphoma. *European Molecular Biology Organization* 25(11), 2453-2464. 2006.
55. Feige, J.N. *et al.* Fluorescence imaging reveals the nuclear behavior of PPAR/RXR heterodimers in the absence and presence of ligand. *J. Biol. Chem.* 280(18), 17880-17890. 6-5-2005.
56. Cazzalini, O. *et al.* Interaction of p21 (CDKN1A) with PCNA regulates the histone acetyltransferase activity of p300 in nucleotide excision repair. *Nucleic Acids Res.* 36(5), 1713-1722. 31-3-2008.

57. Musri,M.M., Gomis,R. & Parrizas,M. Chromatin and chromatin-modifying proteins in adipogenesis. *Biochemistry and Cell Biology* 85(1), 397-410. 6-1-2007.
58. Musri,M.M., Gomis,R. & Parrizas,M. Chromatin and chromatin-modifying proteins in adipogenesis. *Biochemistry and Cell Biology* 85(1), 397-410. 6-1-2007.
59. Musri,M.M., Gomis,R. & Parrizas,M. Chromatin and chromatin-modifying proteins in adipogenesis. *Biochemistry and Cell Biology* 85(1), 397-410. 6-1-2007.
60. Karamanlidis,G., Karamitri,A., Docherty,K., Hazlerigg,D.G. & Lomax,M.A. C/EBP β reprograms white 3t3-l1 preadipocytes to a brown adipocyte pattern of gene expression. *J Biol.Chem.* 282(34), 24660-24669. 4-8-2007.
61. Karamanlidis,G., Karamitri,A., Docherty,K., Hazlerigg,D.G. & Lomax,M.A. C/EBP β reprograms white 3t3-l1 preadipocytes to a brown adipocyte pattern of gene expression. *J Biol.Chem.* 282(34), 24660-24669. 4-8-2007.
62. Nedergaard,J., Matthias,A., Golozoubova,V., Jacobsson,A. & Cannon,B. UCP1: The original uncoupling protein - and perhaps the only one? *Journal of Bioenergetics and Biomembranes* 31(5), 475-491. 1999.
63. Nedergaard,J., Bengtsson,T. & Cannon,B. Unexpected evidence for active brown adipose tissue in adult humans. *Am.J.Physiol Endocrinol.Metab* 293, 444-452. 23-4-2007.
64. Yoo,E.J., Chung,J., Choe,S.S., Kim,K.H. & Kim,J.B. Down-regulation of Histone Deacetylases Stimulates Adipocyte Differentiation. *J. Biol. Chem.* 281, 6608-6615 (2007).
65. Yoo,E.J., Chung,J., Choe,S.S., Kim,K.H. & Kim,J.B. Down-regulation of Histone Deacetylases Stimulates Adipocyte Differentiation. *J. Biol. Chem.* 281, 6608-6615 (2007).
66. Saye,J.A., Cassis,L.A., Sturgill,T.W., Lynch,K.R. & Peach,M.J. Angiotensinogen gene expression in 3T3-L1 cells. *Am. J. Physiol Cell Physiol* 256, 448-451 (2007).
67. Pantoja,C., Huff,J.T. & Yamamoto,K.R. Glucocorticoid signaling defines a novel commitment state during adipogenesis in vitro. *Mol.Biol.Cell.* 2008.
68. Farmer,S.R. Regulation of PPAR γ activity during adipogenesis. *Int.J.Obesity* 29, S13-S16. 2005.

69. Musri,M.M., Gomis,R. & Parrizas,M. Chromatin and chromatin-modifying proteins in adipogenesis. *Biochemistry and Cell Biology* 85(1), 397-410. 6-1-2007.
70. Goethe,R., Basler,T. & Phi-van,L. Regulation of C/EBPb mRNA expression and C/EBPb promoter activity by protein kinases A and C in a myelomonocytic cell line (HD11). *Inflammation Research* 56, 274-281. 2008.
71. Reichert,M. & Eick,D. Analysis of cell cycle arrest in adipocyte differentiation. *Oncogene* 18, 459-466. 1999.
72. Musri,M.M., Gomis,R. & Parrizas,M. Chromatin and chromatin-modifying proteins in adipogenesis. *Biochemistry and Cell Biology* 85(1), 397-410. 6-1-2007.
73. Tontonoz,P., Hu,E. & Spiegelman,B.M. Regulation of adipocyte gene expression and differentiation by peroxisome proliferator activated receptor gamma. *Curr. Opin. Genet. Dev.* 5, 571-576 (1995).
74. Rosen,E.D. The transcriptional basis of adipocyte development. Prostaglandins leukotrienes and Essential Fatty Acids 73(1), 31-34. 2005.
75. Musri,M.M., Gomis,R. & Parrizas,M. Chromatin and chromatin-modifying proteins in adipogenesis. *Biochemistry and Cell Biology* 85(1), 397-410. 6-1-2007.
76. Musri,M.M., Gomis,R. & Parrizas,M. Chromatin and chromatin-modifying proteins in adipogenesis. *Biochemistry and Cell Biology* 85(1), 397-410. 6-1-2007.
77. Musri,M.M., Gomis,R. & Parrizas,M. Chromatin and chromatin-modifying proteins in adipogenesis. *Biochemistry and Cell Biology* 85(1), 397-410. 6-1-2007.
78. Reaven,G.M. Is Insulin resistance becoming a global epidemic? *Diabetes* 37, 1595. 1988.
79. Semple,R.K., Chatterjee,V.K.K. & O'rahilly,S. PPARg and human metabolic disease. *J.Clin.Invest* 116(3), 581-589. 2006.
80. Kjos,S.L. & Buchanan,T.A. Gestational Diabetes Mellitus. *Journal of Medicine* 341(1749), 1756. 1999.
81. Semple,R.K., Chatterjee,V.K.K. & O'rahilly,S. PPARg and human metabolic disease. *J.Clin.Invest* 116(3), 581-589. 2006.

82. Semple,R.K., Chatterjee,V.K.K. & O'rahilly,S. PPARg and human metabolic disease. *J.Clin.Invest* 116(3), 581-589. 2006.
83. Semple,R.K., Chatterjee,V.K.K. & O'rahilly,S. PPARg and human metabolic disease. *J.Clin.Invest* 116(3), 581-589. 2006.
84. Semple,R.K., Chatterjee,V.K.K. & O'rahilly,S. PPARg and human metabolic disease. *J.Clin.Invest* 116(3), 581-589. 2006.
85. Savicky,M. Characterization of human mesoderm induction-early response 1 (hMI-ER1) as a nuclear hormone receptor cofactor. 2004.
86. Jenkins,G.H. In vitro interaction of a transcriptional regulatory protein, hMIER1 alpha, with retinoic acid receptors and retinoid x receptors. 2007.
87. Savicky,M. Characterization of human mesoderm induction-early response 1 (hMI-ER1) as a nuclear hormone receptor cofactor. 2004.
88. Ryan,P.J. & Gillespie,L.L. Phosphorylation of phospholipase C gamma 1 and its association with the FGF receptor is developmentally regulated and occurs during mesoderm induction in *Xenopus laevis*. *Developmental Biology* 166(1), 101-111. 1994.
89. McCarthy,P.L. *et al.* Changes in subcellular localization of MI-ER1a, a novel estrogen receptor alpha interacting protein, is associated with breast cancer progression. *British Journal of Cancer* . 2008.
90. Gilsbach,R., Kouta,M., Bonisch,H. & Bruss,M. Comparison of in vitro and in vivo reference genes for internal standardization of real-time PCR data. *Biotechniques* 40(2), 173-177. 2006.
91. Paterno,G.D. *et al.* Genomic organization of the human mi-er1 gene and characterization of alternatively spliced isoforms: regulated use of a facultative intron determines subcellular localization. *Gene* 295, 79-88 (2002).
92. Savicky,M. Characterization of human mesoderm induction-early response 1 (hMI-ER1) as a nuclear hormone receptor cofactor. 2004.
93. Paterno,G.D. *et al.* Genomic organization of the human mi-er1 gene and characterization of alternatively spliced isoforms: regulated use of a facultative intron determines subcellular localization. *Gene* 295, 79-88 (2002).
94. Ryan,P.J., Paterno,G.D. & Gillespie,L.L. Identification of phosphorylated proteins associated with the fibroblast growth factor receptor type 1 during

- early xenopus development. *Biochem.Biophys.Res.Commun.* 244(3), 763-767. 1998.
95. Paterno,G.D. *et al.* Genomic organization of the human mi-er1 gene and characterization of alternatively spliced isoforms: regulated use of a facultative intron determines subcellular localization. *Gene* 295, 79-88 (2002).
 96. Ding,Z., Gillespie,L.L. & Paterno,G.D. Human MI-ER1 alpha and beta function as transcriptional repressors by recruitment of histone deacetylase 1 to their conserved ELM2 domain. *Mol. Cell Biol.* 23, 250-258 (2003).
 97. Morita,K. *et al.* Selective allosteric ligand activation of the retinoid x receptor heterodimers of NGF1-B and Nurr1. *Biochemical Pharmacology* 71, 98-107 (2005).
 98. Matsusue,K., Peters,J.M. & Gonzalez,F.J. PPAR beta/delta potentiates PPAR gamma-stimulated adipocyte differentiation. *FASEB J.* 18(12), 1477-1479. 2004.
 99. Qiang,L., Wang,H. & Farmer,S.R. Adiponectin secretion is regulated by SIRT1 and the endoplasmic reticulum oxidoreductase Ero1-La. *Mol.Cell Biol.* 27(13), 4698-4707. 2007.
 100. Finck,B.N. & Kelly,D.P. PGC-1 coactivators: inducible regulators of energy metabolism in health and disease. *J.Clin.Invest* 116(3), 615-622. 1-3-2006.
 101. Blackmore,T. An investigation into the role of human mesoderm induction-early response 1 (hMI-ER1) in regulating a histone acetyltransferase, a chromatin remodeling enzyme. *Biomedical Central, Research Notes* . 2004.
 102. Finck,B.N. & Kelly,D.P. PGC-1 coactivators: inducible regulators of energy metabolism in health and disease. *J.Clin.Invest* 116(3), 615-622. 1-3-2006.
 103. Savicky,M. Characterization of human mesoderm induction-early response 1 (hMI-ER1) as a nuclear hormone receptor cofactor. 2004.
 104. Savicky,M. Characterization of human mesoderm induction-early response 1 (hMI-ER1) as a nuclear hormone receptor cofactor. 2004.
 105. Liu,B., Gross,M., Hoeve,J.T. & Shuai,K. A transcriptional corepressor of Stat1 with an essential LXXLL signature motif. *Proc.Natl.Acad.Sci.U.S.A* 98(6), 3203-3207. 2001.
 106. Savicky,M. Characterization of human mesoderm induction-early response 1 (hMI-ER1) as a nuclear hormone receptor cofactor. 2004.

107. Sterner,D.E., Wang,X., Bloom,M.H., Simon,G.M. & Berger,S.L. The SANT domain of Ada2 is required for normal acetylation of histones by the Yeast SAGA complex. *J.Biol.Chem.* 277(10), 8178-8186. 26-12-2001.
108. Wang,L., Charroux,B., Kerridge,S. & Tsai,C. Atrophen recruits HDAC1/2 and G9a to modify histone H3K9 and to determine cell fates. *European Molecular Biology Organization* 9(6), 555-562. 28-3-2008.
109. Li,D., Kang,Q. & Wang,D. Constitutive coactivator of PPAR gamma, a novel coactivator of PPAR gamma that promotes adipogenesis. *Mol.Endocrinol.* 21(10), 2320-2333. 10-1-2007.
110. Gelman,L. *et al.* p300 interacts with the N- and C-terminal part of PPARgamma 2 in a ligand-independent and - dependent manner, respectively. *J.Biol.Chem.* 274(12), 7681-7688. 19-3-1999.
111. Feige,J.N. *et al.* Fluorescence imaging reveals the nuclear behavior of PPAR/RXR heterodimers in the absence and presence of ligand. *J.Biol.Chem.* 280(18), 17880-17890. 6-5-2005.
112. Berger,J. & Moller,D.E. The mechanisms of action of ppars. *Ann.Rev.Med.* 53, 409-435. 2002.
113. Reilly,S.M. & Lee,C.H. PPAR delta as a therapeutic target in metabolic disease. *FEBS Letters* 582(1), 26-31. 2007.
114. Sulistio,M.S., Zion,A., Thukral,N. & Chilton,R. PPAR gamma agonists and coronary atherosclerosis. *Curr.Atherosclerosis Report* 10(2), 134-141. 2008.
115. Balakumar,P., Rose,M., Ganti,S.S., Krishan,P. & Singh,M. PPAR dual agonists: Are they opening Pandora's Box? *Pharmacological Research* 56(2), 91-98. 2007.
116. Furuta,M. *et al.* Troglitazone improves GLUT4 expression in adipose tissue in an animal model of obese type 2 diabetes mellitus. *Diabetes Res Clin Pract* 56(3), 159-171. 6-1-2002.
117. Puigserver,P. & Spiegelman,B. Peroxisome proliferator-activated receptor gamma coactivator 1alpha (PGC-1alpha): Transcriptional coactivator and metabolic regulator. *Endocrine Reviews* 24(1), 78-90. 2003.
118. Li,D., Kang,Q. & Wang,D. Constitutive coactivator of PPAR gamma, a novel coactivator of PPAR gamma that promotes adipogenesis. *Mol.Endocrinol.* 21(10), 2320-2333. 10-1-2007.

119. Vega,R.B., Huss,J.M. & Kelly,D.P. The coactivator PGC-1 cooperates with peroxisome proliferator-activated receptor alpha in transcriptional control of nuclear genes encoding mitochondrial fatty acid oxidation enzymes. *Mol.Cell Biol.* 20(5), 1868-1876. 3-1-2000.
120. Corton,J.C. & Brown-Borg,H.M. Peroxisome proliferator-activated receptor gamma coactivator 1 in caloric restriction and other models of longevity. *J.Gerontol.A.Biol.Sci.Med.Sci.* 60(12), 1494-1509. 2005.
121. Finck,B.N. & Kelly,D.P. PGC-1 coactivators: inducible regulators of energy metabolism in health and disease. *J.Clin.Invest* 116(3), 615-622. 1-3-2006.
122. Hofbauer,K.G., Keller,U. & Boss,O. *Pharmacotherapy of Obesity*., pp. 353-354 (CRC Press,2008).
123. Ding,Z., Gillespie,L.L. & Paterno,G.D. Human MI-ER1 alpha and beta function as transcriptional repressors by recruitment of histone deacetylase 1 to their conserved ELM2 domain. *Mol. Cell Biol.* 23, 250-258 (2003).
124. Feige,J.N. & Auwerx,J. Transcriptional coregulators in the control of energy homeostasis. *Trends Cell Biol* 17(6), 292-301. 2007.
125. Kim,H.I. *et al.* Identification and functional characterization of the peroxisomal proliferator response element in rat GLUT2 promoter. *Diabetes* 49, 1517-1524 (2000).
126. Hassan,M. *et al.* Phloretin enhances adipocyte differentiation and adiponectin expression in 3T3-L1 cells. *Biochem.Biophys.Res.Commun.* 361, 208-213. 7-3-2007.
127. Fu,M. *et al.* A Nuclear Receptor Atlas: 3T3-L1 Adipogenesis. *Mol.Endocrinol.* 19(10), 2437-2450. 2005.
128. Imagawa,M., Tsuchiya,T. & Nishihara,T. Identification of Inducible Genes at the early stage of adipocyte differentiation of 3T3-L1 cells. *Biochem.Biophys.Res.Commun.* 254, 299-305. 1999.
129. Tontonoz,P., Kim,B.J., Graves,R.A. & Spiegelman,B. ADD1: a novel helix-loop-helix transcription factor associated with adipocyte determination and differentiation. *Mol.Cell Biol.* 13(8), 4753-4759. 8-1-1993.
130. Li,D., Kang,Q. & Wang,D. Constitutive coactivator of PPAR gamma, a novel coactivator of PPAR gamma that promotes adipogenesis. *Mol.Endocrinol.* 21(10), 2320-2333. 10-1-2007.

131. Tiraby,C. *et al.* Acquisition of brown fat cell features by human white adipocytes. *J Biol.Chem.* 278(35), 33370-33376. 29-8-2003.
132. Nedergaard,J., Bengtsson,T. & Cannon,B. Unexpected evidence for active brown adipose tissue in adult humans. *Am.J.Physiol Endocrinol.Metab* 293, 444-452. 23-4-2007.
133. Tiraby,C. *et al.* Acquisition of brown fat cell features by human white adipocytes. *J Biol.Chem.* 278(35), 33370-33376. 29-8-2003.
134. Musri,M.M., Gomis,R. & Parrizas,M. Chromatin and chromatin-modifying proteins in adipogenesis. *Biochemistry and Cell Biology* 85(1), 397-410. 6-1-2007.
135. Paterno,G.D. *et al.* Genomic organization of the human mi-er1 gene and characterization of alternatively spliced isoforms: regulated use of a facultative intron determines subcellular localization. *Gene* 295, 79-88 (2002).
136. Burgermeister,E. & Seger,R. MAPK Kinases as Nucleo-cytoplasmic shuttles for PPAR gamma. *Cell Cycle* 6, 1539-1548 (2007).
137. Su,J.L., Winegar,D.A., Wisely,G.B., Sigel,C.S. & Hull-Ryde,E.A. Use of a PPAR gamma-specific monoclonal antibody to demonstrate thiazolidinediones induce PPAR gamma receptor expression in vitro. *Hybridoma* 18, 273-280 (1999).
138. Post,J.N., Luchman,H.A., Mercer,F.C., Paterno,G.D. & Gillespie,L.L. Developmentally regulated cytoplasmic retention of the transcription factor XMI-ER1 requires sequence in the acidic activation domain. *Int.J.Biochem.Cell Biol.* 37, 463-477. 2004.
139. Iyengar,P. *et al.* Adipocyte-secreted factors synergistically promote mammary tumorigenesis through induction of anti-apoptotic transcriptional programs and proto-oncogene stabilization. *Oncogene* 22, 6408-6423. 2003.
140. Puigserver,P. *et al.* Activation of PPAR gamma coactivator 1 through transcription factor docking. *Science* 286(5443), 1368-1371. 1999.
141. Wong,C.W., McNally,C., Nickbarg,E., Komm,B.S. & Cheskis,B.J. Estrogen receptor-interacting protein that modulates its nongenomic activity-crosstalk with src/erk phosphorylation cascade. *Proc.Natl.Acad.Sci.U.S.A* 99(23), 14783-14788. 2008.
142. Takedo,K., Ichiki,T., Tokunou,T., Iino,N. & Takeshita,A. 15 deoxy delta 12, 14 prostaglandin J2 and thiazolidinediones activate the MEK/ERK pathway

through phosphatidylinositol 3-kinase in vascular smooth muscle cells. *J.Biol.Chem.* 276(52), 48950-48955. 2001.

143. Thuillier,P., Baillie,R., Sha,X. & Clarke,S.D. Cytosolic and nuclear distribution of PPAR gamma 2 in differentiating 3T3-L1 preadipocytes. *Journal of Lipid Research* 39, 2329-2338. 1998.
144. Eto,K. *et al.* Genetic manipulations of fatty acid metabolism in beta-cells are associated with dysregulated insulin secretion. *Diabetes* 51 Suppl 3, S414-S420 (2002).
145. Prigeon,R.L., Kahn,S.E. & Porte,D. Effect of troglitazone on b-cell function, insulin sensitivity, and glycemic control in subjects with type 2 diabetes mellitus. *J.Clin.Endocrinol.Metab* 83(3), 819-823. 1998.
146. Eto,K. *et al.* Genetic manipulations of fatty acid metabolism in beta-cells are associated with dysregulated insulin secretion. *Diabetes* 51 Suppl 3, S414-S420 (2002).
147. Li,D., Kang,Q. & Wang,D. Constitutive coactivator of PPAR gamma, a novel coactivator of PPAR gamma that promotes adipogenesis. *Mol.Endocrinol.* 21(10), 2320-2333. 10-1-2007.
148. Li,D., Kang,Q. & Wang,D. Constitutive coactivator of PPAR gamma, a novel coactivator of PPAR gamma that promotes adipogenesis. *Mol.Endocrinol.* 21(10), 2320-2333. 10-1-2007.
149. Thorne,L.B., McCarthy,P.L., Paterno,G.D. & Gillespie,L.L. Protein expression of the transcriptional regulator MI-ER1 alpha in adult mouse tissues. *J Mol. Histol.* (2007).



